NUCLEAR SPIN-LATTICE RELAXATION IN SOLID METHANE AT LOW TEMPERATURES

by

Gerhardus A. de Wit
B. Sc., The University of British Columbia, 1961
M. Sc., The University of British Columbia, 1963

A THESIS SUBMITTED IN PARTIAL FULFILMENT
OF THE REQUIREMENTS FOR THE
DEGREE OF
DOCTOR OF PHILOSOPHY

in the Department
of
Physics

We accept this thesis as conforming to the
required standard

THE UNIVERSITY OF BRITISH COLUMBIA
February, 1966

In presenting this thesis in partial fulfilment of the requirements for an advanced degree at the University of British Columbia, I agree that the Library shall make it freely available for reference and study. I further agree that permission for extensive copying of this thesis for scholarly purposes may be granted by the Head of my Department or by his representatives. It is understood that copying or publication of this thesis for financial gain shall not be allowed without my written permission.

Department of Physics

The University of British Columbia
Vancouver 8, Canada

Date March 7, 1966.

The University of British Columbia

FACULTY OF GRADUATE STUDIES

PROGRAMME OF THE

FINAL ORAL EXAMINATION

FOR THE DEGREE OF

DOCTOR OF PHILOSOPHY

of

GERHARDUS A. de WIT

B.Sc., The University of British Columbia, 1961

M.Sc., The University of British Columbia, 1963

WEDNESDAY, MARCH 2, 1966, AT 3:30 P.M.

IN ROOM 301, HENNINGS BUILDING

COMMITTEE IN CHARGE

Chairman: I. McT. Cowan

M. Bloom
L. G. Harrison
K. B. Harvey
P. W. Matthews
B. G. Turrell
D. Ll. Williams

External Examiner: K. Tomita
Kyoto University, Kyoto, Japan

Research Supervisor: M. Bloom

NUCLEAR SPIN-LATTICE RELAXATION IN SOLID METHANE AT LOW TEMPERATURES

ABSTRACT

The spin-lattice relaxation time T_1 has been measured in the temperature range 1.2 to 55°K at 28.5 mcs. for the proton resonance, and at 4.4 mcs for the deuteron resonance using N.M.R. pulse techniques. The proton T_1 has been measured for CH_4, CH_3D, CD_3H, 50%CH_4-50%Kr, 90%CH_4-10%Kr, 67%CD_4-33%CH_4, 10%CD_4-90%CH_4, and also for CH_4 at 4.4 mcs. The deuteron T_1 has been measured for CD_4, CD_3H, and 67%CD_4-33%CH_4.

It is found that a drastic change in the temperature dependence of T_1 occurs in the temperature region below the phase transitions and that at most of the phase transition temperatures there is either a discontinuous change in T_1 or a change in the slope of T_1 versus T. A minimum in T_1 is found at low temperatures for all the systems studied. An analysis of the data based on conventional N.M.R. theory shows in most cases that the correlation time $\tau_c \propto T^{-7}$ in the neighbourhood of 20°K, and that τ_c is almost independent of temperature near 1.2°K. It is postulated that phonon-molecular interactions, involving direct and Raman processes, can account for the temperature dependence of τ_c. The values of T_1 at the minimum are completely determined by conventional theory. In most cases, however, the predicted values are of the order of 20 times too short. An unexplained minimum in T_1 was observed in CH_4, CH_4-CD_4, and CH_4-Kr mixtures above the upper phase transitions.

To investigate the origin of some of the inadequacies of the conventional theory, the two energy level scheme proposed by Colwell, Gill, and Morrison (1965) is used, where each of the two levels may be degenerate. Simple rate equations are used to calculate the conditional probabilities and the correlation functions for the two level model. It is found that the effective interaction strength is temperature dependent, that the correlation function can be described by a simple exponential under certain conditions, and that the interaction strength has no simple relationship with the classical value.

GRADUATE STUDIES

Field of Study: Nuclear Magnetic Resonance

Quantum Theory of Solids	R. Barrie
Advanced Magnetism	M. Bloom
Low Temperature Physics	J. B. Brown
Electromagnetic Theory	G. M. Volkoff
Statistical Mechanics	R. Barrie

Related Studies:

Quantum Chemistry	J. A. R. Coope

PUBLICATIONS

Gerald A. de Wit and Meyer Bloom "Nuclear Spin Relaxation in Liquid and Solid Methane: Isotope Effects", Can. J. Phys. 43, 986 (1965).

ABSTRACT

The spin-lattice relaxation time T_1 has been measured in the temperature range 1.2 to 55°K at 28.5 mcs. for the proton resonance, and at 4.4 mcs for the deuteron resonance using N.M.R. pulse techniques. The proton T_1 has been measured for CH_4, CH_3D, CD_3H, 50%CH_4-50%Kr, 90%CH_4-10%Kr, 67%CD_4-33%CH_4, 10%CD_4-90%CH_4, and also for CH_4 at 4.4 mcs. The deuteron T_1 has been measured for CD_4, CD_3H, and 67%CD_4-33%CH_4.

It is found that a drastic change in the temperature dependence of T_1 occurs in the temperature region below the phase transitions and that at most of the phase transition temperatures there is either a discontinuous change in T_1 or a change in the slope of T_1 versus T. A minimum in T_1 is found at low temperatures for all the systems studied. An analysis of the data based on conventional N.M.R. theory shows in most cases that the correlation time $\tau_c \propto T^{-7}$ in the neighbourhood of 20°K, and that τ_c is almost independent of temperature near 1.2°K. It is postulated that phonon-molecular interactions, involving direct and Raman processes, can account for the temperature dependence of τ_c. The values of T_1 at the minimum are completely determined by conventional theory. In most cases, however, the predicted values are of the order of 20 times too short. An unexplained minimum in T_1 was observed in CH_4, CH_4-CD_4, and CH_4-Kr mixtures above the upper phase transitions.

To investigate the origin of some of the inadequacies of the conventional theory, the two energy level scheme proposed by Colwell, Gill, and Morrison (1965) is used, where each of the two levels may be degenerate. Simple rate equations are used to calculate the conditional probabilities and the correlation functions for the two level model. It is found that the effective interaction strength is temperature dependent, that the correlation function can be described by a simple exponential under certain conditions, and that the interaction strength has no simple relationship with the classical value.

TABLE OF CONTENTS

LIST OF TABLES

LIST OF ILLUSTRATIONS

ACKNOWLEDGEMENTS

I would like to express my deepest appreciation to Dr. Myer Bloom, my supervisor, for his constant encouragement and guidance.

Without the many sacrifices and the everready assistance of my wife, this thesis would have never been written.

I would like to thank Dr. K. W. Gray and Dr. L. McLachlin for many stimulating discussions.

I am indebted to Mr. John Lees for his indispensable services, as our glassblower.

It is my pleasure to have had the assistance of Mr. Peter Haas in the construction of the equipment and the preparation of the drawings.

My fellow-students and the faculty members in the Nuclear Magnetic Resonance group are hereby thanked for the many ways in which they have contributed to this thesis.

The National Research Council is gratefully acknowledged for providing financial assistance throughout my post-graduate education.

CHAPTER 1.

INTRODUCTION

This thesis is a study of the low temperature magnetic relaxation properties of solid methane, its deuterated modifications, and some mixtures of methane (CH_4) with CD_4 or with Kr. As is well known, the methanes, $CH_{4-n}D_n$, in the solid are all characterized by two λ singularities in the specific heat. The ultimate aim of this work is to obtain more conclusive knowledge about the nature of these phase transitions.

Nuclear magnetic resonance is capable of providing much information about the dynamics of any systems with which the spins interact and exchange energy; these systems are collectively called the "lattice". The interactions between the lattice and the spin system are weak and disturb the "lattice" negligibly. The "lattice" consists of the molecular rotational and vibrational degrees of freedom. In the next few pages, a brief description will be presented of how certain nonequilibrium states of the spin system can be prepared, of how the approach to equilibrium can be monitored, and of how studies of this recovery can be related to microscopic properties of the spin system and the lattice.

First, some of the properties of a nuclear spin will be described. Many atomic nuclei possess a non-zero spin angular momentum $\hbar\overline{I}$ and a magnetic moment $\gamma\hbar\overline{I}$ colinear with it. The application of a magnetic field $\overline{H}_o$ produces

a Zeeman interaction energy of the nuclear spin

$$\begin{aligned} \mathcal{H} &= -\bar{\mu}\cdot\bar{H}_0 \\ &= -\gamma\hbar H_0 I_z , \end{aligned} \tag{1-1}$$

if $\bar{H}_0$ is taken to be in the z-direction. The allowed energies of a single spin are,

$$E_m = -\gamma\hbar H_0 \; m \qquad m = I,\ I-1,\ldots,-I.$$

Next, consider an ensemble of weakly interacting spins in thermal equilibrium with their environment, the "lattice". The temperature of the spin system will be the same as that of the "lattice". The populations of the energy levels E_m are given by a Boltzman distribution,

$$P_m = \frac{e^{-E_m/kT}}{\sum_{m=-I}^{I} e^{-E_m/kT}}$$

The magnetization of an ensemble of N spins is in the z-direction and is given by

$$\begin{aligned} M_z = M_0 &= N\sum_{m=-I}^{I} P_m \gamma\hbar m \\ &= \frac{N\gamma^2\hbar^2 I(I+1)}{3k}\,\frac{H_0}{T} \end{aligned} \tag{1-2}$$

where the high temperature approximation has been made,

$$\gamma\hbar H_0/kT \ll 1$$

This is the well known Curie law.

To detect the existence of this set of energy levels, an interaction, which can cause transitions between these levels, is required. An alternating magnetic field $2H_1\cos\omega t$ perpendicular to $\bar{H}_0$ provides such an interaction, since it has

the following properties: (1) it has non-zero matrix elements $\langle m| I_x |m'\rangle$ for $m - m' = -1$

(2) it conserves energy if its frequency $\omega = \gamma H_o$.

Nuclear magnetic resonance is concerned with this resonant exchange of energy between a radio frequency field and a system of nuclear spins in a magnetic field $\overline{H}_o$.

Consider a system of non-interacting nuclei possessing spin $\frac{1}{2}$, and specify the number of nuclei in the two m states $+\frac{1}{2}$ and $-\frac{1}{2}$ by N^+ and N^- respectively. Now the application of an alternating field gives rise to a transition probability $W_{+\to-}$ between states $m = +\frac{1}{2}$ and $m = -\frac{1}{2}$ and $W_{-\to+}$ for the inverse transition. The equations governing the populations N^+ and N^- can be written as

$$\frac{dN^+}{dt} = N^- W_{-\to+} - N^+ W_{+\to-} \qquad (1\text{-}3)$$

From time dependent perturbation theory, it is known that

$$W_{+\to-} = W_{-\to+} = W$$

$$\text{i.e.} \quad \frac{dn}{dt} = -2Wn \qquad \text{where } n = N^+ - N^- \qquad (1\text{-}4)$$

This equation emphasizes the fact that for a net absorption of energy 'n' must be non-zero, and that the absorption of energy from the alternating field would eventually vanish as $n \to 0$. The condition $n = 0$ implies that the spin system is characterized by an infinite temperature. In actual fact, energy is always absorbed. There must therefore exist another mechanism for inducing transitions between $m = +\frac{1}{2}$ and $m = -\frac{1}{2}$. This mechanism arises through the coupling of the spins with

another system, the lattice.

Let $W_{s\to s'}$ denote the probability that this coupling with the lattice induces a transition between two well defined states s and s' of the spin system and the reverse process by $W_{s'\to s}$. The transition probabilities $W_{s'\to s}$ and $W_{s\to s'}$ depend intimately upon the initial and final state of the lattice. The initial and final states of the spin system and the lattice are restricted to those conserving the energy of the combined system. The transition probability will depend on the matrix elements connecting the initial and final states of the combined system, and also on the probability that the lattice will be in a state that permits the transition.

Denote by P_f the probability of finding the lattice in state $|f\rangle$, and $W_{fs\to f's'}$ the probability of going from a state $|f\rangle|s\rangle$ of the entire spin-lattice system to another $|f'\rangle|s'\rangle$, such that $E_f + E_s = E_{f'} + E_{s'}$. As the spin-lattice system is a closed system, according to the general principles of quantum mechanics $W_{fs\to f's'} = W_{f's'\to fs}$
In addition, it is usually assumed that the lattice is always in thermal equilibrium with itself, and has an infinite specific heat, such that $P_f = \exp -(E_f/kT)$
It is easily shown that

$$\frac{W_{s\to s'}}{W_{s'\to s}} = \frac{\sum_{ff'} P_f\, W_{fs\to f's'}}{\sum_{ff'} P_{f'}\, W_{f's'\to fs}} = \exp\,(E_s - E_{s'})/kT \qquad (1\text{-}5)$$

This condition will lead to a Boltzman distribution for the populations of the spin system characterized by the same

temperature as that of the lattice. This approach to equilibrium has associated with it a time constant T_1, the spin-lattice relaxation time; it will intimately depend on the transition probabilities $W_{s \to s'}$. The approach to equilibrium in many cases is exponential, but this is not always the case.

The nature of the interaction between the spin system and its surroundings, uniquely determines the matrix elements involved in the expression for $W_{s \to s'}$. These interactions can be magnetic, dipole-dipole interactions between the nuclei and interactions between the nuclei and other local magnetic fields; or, in the case of a nucleus such as the deuteron nucleus, which has spin greater than $\frac{1}{2}$, between the electric field gradients and the nuclear quadrupole moments. In addition, the transition probabilities depend on details of the density of states for the normal modes of the lattice. Thus, measurements of T_1 implicitly provide information about the nature of the spin-lattice interactions and the lattice modes.

Classical Treatment 1:1

Many magnetic resonance phenomena and techniques can be understood classically. According to classical electromagnetic theory, the equation of motion of $\overline{M}$ is,

$$\frac{d\bar{M}}{dt} = \gamma \bar{M} \wedge \bar{H} \qquad (1\text{-}6)$$

The Quantum Mechanical expectation values can be shown to obey this equation of motion; all the results derived below can also be derived Quantum Mechanically for an ensemble of weakly interacting nuclear spins. Temporarily, all relaxation effects will be neglected.

Equation (1-6) can be solved when both the main magnetic field $\bar{H}_o$ and the rotating r.f. field perpendicular to $\bar{H}_o$ are present. It is convenient to transform to a rotating co-ordinate frame with angular velocity ω about the z-axis. Now the equation of motion becomes

$$\frac{\partial \bar{M}}{\partial t} = \gamma \bar{M} \wedge \left[\bar{H} + \bar{\omega}/\gamma\right] \qquad (1\text{-}7)$$

This has the same form as equation (1-6) provided that the magnetic field $\bar{H}$ is replaced by an effective field $\bar{H}_e = \bar{H} + \bar{\omega}/\gamma$. Consider the case that $\bar{H}$ consists only of the static field $\bar{H}_o = H_o\bar{k}$. In this frame $\frac{\partial \bar{M}}{\partial t} = 0$, when $\bar{\omega} = -\gamma \bar{H}_o$. It can therefore be said that $\bar{M}$ precesses with respect to laboratory frame at a frequence $\omega = -\gamma H_o$, the Larmor frequency.

Now let us add to $\bar{H}_o$, a field $\bar{H}_1$ rotating perpendicular to H_o with frequency ω . Choose the x-axis of the rotating reference frame to be in the direction of $\bar{H}_1$. i.e. $\bar{H}_1 = H_1\,\bar{i}$. The equation of motion for $\bar{M}$ is

$$\frac{\partial \bar{M}}{\partial t} = \gamma \bar{M} \wedge \bar{H}eff$$

where $$\bar{H}_{eff} = \left(H_o + \omega/\gamma\right)\bar{k} + H_1\,\bar{i} \qquad (1\text{-}8)$$

This implies that in the rotating frame $\overline{M}$ precesses about $\overline{H}_{eff}$ at angular frequency $-\gamma H_{eff}$. Usually H_1 is much smaller than H_o, consequently only when $[H_o + \omega/\gamma] \leq H_1$ will the r.f. field have a pronounced effect. It will change the direction of $\overline{H}_{eff}$ from the z-axis to the x-axis as $|H_o + \omega/\gamma| \longrightarrow 0$. At resonance, when $\omega = -\gamma H_o$, the magnetization $\overline{M}$ precesses about the x-axis with angular frequency γH_1. If the H_1 field is applied as a single pulse of width t_ω, then at $t = 0$ the magnetization $\overline{M}$ will start from $\overline{M} = M_o\overline{k}$ and will have precessed about the x-axis through an angle $\theta = \gamma H_1 t_\omega$ at the end of the pulse. Thus, in the special case that $\theta = \pi/2$ the magnetization, as seen from the laboratory frame, will be precessing in the x-y plane at an angular frequency $\omega = -\gamma H_o$ about the z-axis. In N.M.R. measurements r.f. pulses, such that $\theta = \pi/2$ or π; are frequently used and are referred to as "$\pi/2$ or π pulses", respectively.

The equation of motion has to be modified to include the relaxation effects, which were neglected above; these were allowed for in a phenomenological fashion by Bloch (1946). Earlier, it was described how M_z relaxes to M_o in the absence of the r.f. field; this process was characterized by the time constant T_1. Furthermore, as was described in the last paragraph, the application of an r.f. pulse can give rise to a magnetization solely in the x-y plane. When in thermal equilibrium, the spin system possesses only magnetization in the z-direction (this was shown at the

beginning of the chapter). Consequently, there must exist another relaxation mechanism, spin-spin relaxation, characterized by T_2. All these facts can be incorporated in the following simple equations, the Bloch equations:

$$\frac{d\bar{M}}{dt} = \gamma\, \bar{M} \wedge \bar{H} - \frac{M_x \bar{i} + M_y \bar{j}}{T_2} - \frac{(M_z - M_o)\bar{k}}{T_1} \qquad (1\text{-}9)$$

These equations are particularly well suited to the description of transient effects, while at the same time providing a description of steady state effects broadly consistent with the proper quantum mechanical treatment. For example, if $\bar{M} = (M_{x(o)}\ M_{y(o)}\ M_{z(o)})$ at t = o and no r.f. field is present, then the solutions of the Bloch equations in the laboratory frame are:

$$M_x(t) = M_1(o)e^{-t/T_2} \cos(\ t + \phi)$$
$$M_y(t) = M_1(o)e^{-t/T_2} \sin(\ t + \phi) \qquad (1\text{-}10)$$

$$M_z(t) = M_o + (M_{z(o)} - M_o)\ e^{-t/T_1}$$

where $M_1 = [M_x^2(o) + M_y^2(o)]^{\frac{1}{2}}$

Thus, according to the Bloch equations, the return to equilibrium of the spin system is exponential. This behaviour is certainly not generally true. The Bloch equations provide a useful approximate description of the spin dynamics; however, they should not be regarded as a substitute for a more rigorous quantum mechanical treatment.

Now, the concept of spin-spin relaxation will be explained in more detail. As can be shown, using the Bloch

equation, the description of the $\pi/2$ pulse given above still holds as long as $t_\omega << T_2, T_1$. Under those conditions, at the end of the r.f. pulse, there exists coherence between the phases of the wave functions describing the spin system bringing about a transverse magnetization in the x-y plane. The random interactions of the spins with the environment gradually destroy this coherence and the transverse magnetization; this process is called spin-spin relaxation. It is observed that T_1 is always greater than or equal to T_2, since the decay of the transverse magnetization conserves energy in the field H_o, unlike the recovery of the longitudinal magnetization (M_z) in which energy has to be transferred to the lattice.

How are T_1 and T_2 measured experimentally? One method uses the properties of the $\pi/2$ pulse. As was mentioned earlier this holds as long as $t << T_1, T_2$. The $\pi/2$ pulse sets up a precessing magnetization in the x-y plane and the M_z magnetization is then zero. If a coil is wound around the sample with its symmetry axis in the x-y plane, the precessing magnetization will induce a voltage in the coil decaying with a time constant T_2; this is called the free induction tail. Thus, the decay of the transverse magnetization can be monitored. Moreover, the signal induced in the coil is proportional to the M_z magnetization at the beginning of the pulse. This fact immediately suggests a method for measuring T_1: disturb the M_z magnetization from its equilibrium value M_o by applying an r.f. field for a

short time, a $\pi/2$ pulse, for example; monitor the recovery of M_z at time t later by applying a $\pi/2$ pulse; repeat this sequence for many values of 't', allowing the spin system to attain equilibrium between successive sequences of pulses. Experimentally, the r.f. field is produced by an r.f. current passing through the coil situated around the sample. The alternating field, thus produced, can be decomposed into two circularly polarized components with opposite senses of rotation. If one component satisfies the resonance condition, $\omega_o = -\gamma H_o$, then the effect of the other component is negligible as it will be off-resonance by $2\omega_o$.

In this chapter, some of the concepts involved in N.M.R. have been introduced, and it has been shown how they are related to the microscopic properties of the system. In the next chapter, existing knowledge about the methane system at low temperatures will be reviewed. Chapters 3 and 4 deal with the experimental techniques and the theory, respectively.

CHAPTER 2.

PROPERTIES OF THE METHANES

It is well known that solid CH_4 and all of its deuterated modifications exhibit λ anomalies in the specific heat. This study of the low temperature nuclear magnetic relaxation properties was motived at λ by (1) the lack of definitive experiments regarding the nature of these λ anomalies; (2) some interesting results obtained by us in preliminary experiments studying the relaxation properties of the deuteron spin system between 110 and 55°K.

In this chapter, some of the preceding experimental work will be reviewed. Notwithstanding a wealth of experimental data, the nature of the phase transitions is still very much a mystery. Many of the experiments appear to contradict each other; other experimental conclusions are too qualitative to be of much value.

Properties of Methane Molecules: 2:1

In the free methane molecule, the deuterons and protons are situated at the corners of a tetrahedron with the carbon atom at its center. It follows from the geometry, that CH_4 and CD_4 are spherical top molecules and possess a T_d symmetry group; CD_3H and CH_3D are symmetric top molecules with symmetry group C_3.

The wave function of polyatomic molecules are characterized by three quantum numbers J, K, and M. The square of the total angular momentum is quantized and is equal to $J(J + 1)\hbar^2$, where J is the rotational angular momentum quantum number. The projection of the rotational angular momentum on the molecular axis is quantized and equals $K\hbar$ where K = J,...,-J is an integer. Similarly, its projection on the polar axis fixed in space is $M\hbar$ where M = J,...,-J. The energy levels of free spherical top molecules having moment of inertia I_o depend only on J and are $(2J + 1)^2$ degenerate

$$E_{JKM} = \frac{\hbar^2}{2I_o} J(J + 1) . \qquad (2\text{-}1)$$

The symmetric top molecular energy levels are specified by J and K and are 2(2J + 1) degenerate for $K \neq 0$

$$E_{JKM} = B\ J\ (J + 1) + (C - B)K^2 \qquad (2\text{-}2)$$

where B and C depend on the various components of the moment of inertia tensor of the molecule.

The wave function of the methane molecule is usually approximately expressed as a product of functions of the various co-ordinates.

$$\phi_{tot} = \phi_e \phi_v \phi_R \phi_S \qquad (2\text{-}3)$$

where the subscripts e,v,R, and S indicate that the corresponding factor is a function of the electronic (including electron spin), vibrational, rotational and nuclear spin co-ordinates.

This wave function is not unique, since the permutation of identical nuclei generates a number of other wave functions. The correct wave function must be completely symmetrical or antisymmetrical with respect to interchange of any pair of identical nuclei.

Since protons obey the Pauli exclusion principle, CH_4 has antisymmetrical wave functions, whereas CD_4 has symmetrical wave functions. To obtain wave functions with the proper symmetry character, it is necessary to form linear combinations of the degenerate functions discussed above. This problem is simplified since the electronic wave function ϕ_e and the vibrational wave function ϕ_v in the ground state are usually completely symmetrical. Thus, the symmetry properties of ϕ_{tot} depend only on the symmetry properties of $\phi_R$and ϕ_S. Moreover, all rotations of the group T_d correspond to "even" permutations of the nuclei, hence for CH_4 and CD_4 the total wave function ϕ_{tot} belongs to the totally symmetric irreducible representation A.

The symmetry operations which transform the molecule into itself belong to the tetrahedral symmetry group T_d. This group consists of three classes of operations giving rise to three irreducible representations A, E, and T. Each rotational wave function ϕ_R is assigned in accordance with its symmetry properties to one of these irreducible representations and will be denoted by ϕ_R (E), ϕ_R(A), and ϕ_R(T). The ϕ_R provide the basis functions for these representations. Only rotational wave functions with certain J quantum numbers belong to a particular irreducible representation. A

similar assignment of the spin wave functions can be made. In general, the spin wave functions for each irreducible representation have definite values of the total spin of the nuclei in the molecule. Moreover, this relation is not one-to-one; the ϕ_S of each representation can possess more than one value of total spin.

It can be shown, using group-theoretical methods (Maue, 1937), that the only combinations of $\phi_S\phi_R$ producing a totally symmetric wave function are

$$\begin{matrix} \phi_R\,(A) & \phi_S\,(A) \\ \phi_R\,(E) & \phi_S\,(E) \\ \phi_R\,(T) & \phi_S\,(T) \end{matrix} \qquad (2\text{-}4)$$

In other words, each rotational state will have associated with it a restricted set of spin wave functions. The spin wave functions belonging to a particular irreducible representation T,A, or E are said to belong to the spin species ortho, meta, or para, respectively. This is analogous to the familiar case of hydrogen; it possesses two spin species ortho ($I_t = 1$) and para ($I_t = 0$). In analogy with hydrogen, conversion between these three species is very slow, since the magnetic interactions between molecules are normally too weak. Unlike hydrogen, in CD_4 for certain rotational states the permissible spin wave functions possess more than one total spin quantum number e.g. the $\phi_S(A)$ have total spin quantum numbers 0,2,4 and are associated with rotational levels J = 0,3,4 etc. The spin wave functions for CH_4 are characterized by total spin quantum numbers

0,1, and 2 for E,T, and A spin species, respectively. Similar considerations also apply to the symmetric top molecules CD_3H and CH_3D, see Table I.

So far, only the properties of the free molecule have been considered. In actual fact, the coupling between the molecules will modify the free molecular wave functions and energy levels. It is not known to what extent they are modified; not even the nature and the strength of these forces are known with any certainty. One attempt to describe the influence of the intermolecular interactions has been made by Nagamiya (1951). He assumed that the intermolecular forces could be described by a crystalline electric field potential possessing a definite symmetry. Using group theoretical methods, he worked out to what extent the various degeneracies of the free molecular energy levels would be removed by crystalline fields of various symmetries. His results for CH_4 and CD_4 are shown in Figure 1. These results have proven to be extremely useful in analyzing the entropy of the solid methanes at low temperatures.

A different theoretical approach to the description of the intermolecular interactions was used by James and Keenan (1959). They assume that the interactions are due to the octupole moments of the molecular charge distributions and have attempted to provide a detailed model of the low temperature phase transitions in solid methane in terms of these interactions. Since the theory of James and Keenan is completely classical, they feel that, of the isotopic modifications

Modification	T_λ^+ (°K)	T_λ^- (°K)	Some allowed values of J and K			Constants in eqn.2-2	
			Ortho (T)	Meta (A)	Para (E)	B/k (°K)	C/k (°K)
CH_4	20.4	8.0	J = 1 = 2 = 3 = 4	J = 0 = 3 = 4	J = 2 = 4 = 5	7.68	7.68
CD_4	27.0	21.9				3.84	3.84
CH_3D	23.2	15.9	J = 1 K = 1 = 2 = 1 = 2 = 2 = 3 = 1 = 3 = 3	J = 0 K = 0 = 1 = 0 = 2 = 0 = 3 = 0 = 3 = 3		5.59	7.68
CD_3H	26.1	19.9				4.73	3.84

Table 1. Some Properties of Free Methane Molecules

of methane, its predictions would apply best to CD_4, which has the largest moment of inertia.

Nuclear Magnetic Resonance Studies 2:2

The earliest low temperature N.M.R. studies of methane were carried out by Thomas et al. (1950). In their experimental measurements of the spin-lattice relaxation times, inadequate precautions were taken to remove O_2 impurities from their sample. As a consequence, the relaxation process was dominated by the very strong interactions between the paramagnetic O_2 impurities and the nuclear spins on the methane molecules. Many details pertaining to the nuclear relaxation which are reported in this thesis, were obscured by these interactions in the measurements of Thomas et al.

The first theoretical treatment of N.M.R. in solid methane was provided by Tomita (1953). Unfortunately, his theory was applied to the incorrect experimental results discussed above. However, his general approach, which brings out explicitly the role of molecular symmetry with respect to the effects of the intramolecular spin-spin interactions on T_1 and T_2, will be very useful in any attempt to formulate a detailed theory of N.M.R. in low temperature methane. In particular, he shows that the dipolar interactions between the nuclear spins on molecules having spin wave functions $\phi_S(A)$, give no contribution to spin relaxation.

Measurements of the line-width in CH_4, carried out by Wolf (1963) and Thomas et al. (1950), indicated that there was

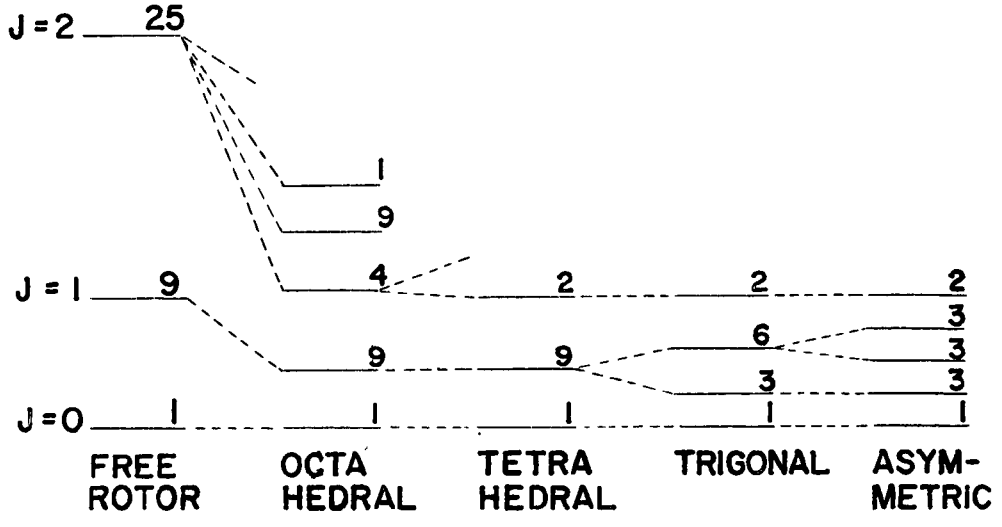

Figure 1. The Molecular Energy Levels in Crystalline Fields with Different Symmetries for CH_4 and CD_4

no significant change in the line-width at either of the two phase transition temperatures. The experimental values of the line-width were much smaller than were calculated assuming a rigid lattice. Actually, the observed values were in reasonable agreement with the calculated values, if the molecules were assumed to be isotropically reorienting. For sufficiently rapid molecular reorientations, the contribution of the intramolecular dipolar interactions (the interactions between nuclei on the same molecule), to the line-width would be considerably reduced. The absence of a change in the line-width at the transition temperatures rules out the proposal by Pauling (1930) that the transition involved a change from oscillations of the molecules in the low temperature phase to free rotation in the high temperature phase.

Another set of pertinent results was reported by de Wit and Bloom (1965). Measurements of the deuteron spin-lattice relaxation time between 55-110°K indicated that the correlation time for molecular reorientations (to be defined in Chapter 4) was a very slowly decreasing function of temperature over the entire temperature range, with no change being observable at the melting point 90°K. Moreover, by measuring the spin-lattice relaxation times in mixtures of CH_4 and CD_4, thus varying the intermolecular dipolar interactions, it was conclusively shown that below 65°K, the interactions causing relaxation are solely intramolecular.

Specific Heat Studies 2:3

Specific heat studies of the methane system were first carried out in 1929. Clusius, in 1929, discovered the upper phase transition at 20.4°K in solid CH_4. Subsequently, Clusius and Popp (1937), found that CD_4 and CDH_3 exhibited two phase transitions. These occurred at 27.0°K and 21.9°K for CD_4, and at 23.2°K and 15.9°K for CH_3D. The other methanes CD_2H_2 and CD_3H have also been found to possess two phase transitions, see Table I (Sperandio, 1961). It may be noted that the upper phase transition temperatures vary almost linearly with 'n' for $CH_{4-n}D_n$. This linearity holds for the lower phase transitions between CH_2D_2 and CD_4, but does not hold for CH_3D and CH_4 (as they do not lie on the straight line). In addition, the lower phase transition is sharper than the upper phase transition, except for the case of CH_4.

Only recently has the lower phase transition in CH_4, which occurs at 8°K, been discovered by Colwell, Gill and Morrison (1962). This phase transition was not very pronounced and was rather difficult to observe. The discovery of the lower phase transition in CH_4 removed the puzzling feature that CH_4 was apparently the only methane modification which was not characterized by <u>two</u> specific heat anomalies. The observations of Morrison et al. have been supported by a re-investigation of the high pressure calorimetric behaviour of CH_4 by Rosenshein and Whitney (1964). They found, contrary to earlier experimental work (Stewart (1959) and Stevenson (1957)), that the lower phase transition at higher pressures

in CH_4 when extrapolated to zero pressure, corresponded to the phase transition temperature observed by Morrison et al. As all methanes possess two phase transition temperatures and can exist in three distinct phases, the following conventions will be adopted: T_λ^+ and T_λ^- denote the upper and lower phase transition temperatures, respectively; and phase I will be the phase above T_λ^+ ; phase II, the phase between T_λ^- and T_λ^+ ; phase III, the phase below T_λ^- .

Studies were also carried out on mixtures of CH_4 and CD_4. It was found that the upper transition temperatures varied linearly as a function of the mixing ratio between those of pure CH_4 and CD_4. For a mixing ratio of CH_4 and CD_4 equal to the stoichiometric ratio of deuterons to protons in a given isotopic modification of methane, T_λ^+ is roughly the same as that of the given isotopic modification! For example, a 25% CH_4-75%CD_4 mixture has $T_\lambda^+ = 25.4^\circ K$, while CHD_3 has $T_\lambda^+ = 25.9^\circ K$. Moreover, it was found that the lower phase transition temperature varied linearly with the mixing ratio, if the CD_4 content was larger than 60%; below 60%, the transition temperature dropped more rapidly (Bartholome et al. 1938).

Methane and krypton can be mixed to form solid solutions (Stackelberg et al., 1936). Solids of pure methane and pure krypton each have the same crystal structure (f.c.c.) and their lattice constants differ by only 1.5%. When Kr is added, the specific heat maximum is broadened, its peak value is decreased, and the temperature at which the peak occurs is shifted downwards (Eucken and Veith, 1936). For Kr concentrations greater

than 16%, the maximum in the specific heat versus temperature curve is unobservable.

A recent paper by Colwell, Gill and Morrison (1965) is of special interest since the conclusions from specific heat measurements, and our conclusions from magnetic resonance agree in principle. They measured the heat capacities of the partially deuterated methanes between 2.5 and 27°K. In addition, to the two transitions for each methane, they observed large heat capacity anomalies below 8°K for CH_3D, CH_2D_2 and CHD_3. These anomalies are interpreted as the high temperature tails of Schottky anomalies (Rosenberg, 1964). In the analysis of their data, they assume that no conversion takes place between the different species, and that in solid methane the coupling between the molecules is weak enough to consider the energy states to be those of the free molecule weakly perturbed by crystalline fields in the solid. In particular, they interpret these anomalies in terms of removal of the rotational degeneracies by the crystalline electric field. They are able to draw some conclusions regarding the size of the energy level splitting, the crystal field symmetry, and the degeneracies of the levels.

N.M.R. measurements were carried out on mixtures of CH_4 with CD_4, and of CH_4 with Kr, in addition to measurements of CH_4 and its isotopic modifications. These experiments were carried out to correlate the magnetic relaxation behaviour with the interesting results of the specific heat measurements discussed above.

Miscellaneous Measurements 2:4

A series of infra-red and Raman experiments have been reported drawing contradictory conclusions from their experiments. Welsh et al. (1952) have studied the Raman spectra of methane as a liquid and as a solid just below its melting point. They concluded that rotation was essentially free in the liquid, and certain aspects of the spectrum in the solid also led them to conclude that the rotational freedom was unchanged by solidification. However, Savitsky and Hornig (1962) contradicted these results. They examined the infra-red spectra of the solid phases I, II, and III of CH_4 and CD_4, and concluded from the absence of observable rotational fine structure that a barrier in excess of several hundred degrees Kelvin must hinder molecular rotation. It should be mentioned that their measurements were limited to temperatures less than $40^{\circ}K$. Recently, Ewing (1964) has shown that the observed spectra of liquid and solid methane do not conflict with the hypothesis that the molecules are undergoing hindered rotation in these phases.

The above contradictory results prompted a theoretical study by Gordon (1965). He shows how the infra-red and Raman line shapes are the Fourier transforms of the time correlation functions of the first and second order spherical harmonics, respectively. To compare the results of the Raman and infra-red studies with each other, the correlation functions should be compared.

To support his contention, he has calculated the Fourier transforms of the Raman spectrum obtained by Welch et al., and the infra-red spectrum by Ewing. He finds that for $t < 10^{-13}$ sec, the correlation functions are indistinguishable from those of the free rotational motion. Both the Raman and infrared correlation functions show the exponential decay for $t > 3 \times 10^{-13}$ sec that is expected for rotors hindered by random intermolecular torques. However, the Raman correlation function decays faster than the infrared function; it has fallen to a much smaller value by the time the exponential description becomes valid. Therefore, the Raman spectrum resembles the free rotational spectrum considerably more than the infrared one does.

X-ray studies by Mooy (1931) and McLannan et al. (1929), showed that solid CH_4 has f.c.c. lattice with the same lattice constants above and below the phase transition. On the other hand, Schallamach (1939) found that frequently additional lines not associated with f.c.c. lattice would appear below the phase transition, which would invariably be accompanied by a 1.6% increase in the lattice constants. Moreover, there are contradicting reports about the existence or absence of birefringence below the phase transition; birefringence would not exist if the crystal is f.c.c.. Thus, it is not at all clear whether or not there is a small change in the crystal structure on passing through the phase transition. In the discussion of the results this point will be referred to again.

Some interesting results have been obtained by Rosenshein et al. (1964) from ultrasonic attenuation and sound velocity measurements in CH_4. The velocity of sound exhibits an appreciable change at the upper phase transition. Moreover, there appears to be a maximum in the attenuation a few degrees above the upper phase transition; there is an interesting correspondence between this maximum and certain features in the spin lattice relaxation data of CH_4, which will be discussed in Chapter 5. No explanation of their results is provided by them.

Inelastic neutron scattering studies of CH_4 have been reported by Stiller and Hautecler (1962) and Dasannacharya et al. (1964); they arrive at the conclusion that hindered rotations are non-existent, and that the only motions of the molecules are librations, small angle oscillations about a certain axis.

CHAPTER 3.

EXPERIMENTAL METHOD AND APPARATUS

Relaxation Time Measurements 3:1

All relaxation time measurements reported in this thesis were carried out at 28.5 and 4.4 mcs using the pulse method developed by Hahn (1950). In this method, a radio frequency field is applied in the form of pulses; we are interested in the transient signals after the pulses. Under conditions previously discussed in the Introduction, the pulse rotates the magnetization of the spin system into the x-y plane; the equilibrium magnetization before the pulse is applied being along the z direction. The precession of the magnetization about the main magnetic field induces a transient signal, called the induction tail, in the coil around the sample oriented in the x-y plane.

As discussed earlier, the return of M_z to its equilibrium value M_o , is usually exponential and is described by the time constant T_1, the spin lattice relaxation time.

To measure T_1 one uses the fact that the amplitude of the induction tail, after a 90° pulse, is proportional to the value of M_z at the beginning of the pulse. One prepares the state of the spin system at $t = 0$, such that $M_z = 0$, by applying a 90° pulse. After a certain time τ, another 90° pulse is applied; the amplitude of the induction tail is a measure of the extent of the recovery of M_z towards its equilibrium value M_o after a time τ . This sequence is repeated many times with different

values of τ . Before repeating the sequence, the spin system has to be allowed to return to equilibrium; this implies one has to wait at least 5 T_1's, to incur an error of less than 1%. The spin-lattice relaxation time is obtained by plotting $\ln(M_o - M(\tau))$ as a function of τ, the slope of the straight line is $-1/T_1$.

An alternative method, which saves time when T_1 is long, involves the application of a train of 15 or more 90^o pulses with a separation between them greater than T_2, but much less than T_1. This prepares the spin system in a state with $M_z = 0$. As before, the application of a 90^o pulse will measure the recovery of M_z towards equilibrium; the procedure for obtaining T_1 is the same as above. Using this method it is not necessary to wait between successive sequences. The reproducibility of T_1 measurements is about 5% in these experiments.

Unlike T_1, the decay of $M_{x,y}$ is not exponential, but in general exhibits a very complicated time dependence. In the solid methanes, the local fields are almost always much larger than the magnetic field inhomogeneity over the sample; therefore no correction had to be applied to obtain the shape of the induction tail.

The Spectrometer 3:2

The apparatus used in pulsed nuclear magnetic resonance has been described in many articles (Hahn 1950, Clark 1964), consequently only the basic features will be described in this section. Each of the major constituents of the spectrometer,

as shown in the block diagram (Figure 2), will now be discussed in turn.

Timing Units 3:2:1

As described in the previous section, pulsed nuclear magnetic resonance (N.M.R.) measurements of spin-lattice or spin-spin relaxation times require pulse sequences consisting either of two radio frequency (r.f.) pulses (the two-pulse sequence), or of a train of r.f. pulses followed by a single r.f. pulse (the saturating train sequence). These two types of pulse sequences are shown in Figure (3). The separation and the number of pulses in the saturating train can be controlled. Further requirements are that the width and the position of the last pulse can be varied independently of the initial pulse or pulses. The electronic circuits used to provide timing pulses for the above pulse sequences and to provide gating pulses for the r.f. oscillator are completely standard (see Figure (3)) and are not shown here. It may be remarked, however, that the output pulses used to gate the oscillator stage have amplitudes of about 80 volts and rise and fall times of approximately 0.1 μsec.

Transmitter 3:2:2 (Figure (4))

The transmitter has to be capable of delivering very intense r.f. pulses, with rise and fall times approximately 0.2 μsec, into a low impedance load. No r.f. leakage can be tolerated between pulses. The simplest method to achieve this

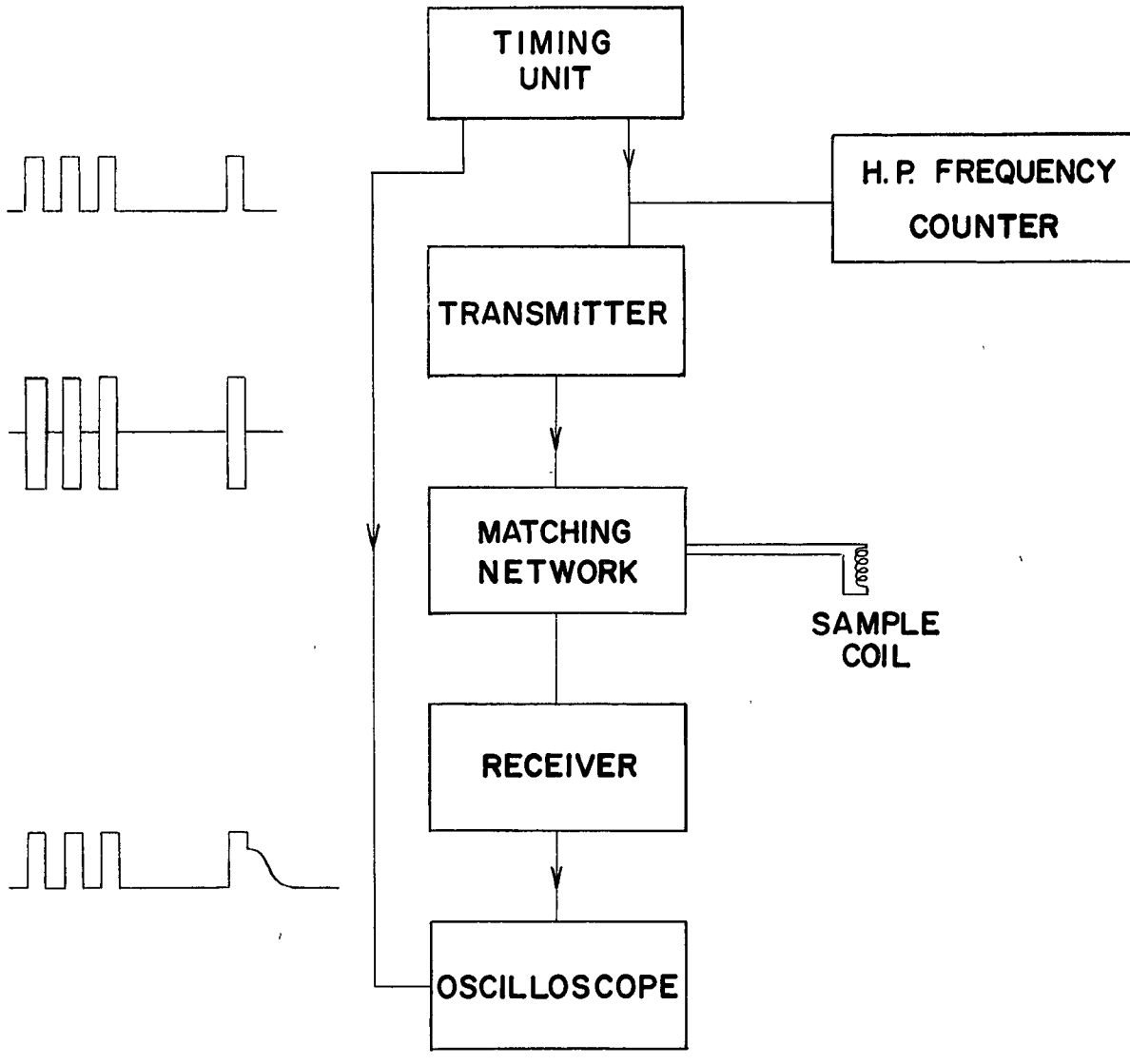

Figure 2. A Block Diagram of the Spectrometer

is to gate the oscillator. The tank circuit of the oscillator is situated in the cathode circuit of a gating tube. During the off cycle, the gating tube is biased on. A d.c. current flows through the coil and thus reduces the Q of the tank circuit so that it cannot oscillate. When a pulse, supplied by the timing unit, biases the gating tube off, the current through the tank circuit is suddenly switched off and the tank circuit rings at its resonant frequency. If there is sufficient feedback, it will oscillate for the duration of the gating pulse. The oscillator is an electron-coupled Hartley circuit to reduce the effects of variations in loading on the frequency.

The oscillator stage is followed by a class A amplifier and two class C amplifiers, all using 6L6 tubes. These stages were capacitance coupled with a tuned circuit in the grid of the next stage. This resulted in better power transfer at 30 mcs, than when transformer coupling was used. The final output stage consisted of an 829-B with both sections in parallel, which was capacitance coupled to an impedance matching network between the transmitter and the sample circuit. To achieve fast rise and fall times, the Q's of all tuned circuits must be quite low.

At 30 mcs, the peak to peak voltage across the sample coil was 1500 volts; at 4.5 mcs, it was 3500 volts.

Sample Circuit 3:2:3

As will be discussed in the Theory chapter, accurate line shapes are obtained only if the r.f. magnetic field is considerably larger than the local magnetic field due to

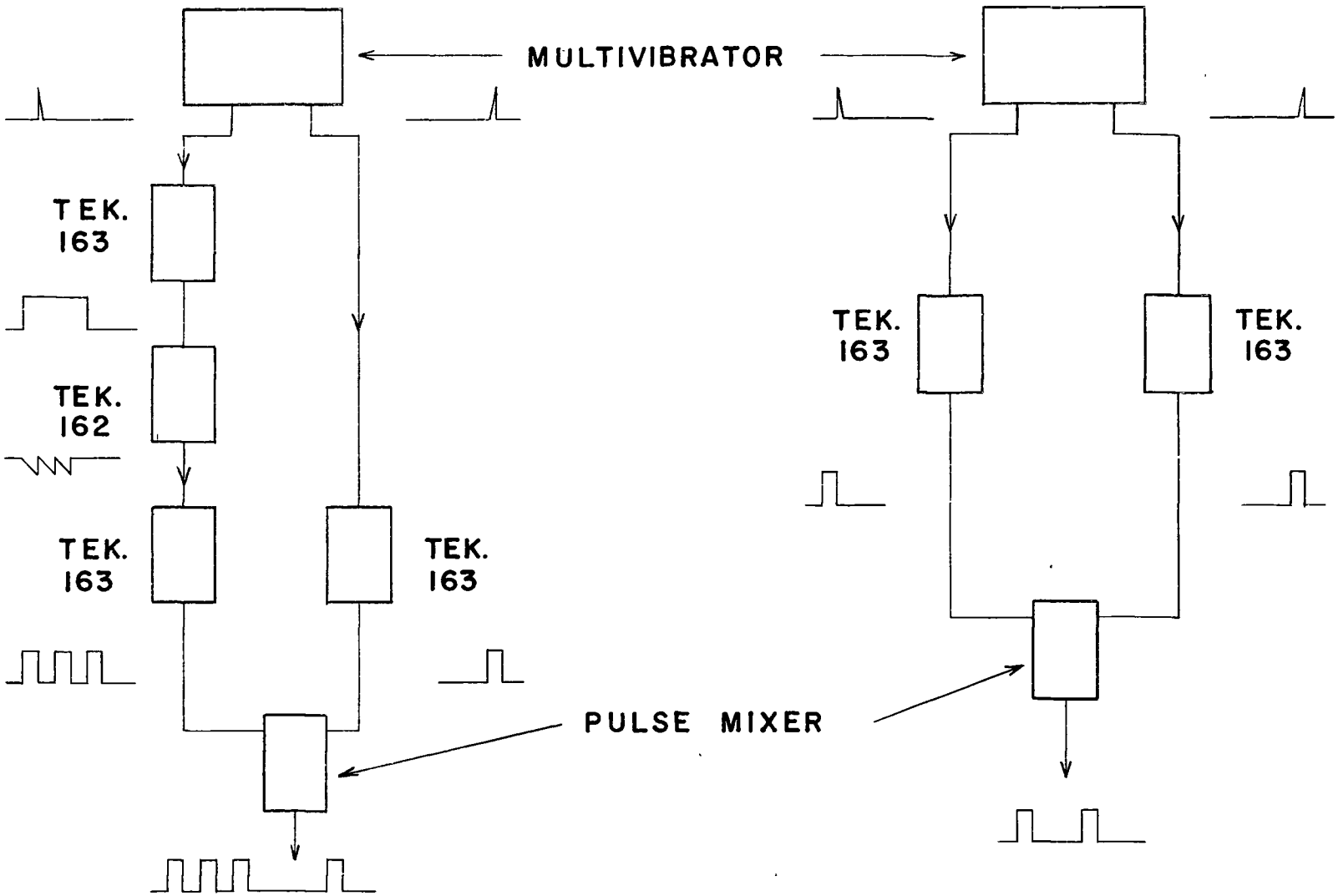

Figure 3. The Two Pulse Sequences Used

interactions of the spin with neighbouring spins. In order to accomplish this, care had to be taken in matching the sample circuit to the transmitter. The sample circuit is shown in Figure (5). The crossed diodes on the transmitter side served three purposes: (1) they increased the Q of the sample circuit, (2) they prevented transmitter noise from being fed into the receiver after the r.f. pulse, by decoupling the transmitter circuitry; (3) they improved the recovery time of the receiver by preventing any r.f. from entering the sample circuit, after the r.f. level in the pulse had dropped below $\frac{1}{2}$ volt.

The inner conductor of the transmission line consisted of silver plated stainless steel tubing, diameter (1/8"); the outer conductor, a $\frac{1}{2}$" stainless steel tube, served as the pumping line as well. These diameters were chosen such that the impedance of the transmission line was as close as possible to 90 ohms, the impedance of the coaxial cable used outside the dewar head. At 28.5 mcs, a half wave transmission line was used between the sample coil and the impedance matching network; at 4.4 mcs, this was eliminated, instead the transmitter and the receiver were placed as close as possible to the sample coil.

Since the r.f. voltages in the sample circuit were large, care had to be exercised to prevent electrical breakdown; in particular, the He exchange gas pressure had to be less than 10 μ.

Another troublesome effect, not noticed at 30 mcs, was large high frequency sinusoidal transients after an r.f.

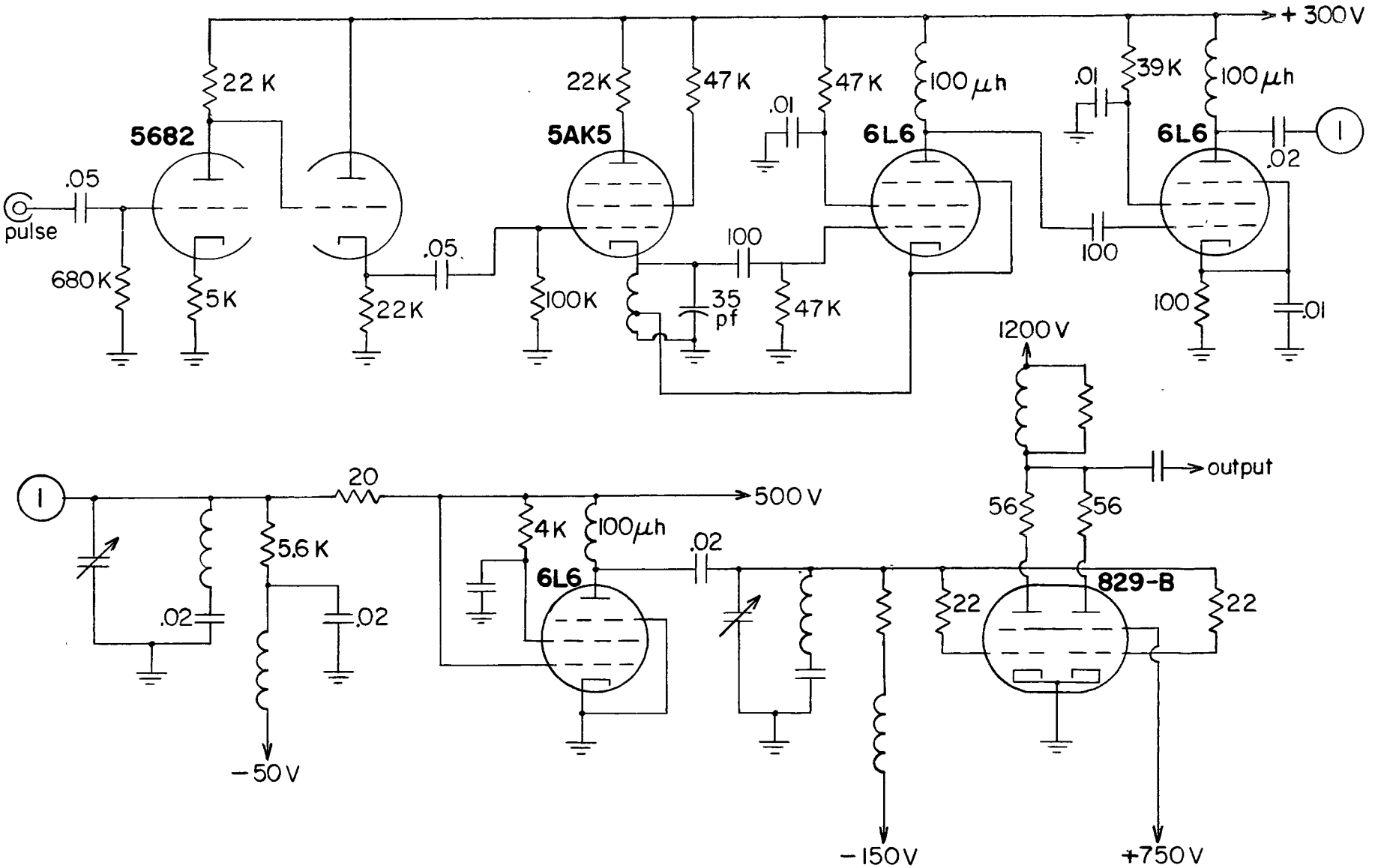

Figure 4. The Transmitter Circuit Diagram

pulse, which appeared only in the presence of the main magnetic field. Their amplitude and frequency could be altered drastically by potting or coating the coil with different substances, but they would usually reappear, if the coil was repeatedly cooled to 4.2°K or if the coating was cracked. We surmised that the interaction between the pulsed r.f. current, which may be 10-20 amps, and the main magnetic field excited some structural resonance in the coil at ultrasonic frequencies. These effects were not seen at 30 mcs because the r.f. currents were smaller, the inductance of the coil was less, and the structure was more rigid. The best potting agents were found to be liquid porcelain "Sauereisen" and "Stycast" epoxy.

Receivers 3:2:4

The single coil sample circuit, described above, suffers from the serious disadvantage of injecting a large r.f. pulse into the input stage of the receiver. For fast recovery, from the large r.f. pulse, which saturates the receiver, all tuned circuits and RC coupling networks must have short time constants. In particular, the last stage and the detector, which handle the maximum signal, must have very fast recovery. Paralysis, which is a temporary cut-off due to grid current being drawn during the pulse, can be avoided by making all grid and cathode circuit time constants short; this suffers from the slight disadvantage of lowering the gain per stage. Supply voltage recovery, if not guarded against, can seriously distort the output and lengthen the recovery time.

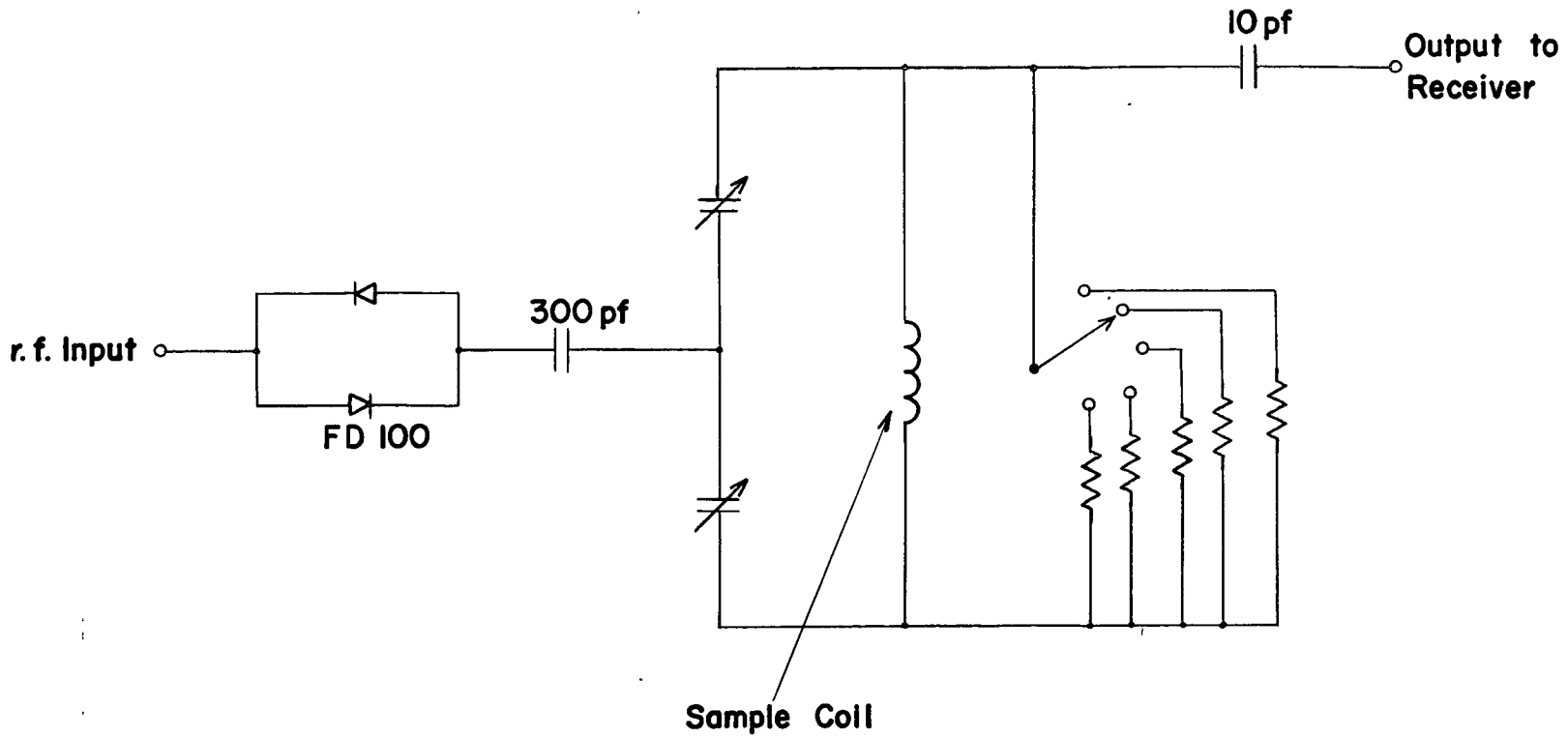

Figure 5. The Sample Circuit

The gain control bias supply, in particular, should have an output impedance of less than 2000 ohms.

The receiver used at 28.5 mcs, was an Arenberg Wide Band amplifier (WA600C). The preamp had a cascode input, two stages of narrow band amplification, and a cathode follower output. The main amplifier was wide band, 10-60 mcs. The overall amplifier had a 7 μs recovery time.

The 4.4 mcs receiver, which we constructed, had a 1 mcs band width and a 6μs recovery time,(see Figure (6)). The preamp, built according to Clark's design (1964), uses a high g_m pentode 7722 in the input with a very low equivalent noise resistance, (200 ohms); followed by a 6DJ8 amplifier and cathode follower stage. The main amplifier consisted of four synchronously tuned amplifying stages, a detector, and a low impedance output stage. The tuned r.f. stages consisted of 6AK5 pentodes, with the individual band widths of each stage being 1.5 mcs. To improve the recovery time of the receiver, pairs of crossed-diodes, FD 100, were used in the plate circuits of the first two amplifying stages.

The linearity of both amplifiers was checked carefully. It was found that the linearity correction was negligible. To keep the operating conditions the same at all times, despite a variation of 80 in the signal strength in the range from 1.2-80°K, we inserted a wide-band Hewlett Packard attenuator between the preamplifier and the main amplifier. This reduced the signal output, but not the signal-to-noise ratio.

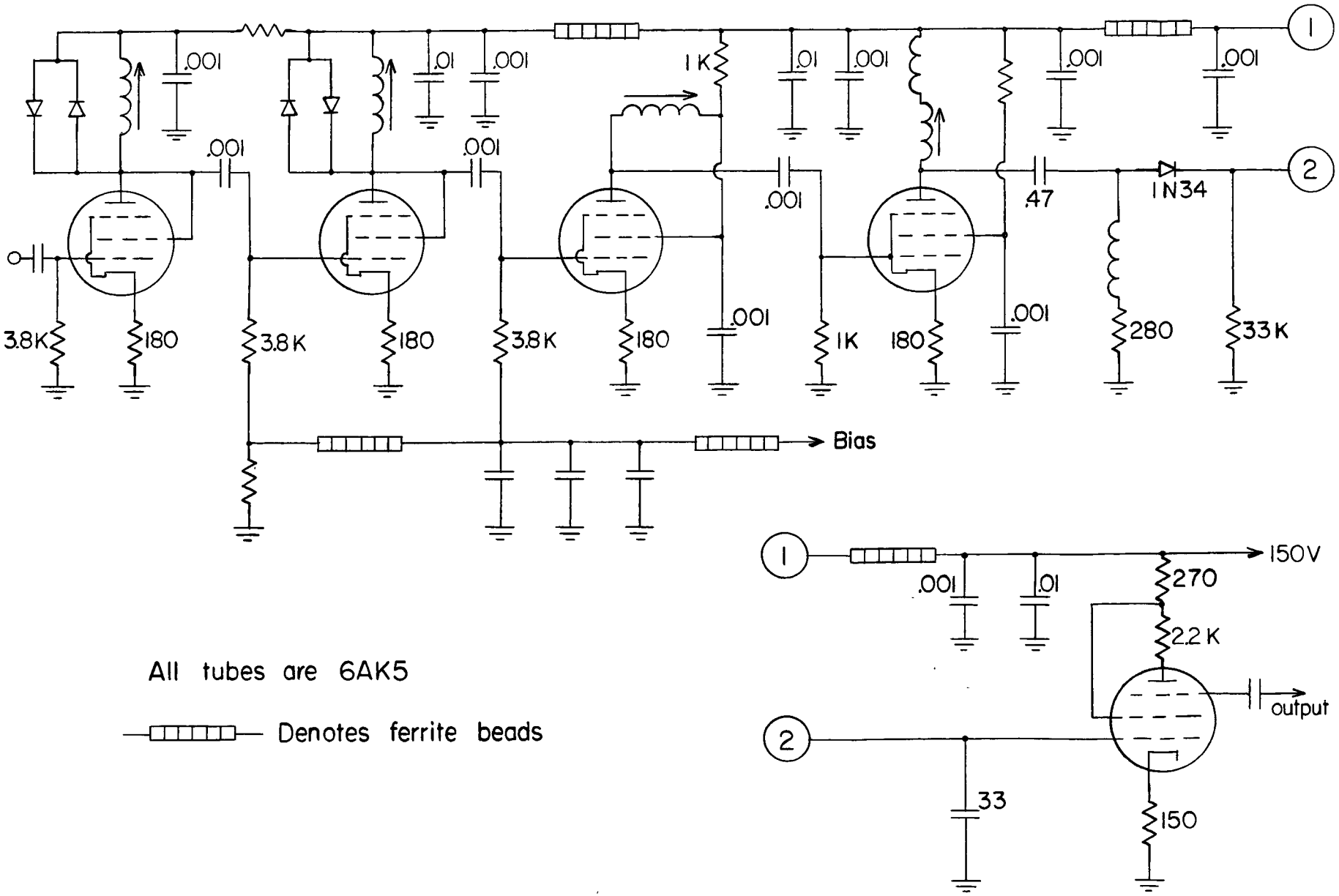

Figure 6. The 44 mcs. Receiver Circuit Diagram

Cryostat 3:3

The design of the cryostat resembles that of an adiabatic calorimeter, the main design criterion being the minimization of any heat leaks. The motivation is, however, different. In the case of the calorimeter, the purpose is to obtain the best possible accuracy; in our case, the aim is to reduce the temperature gradients in the sample and to decrease the helium boil-off rate. These considerations are important as the sample may be at any temperature between $4.2^{\circ}K$ and $50^{\circ}K$. After these introductory remarks, some of the details will be described in the following sections.

The Vacuum Can and the Dewar Head 3:3:1

Figures (7) and (8) show the construction of the dewar head and the vacuum can. The prime concern in the design was to keep the amount of metal to a minimum, so that the consumption of liquid helium was reduced. Only non-magnetic materials were used to keep the magnetic field as homogeneous as possible near the sample; this excludes certain types of stainless steel and brass.

The manifold, shown as A in Figure (7), allowed access to the inner conductor of the transmission line, which ran down the center of the pumping tube. The bottom end of the transmission line was anchored at $4.2^{\circ}K$, to eliminate any heat leak down it. The electrical leads for the thermometers and the heater were brought into the vacuum can using two

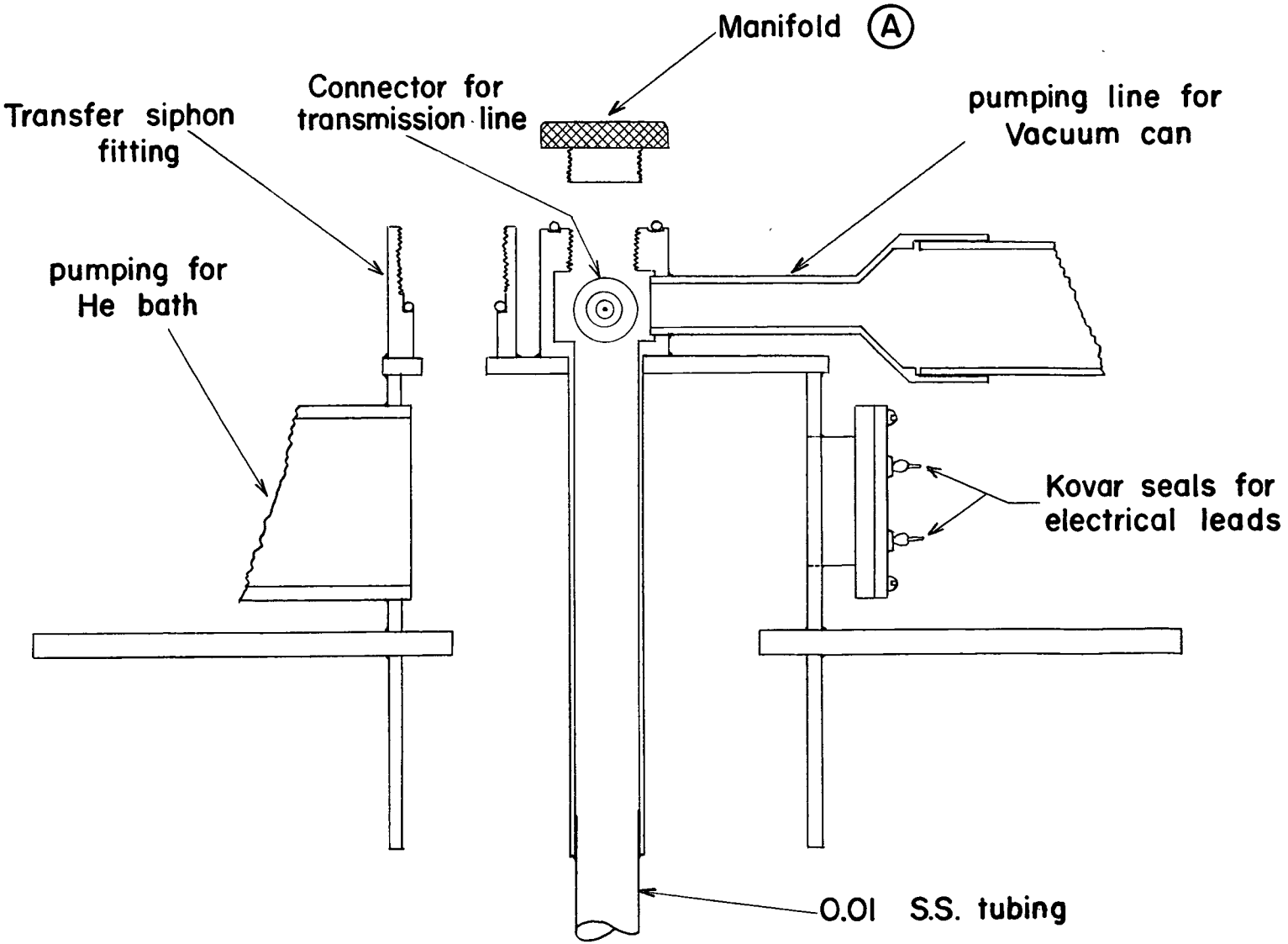

Figure 7. A Diagram of the Dewar Head

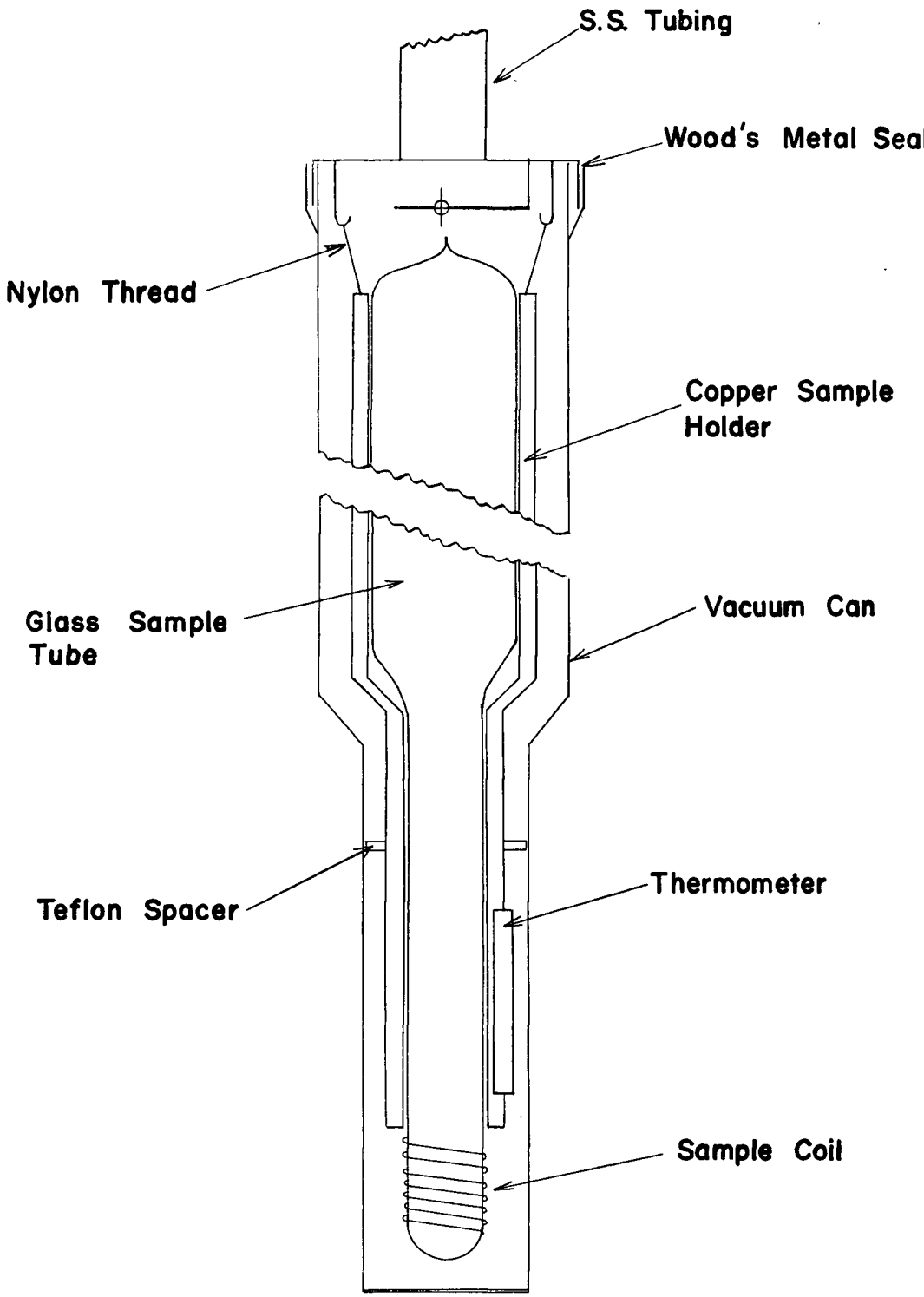

Figure 8. A Diagram Showing the Vacuum Can and Sample Holder

Housekeeper seals fitted with a pinch carrying five tungsten wires each.

The can was soldered to the flange using Woods metal; Indium and Teflon O-ring seals were found to be less reliable and involved the use of more metal. While soldering the flange, the tail end of the can was kept in liquid nitrogen. This condensed the methane in the sample tube, and thus reduced the danger of the sample exploding.

Only copper was used in the construction of the can, because it has a better thermal conductivity coefficient than brass, and it does not spoil the homogeneity of the magnetic field. However, in machining the wall thickness to 30 thousandths of an inch, it became porous to HeII and had to be coated with a thin layer of soft solder.

The Sample Holder 3:3:2

To reduce the temperature gradients, a sample holder was machined from a copper rod. The sample holder completely enclosed the sample, except for the tail end, around which the sample coil was situated. Good thermal contact between the sample holder and the sample was ensured by filling the space between them with Apiezon grease. To reduce heat leaks to a minimum, the sample holder was suspended by two nylon threads and held in place by a teflon spacer. In addition gauge 34 Magnanin wire was used for the thermometer leads, because it is a poor thermal conductor. The radiation baffle shown in

Figure (8), served to intercept any room temperature radiation down the pumping tube, and at the same time anchored the bottom end of the transmission line at 4.2°K.

Two copper tubes soldered into the sample holder served as the thermometer wells. The sample holder also provided a mounting for a 700 ohm Constantan heater, which was bifilar wound to eliminate any stray magnetic fields associated with the heater current. Thermal contact between the heater and the sample holder was provided by two coats of shellac. The heater was evenly spaced over the whole sample holder to avoid any hot spots. To obtain an efficient helium transfer, a helium exchange gas pressure of 3 cm was introduced into the vacuum can. It was found that a moderately fast pumping system was needed to isolate the sample from the bath within a reasonable length of time. Using a Hyvac 6 and an oil diffusion pump connected by a $1\frac{1}{2}$ inch pumping line to the dewar head, a useful vacuum of 0.1 μ or better was obtained after 30 minutes of pumping.

Temperature Measurement and Control 3:4

Temperature Measurement 3:4:1

Two thermometers were used to cover the range from 1.2-55°K, a 100 ohm Speer carbon thermometer Grade 1003, and a Hartman-Braun platinum thermometer model W 4871. The thermometers were fitted into the copper thermometer

wells with some Apiezon grease assuring good thermal contact. The platinum thermometer, which had been calibrated by the N.B.S., was used to measure temperatures above 20°K; the carbon thermometer was used below 20°K. This was necessary because the sensitivity of the platinum thermometer decreases very rapidly below 20°K; and that of the carbon thermometer becomes less sensitive above 25°K.

Calibration points for the carbon thermometer were obtained around 20°K, using the platinum thermometer, and around 4.2°K using the vapour pressure scale of He^4. These calibration points were then used to evaluate the constants A, B, and C in the equation:-

$$\log R + \frac{C}{\log R} = A + B/T$$

This is a semi-empirical relationship, which has been found to describe the temperature variations of the carbon resistance (Clement and Quinnell, 1952). Some of these calibration points were checked for every He run and it was found that changes in carbon resistance implied corrections of the order of 0.01%.

A comparison of the phase transition temperatures obtained from the spin-lattice relaxation time data with those obtained from specific heat measurements, provided a valuable check on the accuracy of the thermometry. Furthermore, the fact that the nuclear spin magnetization obeys the Curie Law, was also used to check relative temperatures of the sample between 4.2 and 15°K with an accuracy of about 3%.

From these checks, it was concluded that the thermometry was accurate to 0.1°K in the range below 10°K, and accurate to 0.2°K from 13°K to 20°K.

To assure ourselves that the magnetic field dependence of the thermometers did not affect our temperature measurements, we measured the resistances of both thermometers for a set of temperatures with the magnetic field on and off. We found that the correction was at the most 0.01°K.

A Rubicon Mueller bridge was used to measure the thermometer resistances, and a Brown null indicator was used for the null amplifier. A Mueller bridge will measure the resistance of a four lead thermometer in the presence of sizeable lead resistances. However, this bridge could only measure resistances up to 70 ohms; whereas the carbon resistance assumes values from 200-500 ohms in the temperature interval 20°K-1.2°K. At lower temperatures, the carbon resistance changes with temperature are fractionally very large. Consequently, a slight loss in accuracy and sensitivity could be tolerated. We therefore decided to extend the range of the Mueller bridge according to the circuit shown in Figure (9). A subsequent check of the sensitivity and the accuracy of the modified bridge, using some accurately measured standard resistances, showed that these were quite adequate.

In the measurement of the carbon resistance below 4.2°K, care had to be exercised to prevent self-heating of the thermometer, which would lead to erroneous temperature readings (Berman, 1952). Below the λ point a measuring current

through the resistor of 1 μamp was used; at 4.2°K and above a 10 μamp current was used. A 1 ma. current was used for the platinum thermometer. It should be noted that all the resistances were measured for both directions of current to eliminate any thermal E.M.F.'s.

An attempt was made to measure the temperature gradient along the sample holder at 20°K, using two calibrated carbon thermometers situated 10 cms. apart. The temperature difference was so small that we could assign only an upper limit of 0.02°K.

Temperature Control 3:4:2

In these experiments, it was imperative to control the temperature to better than 0.1°K over long periods of time at any desired temperature between 4.2 and 55°K. Consequently, we decided to use an electronic feed-back regulator.

The temperature control unit is shown in Figure (10). The sensing element used was either the carbon or the platinum thermometer. The input to the temperature control unit is supplied by the Brown null indicator, which is used here as a d.c. amplifier. As the output voltage of the Brown null indicator contained much 60 cycles/sec, the first stage of the control unit was a McFee difference amplifier to eliminate the 60 cps. component and to amplify the small d.c. component. The next two stages were cathode coupled d.c. amplifiers driving an output cathode follower, the

cathode load of which is the heater. The bias on the grid of the cathode follower determined the average current through the heater. Once the system started regulating the temperature, we were able to adjust the bias such that the mean position of the null indicator was zero.

At low temperatures, the gain of the system was too high and the whole system would oscillate. To remedy this, we just lowered the gain of the control unit until it stopped oscillating.

To measure the temperature, the average current through the heater was maintained, but it was not regulated for the duration of the measurement. The drift of the temperature during the measurement was insignificant.

Because of the high sensitivity, good electrical isolation between the heater and thermometer wiring was essential, otherwise the system would oscillate.

Sample Preparations 3:5

The proton and deuteron spin-lattice relaxation times in the liquid and in the solid methanes have been found to be very sensitive to small concentrations of O_2 in the sample. Since the O_2 molecule is highly paramagnetic, it provides a powerful mechanism for spin-lattice relaxation. As a consequence no information would have been obtained about the nature of the interactions between the methane molecules, if the O_2 impurities had not been removed.

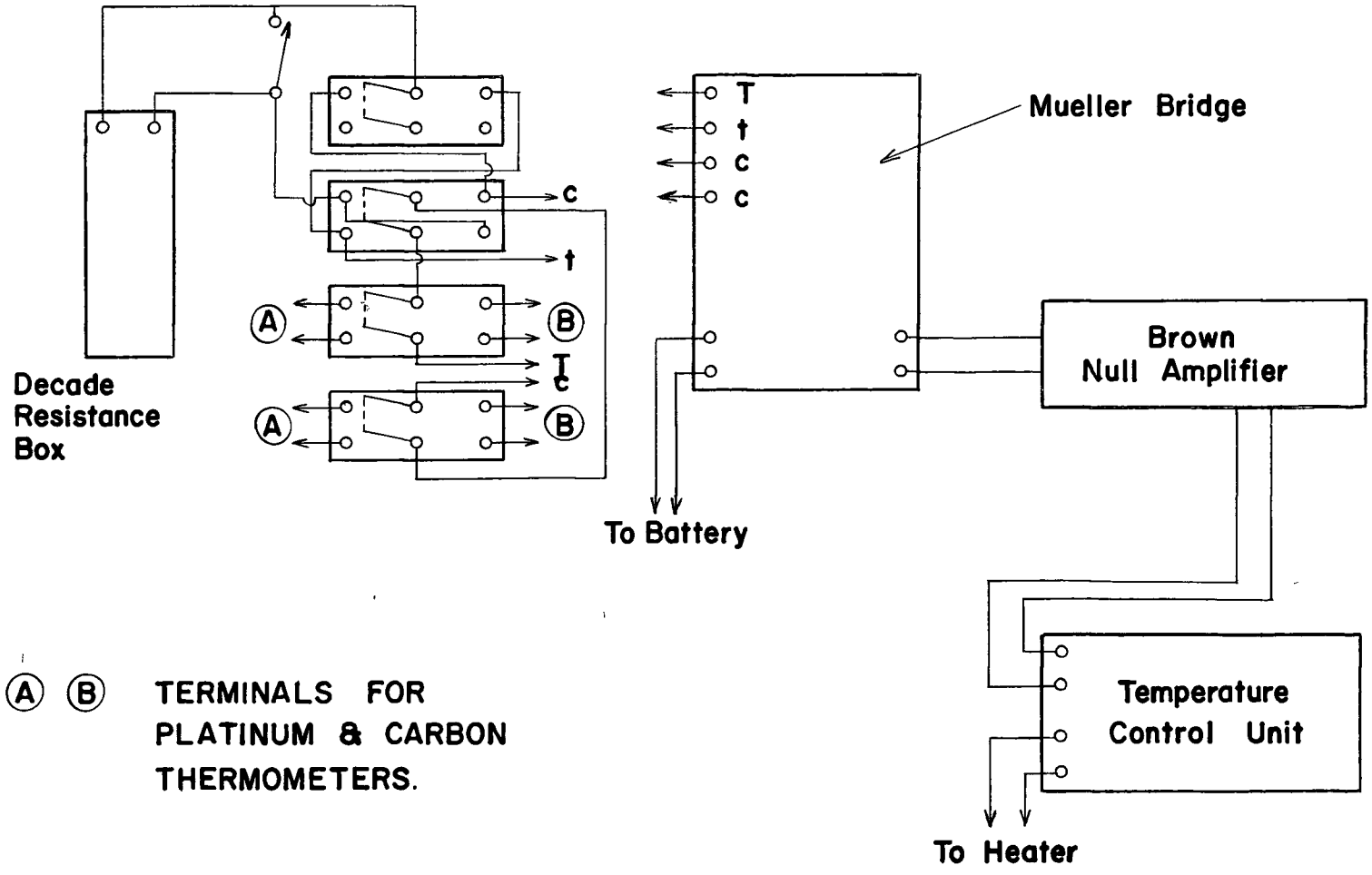

Figure 9. Schematic of the Temperature Regulator

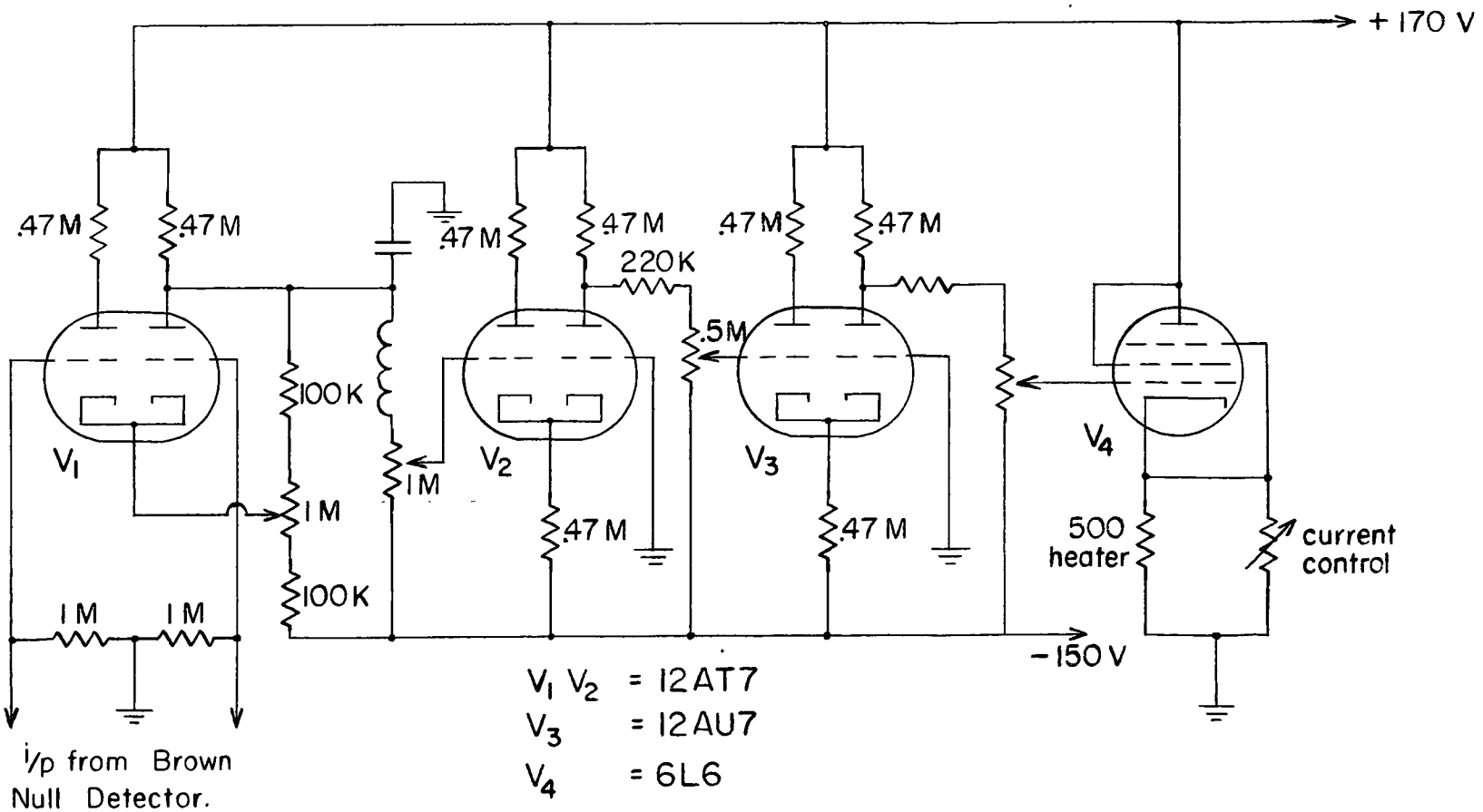

Figure 10. Circuit Diagram of the Temperature Control Unit

The technique found to be most suitable for the removal involved the use of a getter, Misch metal, supplied by Lindsay Chemical Co. The concentration is probably reduced below 2.5×10^{-4}% using this technique (Sandhu et al. 1960).

Two different geometries, shown in Figure (11), were used during the course of these experiments. For both geometries, the relaxation times agreed to within experimental error.

In geometry 'a', the tungsten coil shown in the diagram contains the Misch metal. The sample tube was evacuated to 10^{-6}cm and baked several times while pumping. When the flask had been baked out, it was filled with Argon to a pressure of 1 or 2 mmHg. The getter was then flashed until a diffuse layer was deposited on the inner surface of the flask. The argon was then pumped out, and the methane gas was introduced; the flask was then sealed off from the system.

The sample preparation was the same for geometry 'b', except that the gas was left in contact with the getter for several days, after which the methane was condensed into the sample tube using liquid nitrogen and was sealed off from the gettering bulb. At room temperature, the gas pressure in the sample tube was 25-30 atmospheres, whereas the average bursting pressure was measured to be 70 atmospheres. This geometry was used for most of the low temperature measurements because it meant that the cryostat design could be simplified, and that some of the heat leak and vacuum problems could be virtually eliminated. This particular geometry, however, introduced the

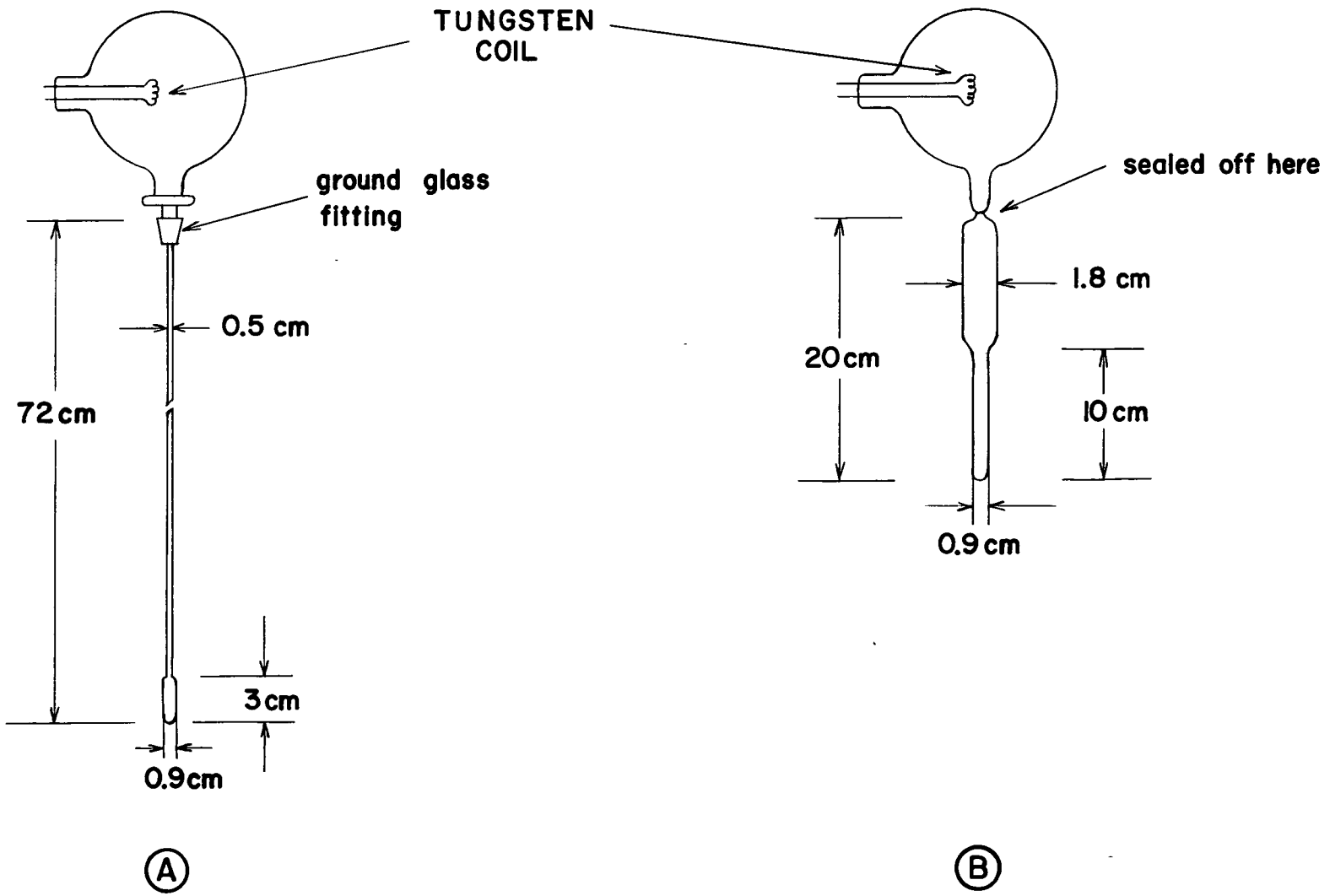

Figure 11. The Two Sample Geometrics Used

possibility of the sample exploding and of possible contamination of the sample by O_2 impurities due to the absence of the getter bulb. The spin-lattice relaxation times were reproducible from sample to sample and over long periods of time for each sample. These measurements were carried out over a period of more than a year and no change in T_1 with time for any sample was ever observed.

Mixtures of CH_4 with CD_4 or Kr were prepared by mixing appropriate amounts of the gases at room temperature. Estimates of CH_4 to CD_4 or to Kr ratios were made from the partial pressures, assuming the gases to be ideal.

CHAPTER 4.

THE THEORY OF RELAXATION

In Chapter 1, the spin-lattice relaxation was described as the exchange of energy between the spin system and the lattice, so that thermal equilibrium will be established between them. A detailed interpretation of the relaxation behaviour will be attempted in terms of the interactions between the nuclei and the degrees of freedom of the lattice.

Many papers have appeared in the literature on the theory of nuclear magnetic relaxation (Redfield 1957, Bloch 1956, Abragam 1961). Some of the gross features of the theory pertaining to the systems under consideration will be reviewed.

Conventional theory 4:1

The problem of calculating spin lattice relaxation times, in general, consists of evaluating the transition probabilities between spin-states due to interactions between the lattice and the spin system. The Hamiltonian describing the spin-lattice interactions for the systems under consideration is:

$$\mathcal{H}_S = \sum_{i<k}\sum_{m=-2}^{2} F^{(m)}(\Omega_{ik})\, A^{(m)}_{ik} + \sum_{i,k'}\sum_{m=-2}^{2} F^{(m)}(\Omega_{ik'})\, A^{(m)}_{ik'} + \sum_{i'<k'}\sum_{m=-2}^{2} F^{(m)}(\Omega_{i'k'})\, A^{(m)}_{i'k'}$$
$$\sum_{i} I_i \cdot \tilde{\tilde{C}} \cdot J + \sum_{i'} I_{i'} \cdot \tilde{\tilde{C}}' \cdot J \qquad (4\text{-}1)$$
$$\sum_{i'}\sum_{m} F^{(m)}(\Omega_{i'}) B^{(m)}_{i'}$$

The first three terms describe the magnetic dipole-dipole interactions between like and unlike nuclear spins. The primed (unprimed) symbols denote those quantities belonging to spins I, for example protons (to spins S, for example deuterons). Ω_{ik} is the direction of the vector $\bar{r}_{ik}$ between spins i and k.

$$
\begin{aligned}
F_{ik}^{0} &= \frac{1}{r_{ik}^{3}}\left(1-3\cos^{2}\theta_{ik}\right) &&= -2\sqrt{\frac{4\pi}{5}}\ \frac{Y_{20}}{r_{ik}^{3}} \\
F_{ik}^{\pm 1} &= \frac{1}{r_{ik}^{3}}\ \sin\theta_{ik}\cos\theta_{ik}\, e^{\pm i\phi_{ik}} &&= \mp\sqrt{\frac{8\pi}{15}}\ \frac{Y_{2\pm 1}}{r_{ik}^{3}} \\
F_{ik}^{\pm 2} &= \frac{1}{r_{ik}^{3}}\ \sin^{2}\theta_{ik}\, e^{\pm 2\phi_{ik}} &&= 4\sqrt{\frac{2\pi}{15}}\ \frac{Y_{2\pm 2}}{r_{ik}^{3}}
\end{aligned}
\qquad (4\text{-}2)
$$

$$
A_{ik}^{0} = -\frac{3}{2}\gamma_i\gamma_k\hbar^{2}\left[-\tfrac{2}{3}I_{zi}I_{zk} + \frac{1}{6}\left(I_{+i}I_{-k} + I_{-i}I_{+k}\right)\right]
$$

$$
A_{ik}^{\pm 1} = -\frac{3}{2}\gamma_i\gamma_k\hbar^{2}\left[I_{zi}I_{\pm k} + I_{\pm i}I_{zk}\right]
$$

$$
A_{ik}^{\pm 2} = -\frac{3}{4}\gamma_i\gamma_k\hbar^{2}\, I_{\pm i}I_{\pm k}
$$

where the $Y_{2m}(\theta,\phi)$ are normalized spherical harmonics.

The next two terms of the Hamiltonian describe the spin rotation interaction, the interaction between the nuclear spin and the current distribution associated with molecular rotation. $\overset{\approx}{C}$ and $\overset{\approx}{C}'$ are the spin-rotation interaction tensors for the two types of nuclei.

The last term is present when one of the types of nuclei has spin $I > \frac{1}{2}$; it describes the interaction between the quadrupole moment of the nucleus and the electric field gradients at the site of the nucleus due to the surrounding electronic and nuclear charges. The functions $F^{m}(\Omega_i)$ are the same as above, except now Ω_i specifies the orientation of the field gradient at the site of nucleus 'i' with respect to the laboratory frame, and

$$B_i^0 = 3I_{zi}^2 - I_i(I_i+1)$$

$$B_i^{\pm 1} = \frac{\sqrt{6}}{2}\left[I_{zi}I_{\pm i} + I_{\pm i}I_{zi}\right] \qquad (4\text{-}3)$$

$$B_i^{\pm 2} = \frac{\sqrt{6}}{2} I_{\pm i}^2$$

All of these contributions to $\mathcal{H}$ involve molecular parameters. As a consequence of those interactions between the molecules which cause the molecules to reorient, these molecular parameters will also be random functions of time. In the general theory of nuclear spin relaxation (Abragam p300), the relaxation probability due to random perturbations involve the Fourier transform of the "correlation function" of these parameters. The "correlation function" $G(\tau)$ of spherical harmonics of order 2, for example, is denoted by

$$G(\tau) = \left\langle Y_{2m}(\Omega_i(t))\; Y^*_{2m}(\Omega_i(t+\tau)) \right\rangle \qquad (4\text{-}4)$$

where $\langle\ \rangle$ signifies an ensemble average. $G(\tau)$ is a function of τ only if, as is generally true for an equilibrium ensemble, the correlation function is invariant under a change in the origin of time. The correlation function $G(\tau) \longrightarrow 0$ as $\tau \longrightarrow \infty$. If the correlation function is exponential, as is often the case, a characteristic time of the system, the correlation time, is defined by $G(\tau) = G(0)\ e^{-\tau/\tau_c}$. General properties of the Fourier spectrum (or "spectral density") $J(\omega)$ of $G(\tau)$ are that the shorter the correlation time, the broader the frequency spectrum; in the limit that $\tau_c \longrightarrow 0$ it approximates a "white spectrum". More

specifically, if the correlation function is exponential, then the spectral density is

$$J(\omega) = \frac{2\tau_c}{1 + \omega^2 \tau_c^2} \qquad (4\text{-}5)$$

and the Fourier component $J(\omega_o)$ attains its maximum amplitude when $\omega_0 \tau_c = 1$. As we shall see later, the fact that $J(\omega)$ goes through such a maximum gives rise to a characteristic minimum in the plot T_1 versus correlation time.

The theory of nuclear spin relaxation originally developed by Bloembergen, Purcell and Pound (B.P.P., 1948), expressed the spin-lattice relaxation process in terms of rate equations involving transition probabilities between nuclear spin states induced by the spin-lattice interactions. This theory was incapable of describing interactions in which the off-diagonal elements of the density matrix played an important role. A more general theory using the density matrix was developed by Redfield and by Wangness and Bloch (Abragam p276). Using this formalism and neglecting cross-correlations arising from the fact that as a molecule moves as a rigid body there is a correlation between the relative motions of various pairs of spins) i.e. assume $\langle Y_{2m}(\Omega_{ij}(t))\ Y_{2m}(\Omega_{k'l}(t+\tau))\rangle$ for $i,j,\neq k,l$, it can be shown that spin-lattice relaxation due to dipolar interactions can be described by a single exponential and the expression for T_1 and T_2 due to interactions between like spins are:

$$\frac{1}{T_1} = \frac{3}{2}\gamma^4\hbar^2 I(I+1)\sum_k{}'\left[J_{ik}^{(1)}(\omega_I) + J_{ik}^{(2)}(2\omega_I)\right]$$
$$\frac{1}{T_2} = \gamma^4\hbar^2 I(I+1)\sum_k{}'\left[\frac{3}{8}J_{ik}^{(2)}(2\omega_I) + \frac{15}{4}J_{ik}^{(1)}(\omega_I) + \frac{3}{8}J_{ik}^{(0)}(0)\right] \qquad (4\text{-}6)$$

A similar expression has been derived for T_1 in the case of dipolar interactions between unlike spins. For a nucleus with spin I = 1 and non-zero quadrupole moment, the quadrupole interaction with an axially symmetric field gradient gives rise to a spin-lattice relaxation time

$$\frac{1}{T_1} = \frac{3}{80}\left(\frac{eQ}{\hbar}\frac{\partial^2 V}{\partial z^2}\right)^2 \left[J^1(\omega_0) + J^2(2\omega_0)\right] \qquad (4\text{-}7)$$

In the theory leading to the above results, it has been explicitly assumed (Redfield, 1957), that

$$\left[\langle H_1^2\rangle \tau_c^2\right]^{1/2} << 1 \qquad (4\text{-}7a)$$

and that $\langle H_1 \rangle = 0$, where H_1 is the perturbation causing relaxation. This assumption is essentially a statement of the fact that the fractional change in the populations has to be small during the time of interest (τ_c) otherwise one does not get simple time-independent rate processes.

The above theory, which essentially treats the lattice classically, suffers from the defect that the spin system relaxes to a steady state described by an infinite temperature. It can be shown that a quantum mechanical description of the lattice will lead to a finite T for the spin system equal to that of the lattice. This result can readily be understood, if one remembers that the lattice is assumed to have infinite heat capacity, i.e. at all times remains in thermal equilibrium, consequently the transition probability will be weighted by the Boltzman factors and will tend to bring the spin system into thermal equilibrium with the lattice. The quantum mechanical description of the lattice becomes

necessary at low temperatures when only a small number of degrees of freedom of the lattice are excited; this will become apparent when we consider a Quantum Mechanical model in Chapter 6.

In the Hamiltonian described earlier, no distinction was made between interactions originating within the molecule (intramolecular interactions), or outside the molecule (intermolecular interactions).

$$\mathcal{H} = \mathcal{H}_{\text{intra}} + \mathcal{H}_{\text{inter}} \tag{4-8}$$

For example, in a molecular solid the contribution to the electric field gradient at the site of a nucleus due to neighbouring molecules is negligible in comparison with that due to charges associated with the molecule on which the nucleus is situated. For the quadrupolar interactions, therefore, the only molecular parameters entering into the Hamiltonian of Equation (4-1) will be the angles of the electric field gradient with respect to the laboratory frame. In actual fact, the deuteron spin-lattice relaxation is dominated by the quadrupolar interactions, the dipolar interactions being much weaker (deWit and Bloom, 1965). The deuteron spin-lattice relaxation gives information about the correlation function of $Y_2(\Omega)$.

The dipolar interactions are both intra- and inter-molecular in origin. The intra-molecular dipolar interactions average to zero under rotations of the molecule. The correlation times for these reorientations are

sufficiently short at all the experimental temperatures so that the assumptions (4-7a) are satisfied and T_1 and T_2 can be evaluated using equations (4-6).

The inter-molecular dipolar interactions are more complicated because the interaction strength between the molecules is determined by the relative spatial locations of the molecules as well as the orientations. Because of this fact, they do not average to zero under rotations alone. Consequently, the spectral density is in general a function of two correlation times, one associated with molecular reorientation and the other with translational motion. If it is assumed that the correlation time for reorientations is much shorter than the correlation time for translational motions, then H_{inter} can be written as (Abragam, p453),

$$\mathcal{H}_{inter} = \left[\mathcal{H}_1 - \langle \mathcal{H}_1 \rangle_{\Omega_1,\Omega_2}\right] + \langle \mathcal{H}_1 \rangle_{\Omega_1,\Omega_2}$$
$$= \mathcal{H}_r + \mathcal{H}_t$$

where $\langle\ \rangle_{\Omega_1,\Omega_2}$ represents an average over all orientations Ω_1 and Ω_2 of each of the molecules. H_r is time dependent primarily through reorientations of the molecule and H_t depends only on the relative positions of the molecules so that its time dependence is due to translational motions only. Now the correlation function for H_{inter} is

$$\langle \mathcal{H}_{inter}(t)\, \mathcal{H}_{inter}(t+\tau) \rangle = \langle \mathcal{H}_r(t)\, \mathcal{H}_r(t+\tau) \rangle + \langle \mathcal{H}_t(t)\, \mathcal{H}_t(t+\tau) \rangle$$
$$+ \langle \mathcal{H}_r(t)\, \mathcal{H}_t(t+\tau) \rangle + \langle \mathcal{H}_t(t)\, \mathcal{H}_r(t+\tau) \rangle$$

The last two terms average to zero, if the translational and the rotational motions of the molecules are uncorrelated.

Thus, the spectral density of H_{inter} is easily seen to be the sum of two terms--the spectral density of H_r involving the rotational correlation time, and the spectral density of H_t involving the correlation time for translational diffusion,

$$\text{i.e.} \quad J_{inter}(\omega) = J_r(\omega) + J_t(\omega) \quad .$$

If the correlation times are sufficiently short to satisfy the assumptions (4-7a), then T_1 and T_2 can be calculated using equations (4-6).

When the correlation time for diffusion is long, the spectral density $J_r(\omega_o)$ is small and the contribution to T_1 is negligible. This is the case below 65°K, where self-diffusion is virtually non-existent, i.e. a truly rigid lattice. The spin-lattice time measurements in mixtures of CH_4 and CD_4 (deWit and Bloom, 1965), and experimental results to be discussed in Chapter 5, showed clearly that those interactions causing relaxation below 65°K are intra-molecular. In other words, the contributions of H_r and H_t to T_1 are both negligible. This result is in agreement with some theoretical predictions by Hubbard (1963), regarding the influence of intermolecular interactions on spin-lattice relaxation.

What effect do these interactions have on the spin-spin relaxation? The contribution to T_2 due to H_r is small, since it is equal to the contribution to T_1 due to H_r. Here, use is made of the fact that $T_1 = T_2$ when $\omega_o \tau_c << 1$. The contribution due to H_t below 65°K is much larger than that due to H_r. It can not be calculated using equation (4-6) because the assumptions (4-7a) are violated, the correlation

time for diffusion τ_o being too long, i.e. $\omega_o \tau_o >> 1$. Van Vleck's moment analyses has to be used and it will be discussed in section 4:3. For $\omega_o \tau_o >> 1$, the contribution of H_t to the line shape is temperature independent. Thus, the entire dependence of the line shape on τ_c is due to the small contribution H_r. This explains why our measurements of spin-lattice relaxation are more sensitive to changes in τ_c than Wolf's (1963) measurements of spin-spin relaxation.

In summary, only the intra-molecular interactions cause appreciable spin-lattice relaxation. One can thus think of nuclear spin-lattice relaxation in methane as a two-step process, as shown in Figure (12): first step, the electric interactions between a molecule and its neighbours cause it to re-orient; second step, the time dependence of intra-molecular interactions due to molecular reorientations causes the spins to relax by exchanging energy with the molecular degrees of freedom. Both the intramolecular dipolar and the quadrupolar interactions involve second order spherical harmonics. Consequently, these interactions are described by the same correlation functions: these correlation functions will be discussed in the next section.

Classical Theory of Molecular Reorientations 4:2

In general, one can define the reduced correlation function $g_\ell(\tau)$ for the spherical harmonics of order ℓ in terms of the correlation function $G_\ell(\tau)$

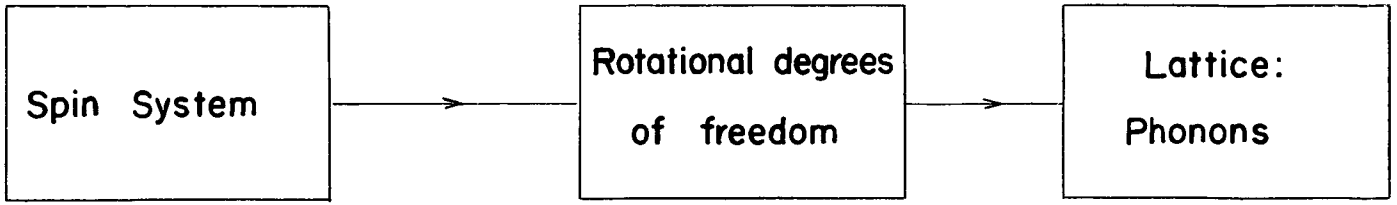

Figure 12. Illustration of the Idea that Relaxation is a Two Step Process

$$G_\ell(\tau) = \langle | Y_{\ell m} \Omega_i(t)|^2 \rangle g_\ell(\tau) = \frac{1}{4\pi} g_\ell(\tau) \qquad (4\text{-}9)$$

Ivanov (1964) has shown that for a general rotational random walk with no restrictions on the size of the individual angular steps, an exponential correlation function is obtained. The rotational diffusion equations of the Debye model (BPP, 1948) is obtained in the limit of small angular steps. The Debye model is widely used by experimentalists in the field of NMR to interpret their experimental data, although there exists some doubt as to the validity of the rotational diffusion equation when applied to molecules in situations such as are encountered in solid methane. The existence of an exponential correlation function enables one to calculate some sort of characteristic time τ_c directly from the experimental measurements of T_1.

Hubbard (1961), using the rotational diffusion equation, calculated the influence of cross-correlations on the spin-lattice relaxation of CH_4. He found that the spin lattice relaxation was governed by three exponentials for all values of $\omega_o \tau_c$, but that one exponential was dominant, and that within the presently available experimental techniques one should observe only one time constant equal to that calculated, neglecting cross correlations.

The spectral densities for eqn. (4-6) are of the form

$$J^{(1)}(\omega) = \frac{4}{15} \frac{1}{b^6} \frac{\tau_c}{1 + \omega^2 \tau_c^2} \qquad (4\text{-}10)$$

$$J^{(0)}(\omega) : J^{(1)}(\omega) : J^{(2)}(\omega) = 6 : 1 : 4$$

For the intramolecular dipolar interaction we obtain using eqn. (4-6)

$$\frac{1}{T_1} = \frac{6}{5}\frac{\gamma^4\hbar^2 I(I+1)}{b^6}\left[\frac{\tau_c}{1+(\omega_0\tau_c)^2} + \frac{4\tau_c}{1+(2\omega_0\tau_c)^2}\right] \qquad (4\text{-}11)$$

Figure (15) is a plot of T_1 versus according to eqn. (4-11). The minimum value of T_1 occurs at $\omega_0\tau_c = 0.62$ and the expression for $(T_1)_{min}$ is

$$\left(\frac{1}{T_1}\right)_{min} = \frac{.95}{\omega_0}\langle\Delta H^2\rangle = 8\text{ms. for } CH_4 \text{ for } \omega_0 = 2\pi\times 28.5\times 10^6$$

where ω_0 is Larmor frequency of the nuclear spins and $\langle\Delta H^2\rangle$ is the mean square average of the magnetic field at the site of a nuclear spin due to the dipolar interactions with the other spins on the same molecule, i.e. the effective strength of the interaction giving rise to relaxation. Similarly, the expression for T_1 due to quadrupolar relaxation also involves the correlation functions of the spherical harmonics $Y_{2m}(\Omega)$. For spins I = 1 and axially symmetric field gradients, such as is the case for CD_4, the expression for T_1 is:

$$\frac{1}{T_1} = \frac{3}{80}\left[\frac{eQ}{\hbar}\frac{\partial^2 V}{\partial z^2}\right]^2\left[\frac{\tau_c}{1+(\omega_0\tau_c)^2} + \frac{4\tau_c}{1+(2\omega_0\tau_c)^2}\right] \qquad (4\text{-}12)$$

An approximate value for $(T_1)_{min}$ is obtained using C. H. Anderson molecular beam measurement of the quadrupole coupling constant.

$$\frac{eQ}{\hbar}\frac{\partial^2 V}{\partial z^2} = 100\text{ kc.} \pm 50\%$$

and

$$\left(\frac{1}{T_1}\right)_{min.} = 8.0\ {}^{+\ (11.1)}_{-\ (6.0)}\ \text{millisec.}$$

The important feature to be noted is that if the correlation functions are exponential, then the value of T_1 at the minimum determines the strength of the interaction causing the relaxation of the spin system; no adjustable parameters are involved. Yet, the value calculated for CH_4 is a factor of 20 smaller than the experimental value; for CD_4, the experimental value of 8.5ms. agrees reasonably well with the value calculated above.

This discrepancy will occupy our attention for the remainder of this thesis; we will discuss the shortcomings of the conventional theory in dealing with a Quantum Mechanical system like CH_4 at low temperatures.

If one included any other interactions, like the spin rotation interactions, the theoretical T_1 would become even shorter. The spin rotation interaction is usually assumed to be non-existent in the solid and the dense liquid states. This is a consequence of the crystalline electric fields present at the molecular sites. These are said to quench the molecular angular momentum i.e. $\langle \bar{J} \rangle = 0$ just as is encountered in crystal field theory of paramagnetic resonance. It might be worth mentioning that the spin-rotation would be strictly additive to the dipolar or quadrupolar contributions, because any cross terms would be zero, as they have different transformation properties.

As yet, a theory predicting the correlation time of molecular reorientations in terms of the intermolecular forces, the collective motions in the solid and the wave

functions of the molecule in the solid, is non-existant. Below the phase transitions probably, the only correct procedure would be to derive the normal modes of the many body problem; as a λ -singularity in the specific heat usually signifies a co-operative transition.

The crystalline electric field, which arises from anisotropic intermolecular forces, is sometimes used to calculate single molecule wave functions and energy levels in solids. Modulation of the anisotropic interactions by phonons can cause transitions between these states. These intermolecular forces are all due to electric interactions between the charge distributions of the various molecules. Examples are the anisotropic interactions between the octupole moments of the charge distribution, and the Van der Waals dispersion forces, which contribute both to the isotropic and anisotropic intermolecular forces.

Line Shape 4:3

As was mentioned at the end of section 4:1, the line shape is dominated by the time-averaged intermolecular dipolar interactions, $\langle H_{inter} \rangle$. The problem of calculating the line shape due to these interactions is the same as the usual line shape problem in which magnetic dipoles are situated in the lattice sites of a rigid lattice. Van Vleck (Abragam p108) has derived general expressions for the moments of the line shape for this type of problem. It is generally found

that the rigid lattice absorption line shape for a non-metal resembles a Gaussian line, but the values of the fourth and higher moments indicate that it is squarer than a Gaussian. The experimentally observed induction tail is shown in Figure (13).

A rigorous theorem can be derived showing that the time evolution of the free induction tail is described by the Fourier transform of the absorption line shape. For this theorem to be valid, the r.f. magnetic field during the pulse has to be much larger than the local field. This condition is satisfied if the width of the $\pi/2$ pulse is much less than T_2. It follows from the above theorem that the induction tail can be expressed in the following form,

$$G(t) = \sum_{n} M_n \frac{t^n}{n!} \qquad (4\text{-}13)$$

where M_n is the n^{th} moment of the absorption line shape

$$M_n = \int_{-\infty}^{\infty} f(\omega - \omega_0)(\omega - \omega_0)^n \, d\omega$$

As the expression (4-13) converges rather slowly, the semi-empirical analytic expression

$$F(t) = \exp\left(\frac{-a^2 t^2}{2}\right) \frac{\sin bt}{bt} \qquad (4\text{-}14)$$

has been employed in several instances and found to provide a remarkable fit of the data. Once the parameters 'a' and 'b' in F(t) have been obtained by fitting it to the experimental induction tail, the moments of the line are given by

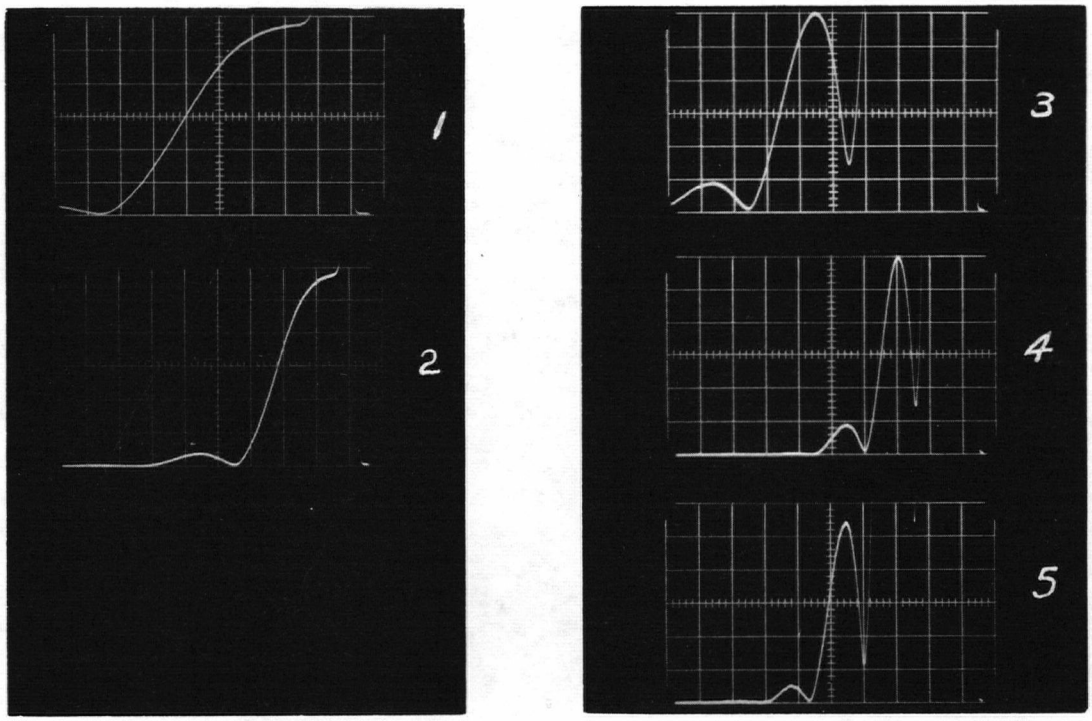

Figure 13. Photographs Showing a Typical Induction Tail for CH_4 at 1.2°K

(1) sweep 5 μsec/cm.

(2) sweep 10 μsec/cm.

(3) sweep 10 μsec/cm; increased gain by factor of 15.

(4) sweep 20 μsec/cm; same gain as (3)

(5) sweep 20 μsec/cm; increased gain by factor of 6.

$$M_2 = a^2 + \frac{1}{3} b^2$$

$$M_4 = 3a^4 + 2a^2b^2 + \frac{1}{5} b^4$$

$$M_6 = 15a^6 + 15a^4b^2 + 3a^2 b^4 + \frac{1}{7} b^6$$

One method for evaluating 'a' and 'b' from the experimental data is as follows. As is easily verified from equation (4-14), the induction tail is zero whenever $bt_n = \pi n$ where n is an integer. Thus, by measuring the times t_n, where the zeros occur in the induction tail, one can evaluate 'b'. The maxima between the zeros occur at times t_k given by

$$\left[\frac{d\ F(t)}{d\ t}\right]_{t=t_k} = 0$$

Using this condition, the following relationship is obtained.

$$a^2 = \frac{b}{t_k} \cot b\, t_k - \frac{1}{t_k^2}$$

Caution should be exercised to check that the expression (4-14) using the experimentally evaluated parameters 'a' and 'b' does indeed fit the complete experimental induction tail.

In the next chapter, we will review the experimental results and point out the discrepancies in view of the conventional theory. In Chapter 6, we will propose a model and discuss possible extensions of the conventional theory to cope with these discrepancies.

CHAPTER 5.

THE EXPERIMENTAL RESULTS

The results of the conventional theory quoted in the previous chapter will now be used to analyze the experimental results. There it was observed that the nuclear spin-lattice relaxation time depends on the strength of the spin-lattice interaction, and the correlation time describing the random character of the interactions. Thus, under appropriate assumptions, the temperature dependence of the correlation time can be extracted from the data. The next and rather difficult task is the explanation of the temperature dependence of the correlation time. A model which partially explains the temperature dependence and other features of the data will be presentedin the next chapter. Some of the discrepancies between the experimental results and the predictions from conventional theory, which will become apparent in this chapter, will also be discussed there.

Certain similarities between the various sets of data are evident, and will now be summarized to aid in the discussion of the individual sets of data. The spin-lattice relaxation time varies slowly with temperature above $30^{o}K$. This slow temperature dependence is in agreement with the earlier experimental results between $55\text{-}110^{o}K$ (de Wit and Bloom, 1965). In contrast, the temperature dependence below the upper phase transition temperature is

very strong. The spin-lattice relaxation time usually decreases by two or three orders of magnitude in this region. All but one of the curves of T_1 versus T go through a minimum. The increase in the spin-lattice relaxation time on the low temperature side of the minimum is usually less than a factor of 10; except in three cases where this increase is rather more spectacular. At the lowest obtainable temperatures (1.2°K), the temperature dependence of T_1 generally becomes much weaker. The temperatures at which the λ-anomalies in the specific heat occur are evident in the spin-lattice relaxation time data in many cases, either as changes in the slope or as discontinuities in the T_1 versus T curve. Now, the experimental results will be presented.

Coupled Spin Systems: 5:1

A discussion of CD_3H and CH_3D should be prefaced by a discussion of the nature of the relaxation when a nucleus, besides interacting with identical neighbouring nuclei having spins I, also interacts with neighbouring unlike nuclei having spins S. Because the splitting of the nuclear Zeeman levels is quite different for the two types of nuclei, the expressions for the relaxation of one type of nucleus as a result of interactions with the other type of nucleus are quite different from the expressions for interactions between nuclei of the same type. As a matter of fact, the

time dependence of the z-component of magnetization of the spin system S, S_z, will be a function of $I_z - I_o$ as well as of $S_z - S_o$, where I_o and S_o are the equilibrium magnetizations. The time dependence is described by a set of coupled differential equations, as given by Abragam p295.

$$\frac{dx}{dt} = -Ax - A'y$$

$$\frac{dy}{dt} = -B'x - By \qquad (5\text{-}1)$$

where $x = I_z - I_o$

$y = S_z - S_o$

where the A's and the B's are relaxation rates and will be explicitly written in the next paragraph. The solutions of these equations are

$$x = \frac{a}{(\lambda_1 - \lambda_2)}\left[-(\lambda_2 + A)\, e^{\lambda_1 t} + (\lambda_1 + A)\, e^{\lambda_2 t}\right]$$

$$y = -\frac{a(\lambda_1 + A)(\lambda_2 + A)}{(\lambda_1 - \lambda_2)A}\left[e^{\lambda_1 t} - e^{+\lambda_2 t}\right] \qquad (5\text{-}2)$$

$$\text{where} \quad \lambda_1, \lambda_2 = \frac{-(A+B) \pm \sqrt{(A-B)^2 + 4A'B'}}{2}$$

The solutions of equations (5-1) were obtained under the initial conditions that at t = 0, x = a, and y = 0. In other words, that the spin system I has been disturbed from thermal equilibrium $I_z \neq I_o$, by an r.f. pulse for example; but the spin system S has not been disturbed and thus the z-component of magnetization is still $S_z = S_o$. This set of initial conditions applies to all the experiments reported

here; r.f. pulses are applied only at the Larmor frequency of one of the spin systems. The above expressions will be used to determine to what extent cross relaxation effects influence the relaxation of a particular spin system.

Now the expression for the A's and B's will be given. The expression for A and B involve two contributions; that due to relaxation by like spins which is given by equations (4-6) and (4-7) and that due to coupling between unlike spins. The contributions due to like spins will be denoted by $1/T_1{}^I$ and $1/T_1{}^S$ for the I and S spin systems, respectively.

$$A = \frac{1}{T_1{}^I} + \gamma_I^2\gamma_S^2\hbar^2 S(S+1)\sum\left[\frac{1}{12}J^{(0)}(\omega_I-\omega_S) + \frac{3}{2}J^{(1)}(\omega_I) + \frac{3}{4}J^{(2)}(\omega_I+\omega_S)\right]$$

$$A' = \gamma_I^2\gamma_S^2\hbar^2 I(I+1)\sum\left[-\frac{1}{12}J^{(0)}(\omega_I-\omega_S) + \frac{3}{4}J^{(2)}(\omega_I+\omega_S)\right] \qquad (5\text{-}3)$$

$$B = \frac{1}{T_1{}^S} + \gamma_I^2\gamma_S^2\hbar^2 I(I+1)\sum\left[\frac{1}{12}J^{(0)}(\omega_S-\omega_I) + \frac{3}{2}J^{(1)}(\omega_S) + \frac{3}{4}J^{(2)}(\omega_S+\omega_I)\right]$$

where B' and $1/T_1{}^{SS}$ are the corresponding expressions given above with the I and S interchanged.

CH_3D: 5:2

The proton relaxation data for CH_3D at 28.5mcs., shown in Figure (14), exhibit the general features outlined above. The reason for discussing CH_3D first is that the breaks in T_1, occurring at both phase transition temperatures in CH_3D

are the most pronounced of those for all the systems studied. It has been previously inferred from entropy measurements (Collwell, Gill and Morrison, 1965) that these phase transitions have to do with ordering of the molecular orientations. The rapid changes of T_1 near the phase transitions and the changes in the temperature dependences of T_1 provide, perhaps, the most direct confirmation of this interpretation of the entropy data. This is so because it is known that below about 65°K, T_1 is governed by intra-molecular interactions and is therefore sensitive only to the strengths of these interactions and the rate of molecular reorientation. In this connection note that the high temperature results between 25 and 55°K join up with the results obtained by Bloom and Sandhu (1962) between 55 and 110°K. The slow temperature dependence between 55 and 110°K, implies that the correlation time is also a slowly varying function of temperature in this range.

Earlier it was noted that if the relaxation is dominated by one mechanism, and if the correlation function is exponential, then the expression for the minimum value in the spin-lattice relaxation time involves no adjustable parameters. It only contains parameters specifying the strength of the interaction and the Larmor frequency of the nuclei in the applied magnetic field. For CH_3D the dominant relaxation mechanism is believed to be the intramolecular dipolar interactions; this conjecture is supported by the present and earlier experiments by us (see section 4:3).

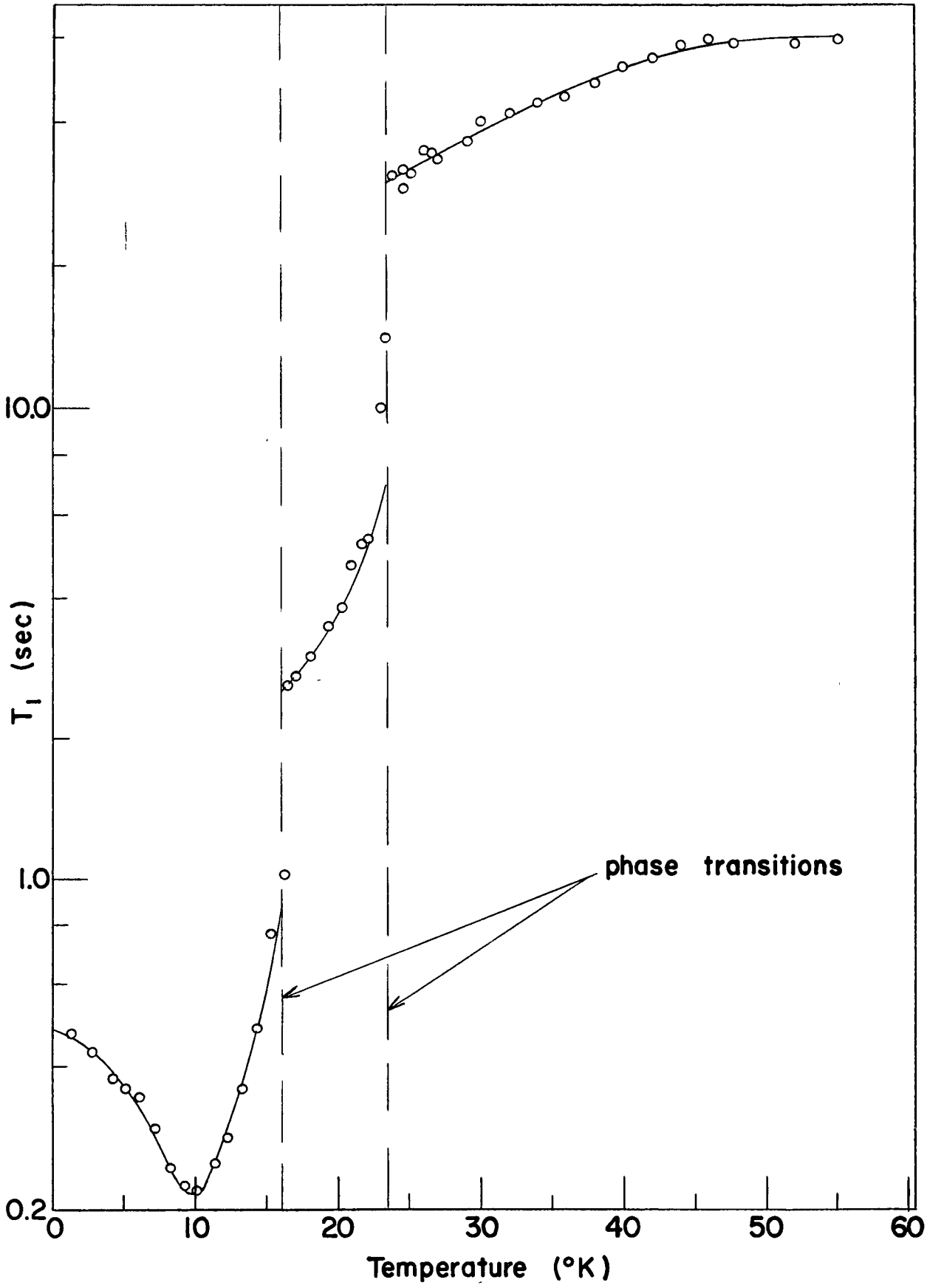

Figure 14. Experimental Values of T_1 Versus T for CH_3D

Now using the results of the previous section, the effect of the coupling between the unlike spins can be taken into account. It may be shown using equations (4-6) and (5-3) that $\frac{1/T_1{}^{I}}{1/T_1{}^{II}} \approx 42$, $\frac{1/T_1{}^{II}}{1/T_1{}^{IS}} \approx 5$, and $\frac{1/T_1{}^{II}}{1/T_1{}^{SI}} \approx 0.8$; these results were calculated using the approximation that for exponential correlation functions the spectral density $J(\omega_I \pm \omega_S) \approx J(\omega_I)$ as $\omega_I = 28.5$ mcs. and $\omega_S = 4.4$mcs. Thus, if the time constants are evaluated and substituted in the equations (5-2), the conclusion is that the relaxation is governed by one exponential with time constant $1/T_1{}^{I}$ to within experimental error. In other words, for all practical purposes the relaxation of proton system, and thus $(T_1)_{min}$, is governed by the interactions with the other protons in the molecule and is given by equation (4-6). From this equation it can be seen that the only difference between the calculation for $(T_1)_{min}$ for CH_3D and that for CH_4 is that the interactions now involve two neighbouring nuclei rather than three as for CH_4. Thus one finds using equation (4-6), that $(T_1)_{min} = 12$ millisec. for CH_3D as compared with 8ms for CH_4. As in the case of CH_4 to be discussed later, there is a discrepancy of a factor of 18 between the experimental and theoretical values of $(T_1)_{min}$. If any other contributions to T_1, due to other relaxation mechanisms, are included, then the discrepancy would be even greater. Despite the fact that the predictions of $(T_1)_{min}$ by the conventional theory appear to be wrong, the

relationship between T_1, τ_c and $(T_1)_{min}$ given by the conventional theory will be used in the next section to obtain the correlation times.

The Analysis of the Data: 5:3

In this section a method of analysis will be described, which is based on the discussion in Chapter 4. We recall the expressions (4-11) and (4-12) for the spin-lattice relaxation time due to dipolar and quadrupolar interactions, respectively. These equations can be rewritten in a form involving only τ_c, ω_o and $(T_1)_{min}$

$$\frac{1}{T_1} = \frac{A}{\omega_o} \quad y \tag{5-4}$$

where y is defined as

$$y = \frac{x}{1+x^2} + \frac{4x}{1+4x^2} \tag{5-5}$$

where $x = \omega_o \tau_c$

The dependence of y on x is shown in Figure (15). It must be emphasized here that owing to the presence of a maximum in y versus x at x = 0.62 and the resulting minimum in T_1, definite values can be assigned to τ_c at any temperature using the value of $\tau_c = 0.62/\omega_o$ at the temperature at which the minimum in T_1 occurs.

$$\left(\frac{1}{T_1}\right)_{min} = \frac{A}{\omega_o} \quad 1.425$$

At a particular temperature τ_c can be obtained from the value of y. The value of y is given by the ratio of T_1 at the particular temperature to $(T_1)_{min}$

$$\frac{(T_1)_{min}}{T_1} = \frac{y}{1.425} \qquad (5\text{-}6)$$

Having evaluated y, two values of x are obtained from the graph of y versus x. One of these two values is eliminated using the criteria that $x < 0.62$ corresponds to the high temperature side of the minimum,and $x > 0.62$ to the low temperature side.

One is faced by the dilemna that the theoretical and experimental values of $(T_1)_{min}$ disagree drastically. One possible explanation, which will be justified in the next chapter, is that at low temperatures or for small J quantum numbers, the effective interaction strength causing the relaxation can not be correctly described classically and has been reduced in strength. If the correlation function is still exponential and <u>if the strength of the interaction does not change appreciably in the temperature range of interest</u>, then the general form of T_1 as a function of τ_c as given by equation (5-4) is still correct. It is this general form of the dependence of T_1 on τ_c which is of importance in this analysis. The only necessary modification to equation (5-6) is the replacement of the theoretical value of $(T_1)_{min}$ by the experimental value, in order to correct for the change in the effective strength of the interaction. The above two assumptions will be examined in detail in the next chapter, where

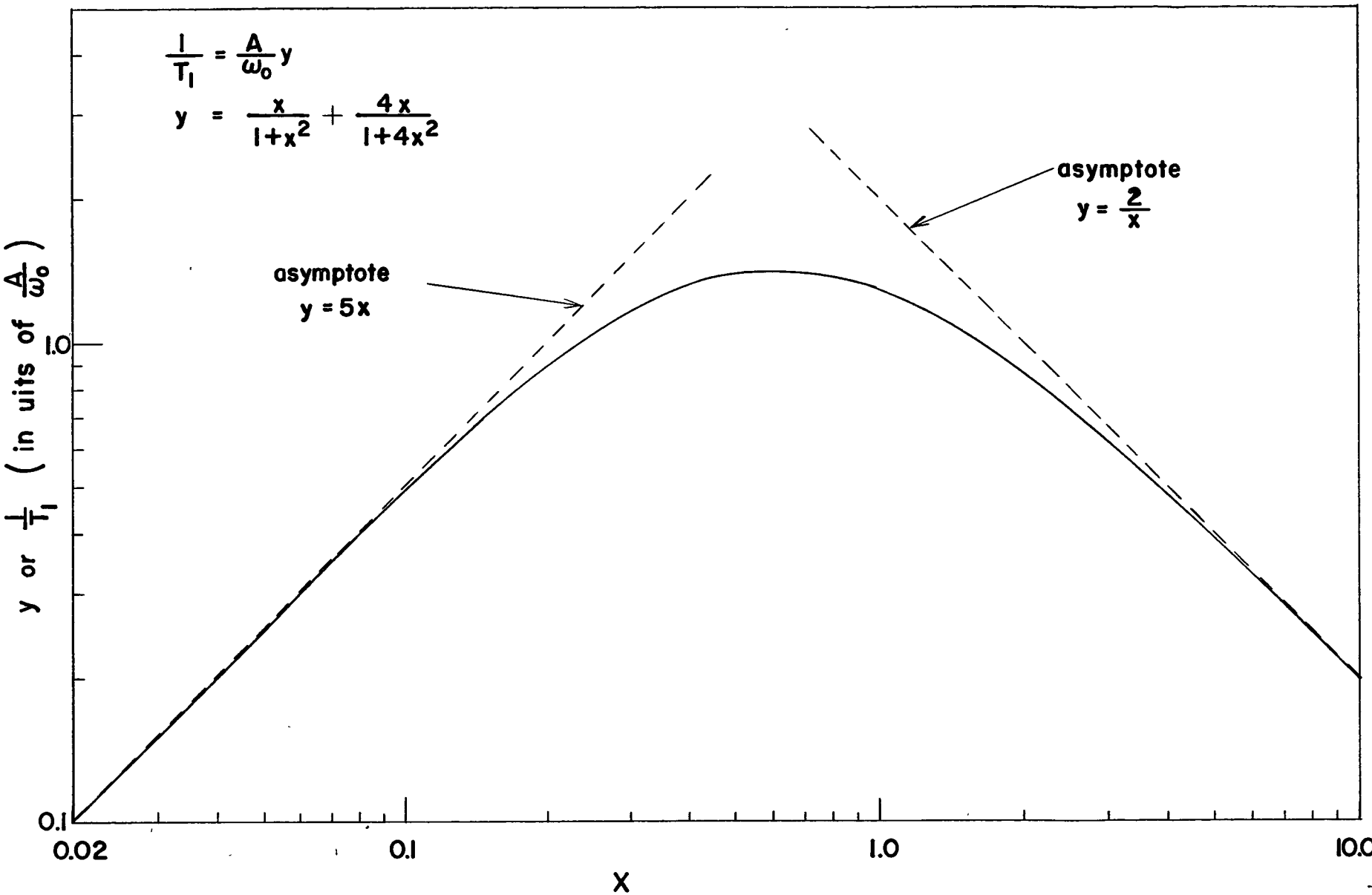

Figure 15. Plot of y and $1/T_1$ Versus x

it will be seen that they are not always valid.

There are two additional assumptions implicit in this analysis. One of the assumptions is the neglect of effects due to cross-correlations between pairs of spins on the molecule. As was discussed earlier, Hubbard has shown this assumption to be correct in the range of validity of the classical diffusion equation, but its validity at low temperature is debatable. The other assumption is that the relaxation of the spin system is dominated by one mechanism. This last assumption is consistent with the interpretation of the data between 55 and 110°K, and is supported by the present experimental results; in particular the data on T_1 versus T for mixtures of CH_4 with CD_4, and the mixtures of CH_4 with Kr (to be discussed later) being especially relevant.

Using the above outlined method of analysis, the values of τ_c versus T have been been obtained for CH_3D and are shown in Figure (16) (log $1/\omega_o\tau_c$ has been plotted versus log T). A surprising feature is the slow temperature dependence at the low temperature end. Moreover, if it is assumed that $1/\tau_c \propto T^7$ then the resulting graph is indicated by the dashed line. The behaviour of the log 1/x versus log T plot at the higher temperatures suggests that a T^7 temperature dependence is not unreasonable. This latter feature is encountered in most of the systems studied and will be discussed in terms of the coupling between the phonons and the molecules in the next chapter. The solid curve is a theoretical fit on the basis of this phonon coupling model.

The first possibility that should be investigated is the possibility of describing the reorientational correlation time by an activation energy as it has often been found to be the case (Andrew and Eades, 1953). The temperature dependence of the correlation time would then be of the form

$$\tau_c = \tau_o e^{T_o/T} \qquad (5\text{-}7)$$

where kT_o is an activation energy corresponding approximately to the height of the rotational barrier between different molecular positions. To check whether the correlation time can be described in this way in Figure(17) $\ln \omega_o \tau_c$ has been plotted versus $1/T$. It is clearly demonstrated by this figure that for no appreciable range of temperatures can the temperature dependence be described by an activation energy. Exactly the same conclusions can be drawn about τ_c versus T in each of the following systems.

CD_4: 5:4

In Figure (18), the experimental values for the spin-lattice relaxation time as a function of temperature of the deuteron spin system in CD_4 are shown. A distinctive feature of the data is the rapid variation of T_1 on the low temperature side of the $(T_1)_{min}$. Another difference between this set of data and that of CH_3D is the occurrence of only a single break in T_1 versus T curve occurring at the upper phase transition temperature. The absence of any discontinuity at the

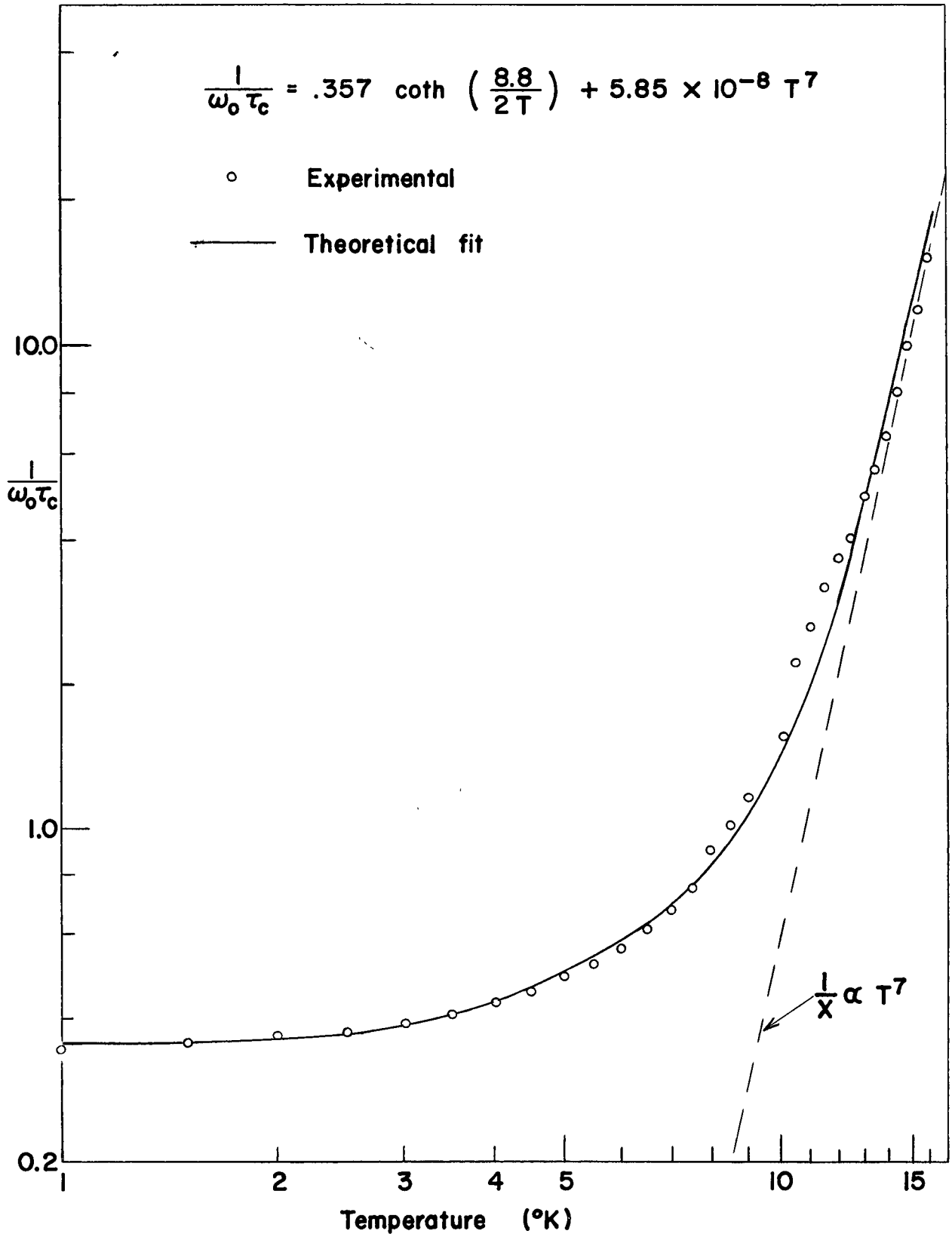

Figure 16. Plot of $1/\omega_0 \tau_c$ Versus T. The Theoretical Fit Obeys the Equation Shown in the Figure

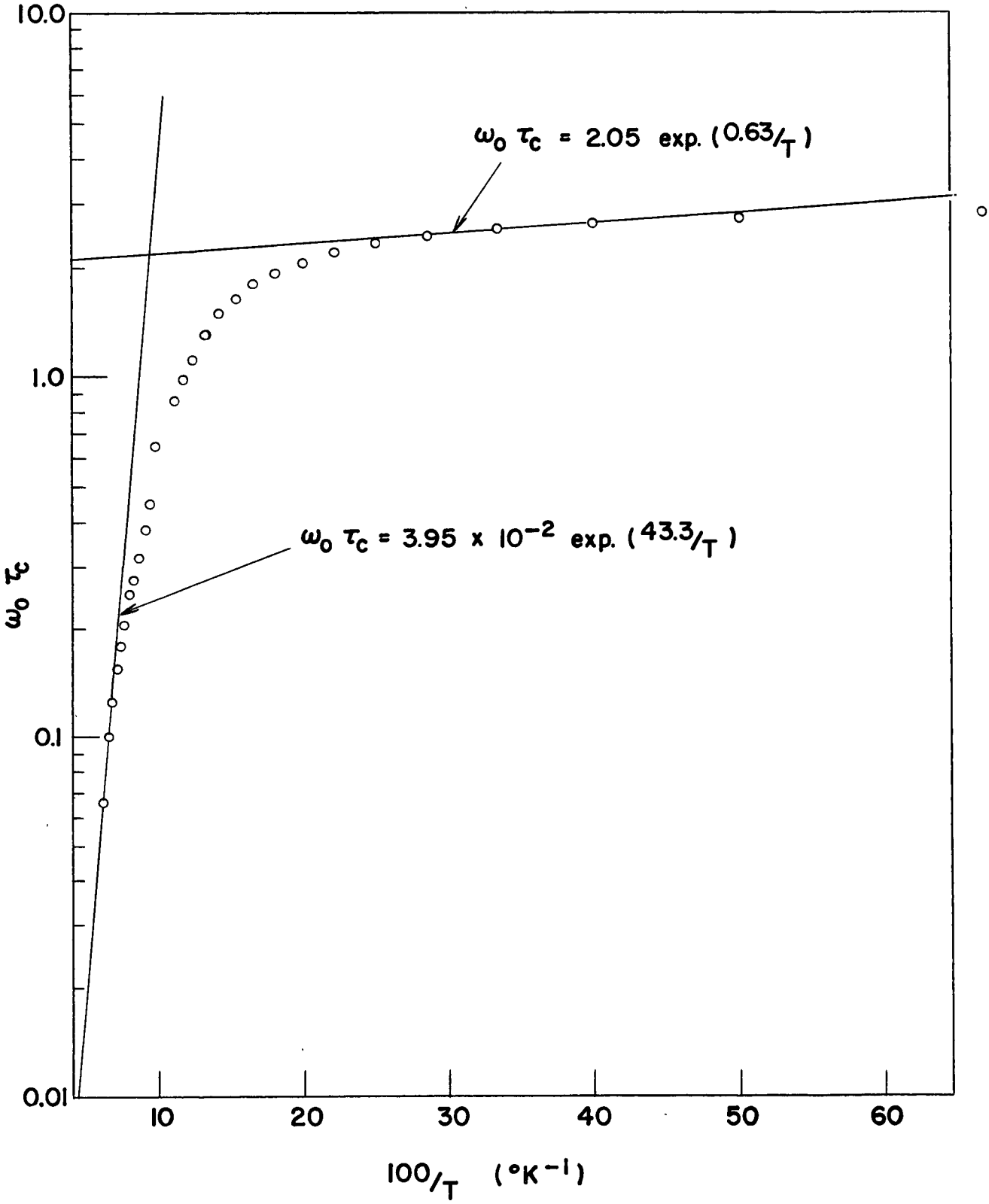

Figure 17. Plot of $\omega_0 \tau_c$ Versus 1/T to check whether Molecular Reorientation is Governed by an Activation Energy

lower phase transition temperature may be due to the experimental errors in the T_1 measurements together with the very steep slope of the T_1 versus T curve at that point. The high temperature values of T_1 join up with the earlier reported measurement between 55 and 110°K.

Using conventional theory and the quadrupole coupling constant for CD_4, the minimum value of T_1 is calculated to be 8 millisec $\pm\binom{11.1}{6.0}$ (see section 4:3), whereas the experimental value is 8.4 millisec. Ramsey and Anderson in a private communication have stated that the uncertainty of their quadrupole coupling constant should be even larger than that quoted by Anderson (1961). Anderson's values were used in calculating the above limits on $(T_1)_{min}$. Thus the apparent agreement between the experimental and theoretical $(T_1)_{min}$ may be misleading.

The graph of log 1/x versus log T obtained using the above procedure is shown in Figure (19). This curve is not smooth as is the one for CH_3D. According to some conjectures the curve should be smooth near the high temperature end. The bumps in ln 1/x versus ln T may be due to the nature of the low lying energy levels in CD_4.

CD_3H: 5:5

For CD_3H, both the proton and deuteron spin-lattice relaxation times have been measured, see Figures (20) and

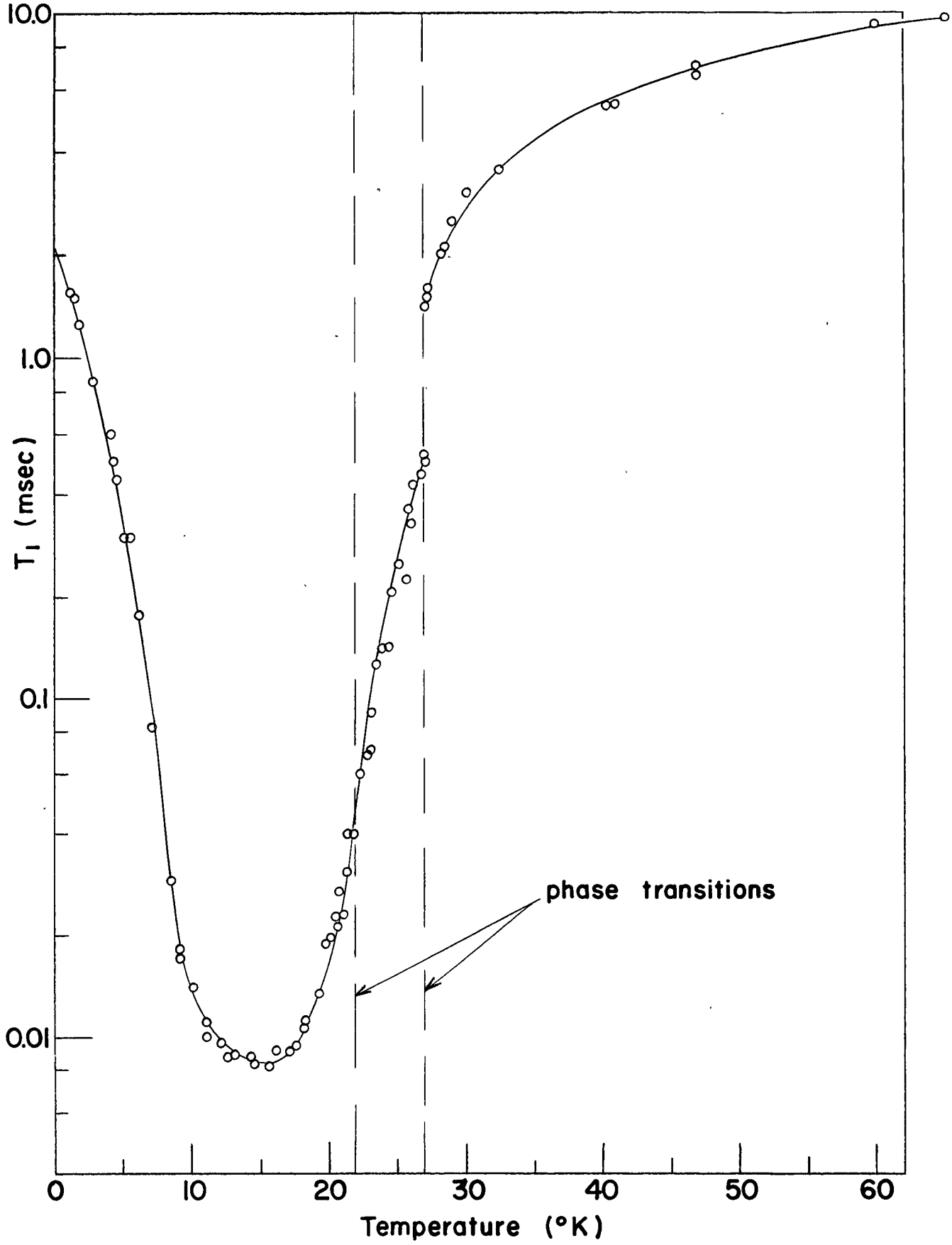

Figure 18. Experimental Values of T Versus T for CD_4

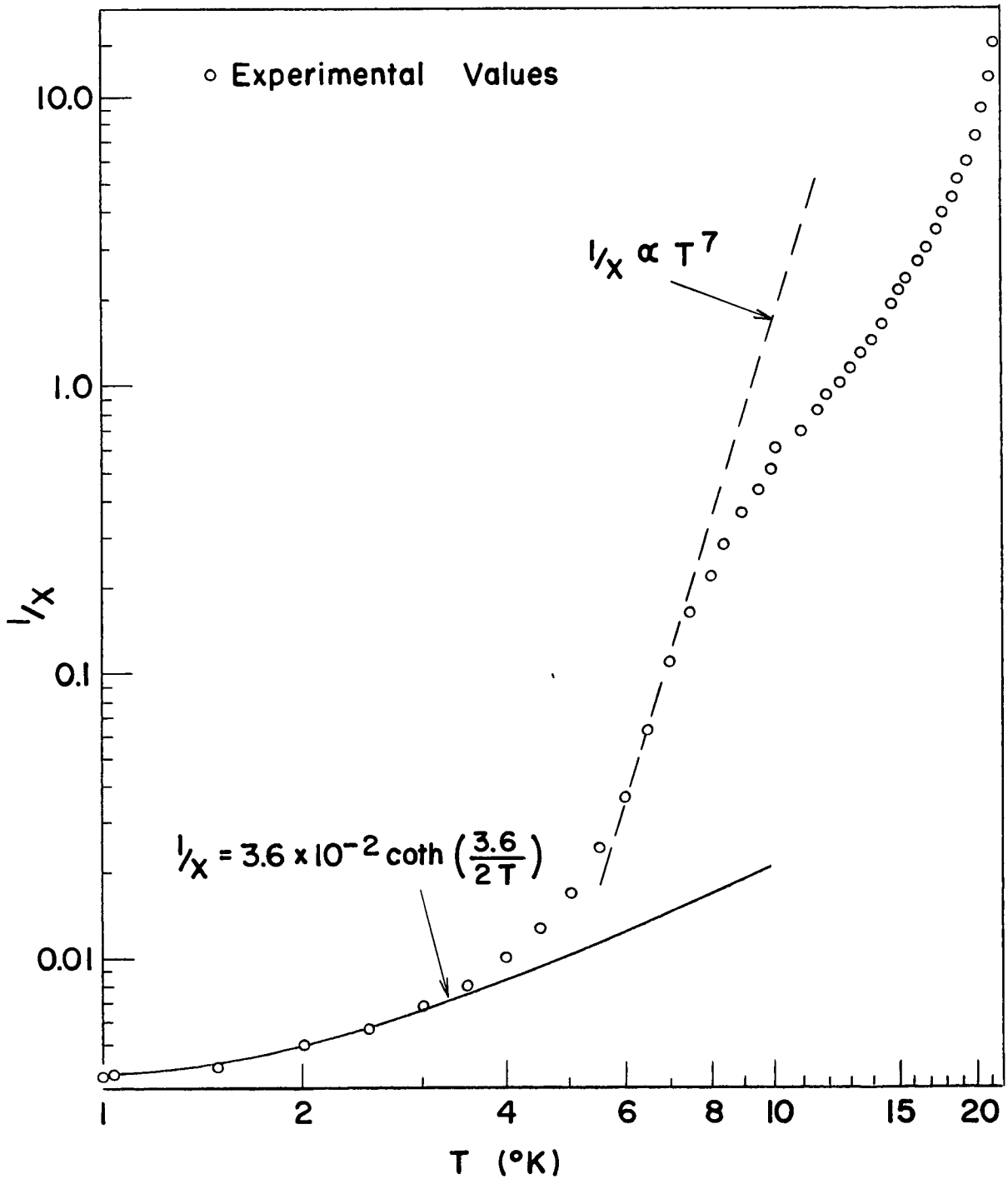

Figure 19. Plot of 1/x Versus T for CD_4

(21). The curves exhibit changes in slope and breaks in T_1 at the two phase transitions.

The value of $(T_1)_{min}$ for the deuteron resonance is 4 millisec. as compared with 8 millisec. for CD_4. If one rather naively assumes that the electric field gradient at the site of deuteron in CD_3H has the same value as that in CD_4, then the theoretical value of $(T_1)_{min}$ for CD_3H is the same as that for CD_4, 8 ms. Now, the question is: how large is the contribution of the intramolecular dipolar interaction to the relaxation of the deuteron, and can it account for the apparently low value of $(T_1)_{min}$ for CD_3H?

If again the approximation is used that $J(\omega_I \pm \omega_S) \approx J(\omega_I)$, then the maximum contribution to the relaxation rates due to the coupling between unlike spins correspond to time constants T_1^{SS} and T_1^{IS} which satisfy the relations $T_1^{SS} \approx$ 800 millisec and $\frac{1/T_1^{SS}}{1/T_1^{IS}} \approx 0.8$, and $\frac{1/T_1^{SS}}{1/T_1^{SI}} \approx 5$. It was noted above that T_1^S, the relaxation time due to quadrupole interactions, was approximately 8 ms. It may be seen using these numbers and equation (5-2) that the relaxation is dominated by the quadrupole interactions. i.e., $T_1 = T_1^S = 8$ ms. Similarly, the proton relaxation is not affected by the deuteron spin system, because the cross-relaxation times T_1^{IS}, etc., are so long, and the deuteron relaxation time is so short. In essence the z-component of the deuteron magnetization $S_z(t)$ remains always approximately equal to S_o when the proton system is disturbed from

equilibrium by an r.f. pulse in the measurement of the proton T_1.

There is another problem in connection with CD_3H, namely, it has been found (Morrison et al., 1965) that the CD_3H supplied by Merck, Sharp and Dohme contains small amounts of CD_4 and CH_2D_2. This fact did not come to our attention until it was too late to have the sample analyzed. These impurities in the CD_3H cause some doubt as to the validity of our results for CD_3H. In particular, the CH_2D_2 impurity is likely to have an appreciable effect on the proton T_1 in CD_3H. This has been discussed elsewhere (de Wit and Bloom, 1965).

CH_4: 5:6

The spin-lattice relaxation time data for the proton resonance at 28.5 mcs. in CH_4 is shown in Figure (22). Although a break in the T_1 versus T curve is evident at the upper phase transition temperature, no change is observed at the lower phase transition; this may be due to the fact that this phase transition is quite broad and difficult to observe (Morrison et al. 1963). The theoretical value of $(T_1)_{min}$ = 8 millisec. was calculated in section 4:3, and is 20 times shorter than the experimental value of 160 millisec. The $(T_1)_{min}$ is rather shallow indicating that in this region τ_c is a slowly varying function of temperature.

That τ_c is slowly varying around $(T_1)_{min}$ is illustrated by the spin-lattice relaxation time measurements

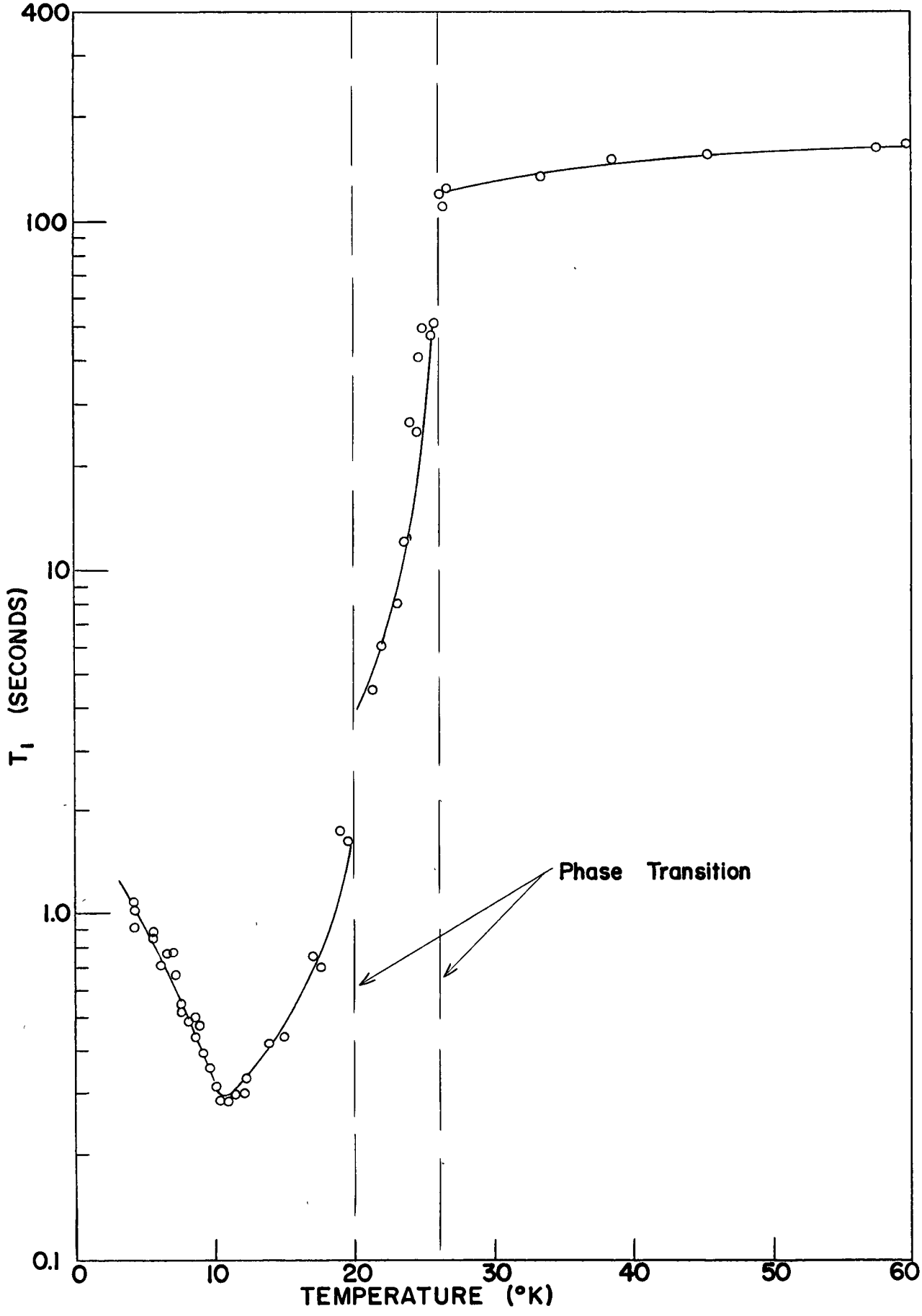

Figure 20. Experimental Values of Proton T_1 Versus T for CD_3H

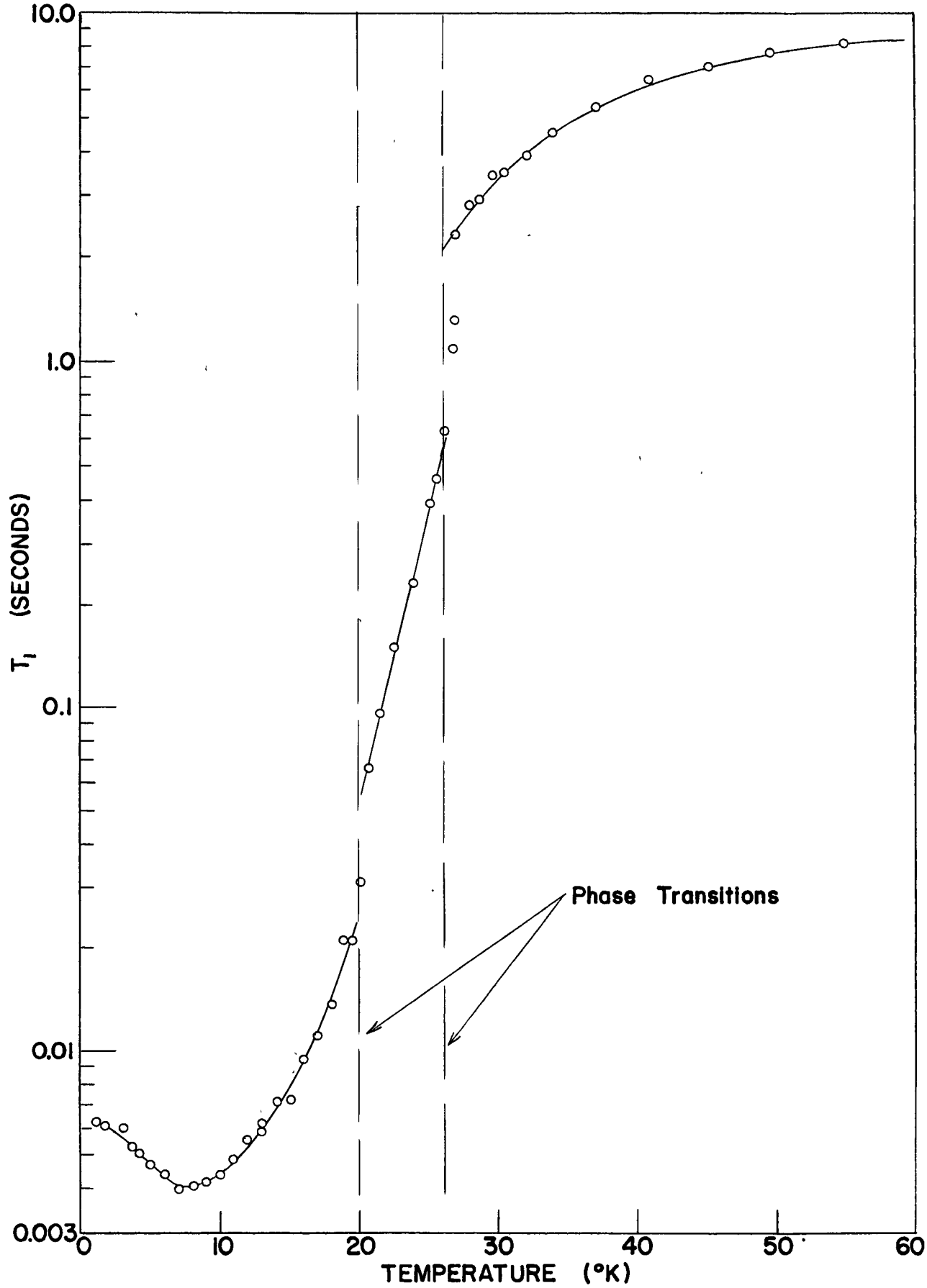

Figure 21. Experimental Values of Deuteron T_1 Versus T for CD_3H

carried out at 4.4 mcs, shown in Figure (23). A noteworthy feature of this set of data is the absence of a minimum in T_1; at the lowest attainable temperatures the spin-lattice relaxation time is still becoming shorter. If one examines the curve of the correlation times, log 1/x versus log T, for the 28.5 mcs CH_4 data shown in Figure (24), then one concludes that the absence of a $(T_1)_{min}$ at 4.4 mcs. is to be expected. Using the value of τ_c given at 1.2°K, one finds that at $\omega_o = 2\pi$ x 4.4 mcs. $\omega_o\tau_c = 0.18$, whereas it has been seen earlier that $(T_1)_{min}$ occurs at $\omega_o\tau_c = 0.62$. The high temperature end of the correlation time curve shows a T^7 behaviour as indicated by the dotted line in Figure (24). In Figure (23) the correlation times obtained from the 28.5 mcs. data have been used to predict the values of T_1 at 4.4 mcs, so as to check the consistency of the assumptions and method of analysis. The agreement between the predicted and experimental results is reasonably good.

A puzzling feature most clearly seen in the 4.4 mcs. data is the minimum in T_1 which occurs at 23°K. This second minimum is also present in the data for the CH_4-Kr and CH_4-CD_4 mixtures. It is rather unfortunate that the existence of this second minimum was not realized when the CH_4 data at 28.5 mcs were taken; in that case T_1 is decreasing, but the data do not go through the second minimum. This second minimum has not been observed for any of the isotopic modifications of CH_4.

Some remarks have to be made about the data obtained in the region of this upper minimum. The plot of log

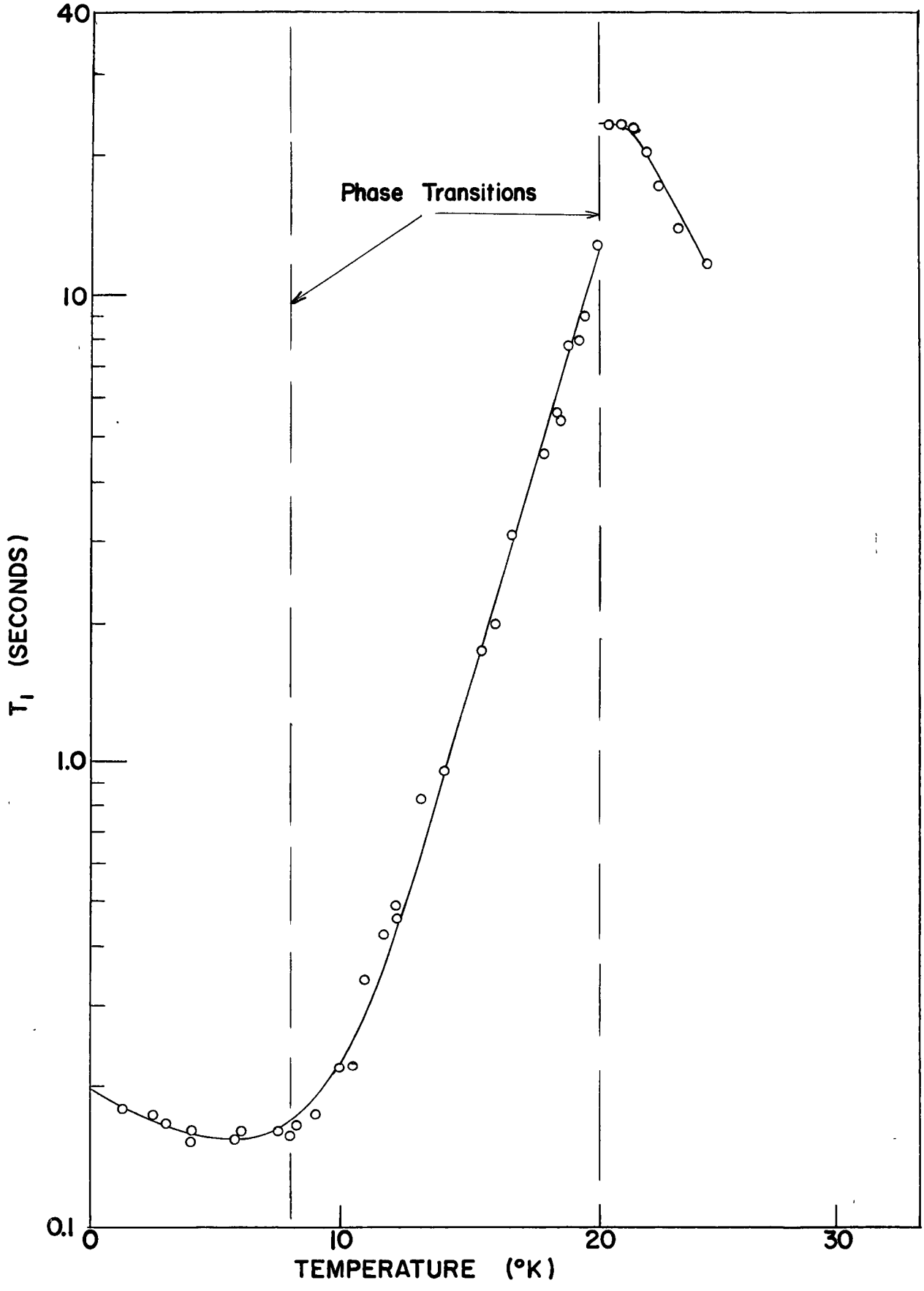

Figure 22. Experimental Values of T_1 Versus T for CH_4 at 30Mcs

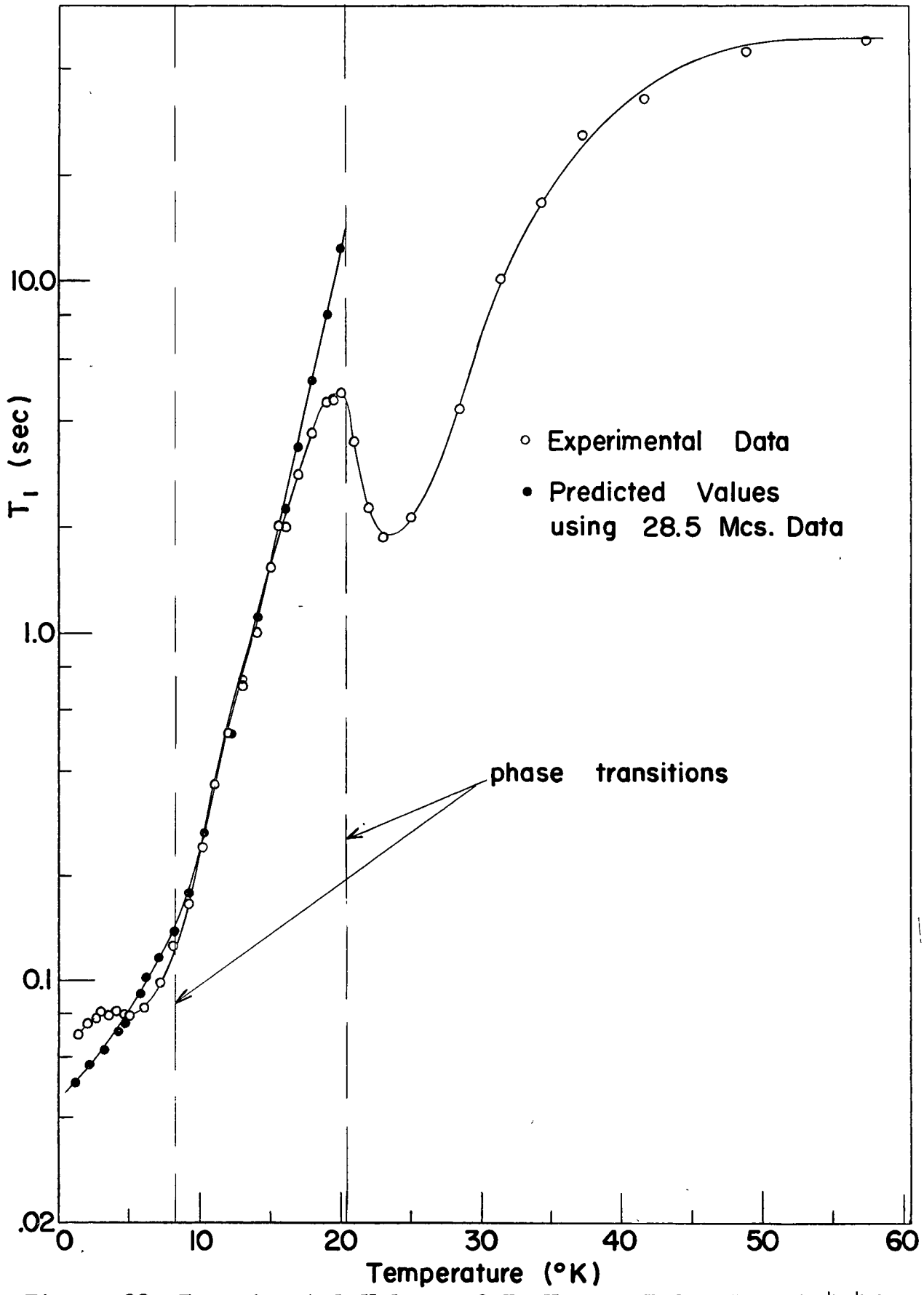

Figure 23. Experimental Values of T_1 Versus T for CH_4 at 4.4Mcs. Also shown are the predicted values using the 30 mcs. data. Note the T_1 minimum above the upper phase transition.

$(A(\infty) - A_t)$ versus t does not consist of a single exponential, i.e., there is no unique T_1, but it can be analyzed as the sum of the two exponentials. A typical plot is shown in Figure (25). In view of the experimental errors associated with $A(\infty) - A_t$ and the fact that the two time constants so obtained usually differ from each other by less than a factor of 4, it is impossible to try a meaningful separation of the two time constants. The values of T_1 shown on the graph are in fact the slopes of the initial straight line portion of the T_1 plots and the value of T_1 thus obtained falls in between the values of the two time constants. One can say with certainty that there are two distinct contributions to the spin-lattice relaxation. Note that the effect of the second minimum of shortening T_1 in the 4.4 mcs. CH_4 data persists even below the phase transition; that is why the departure of the experimental values of T_1 from the predicted values on the basis of the 28.5 mcs. data is greater near the phase transition. The effect of this second minimum on T_1 can not be accounted for at the present time.

Ultrasonic attenuation measurements by Thiele, Whitney and Chase (1964) were carried out at a frequency of 11.8 mcs. These measurements show a peak in the absorption at 23.5°K. This peak implies a correlation time of approximately 1.4×10^{-8} sec. at 23.5°K for whatever mechanism is responsible for the ultrasonic attenuation. The correlation time obtained from their data is to be compared with the

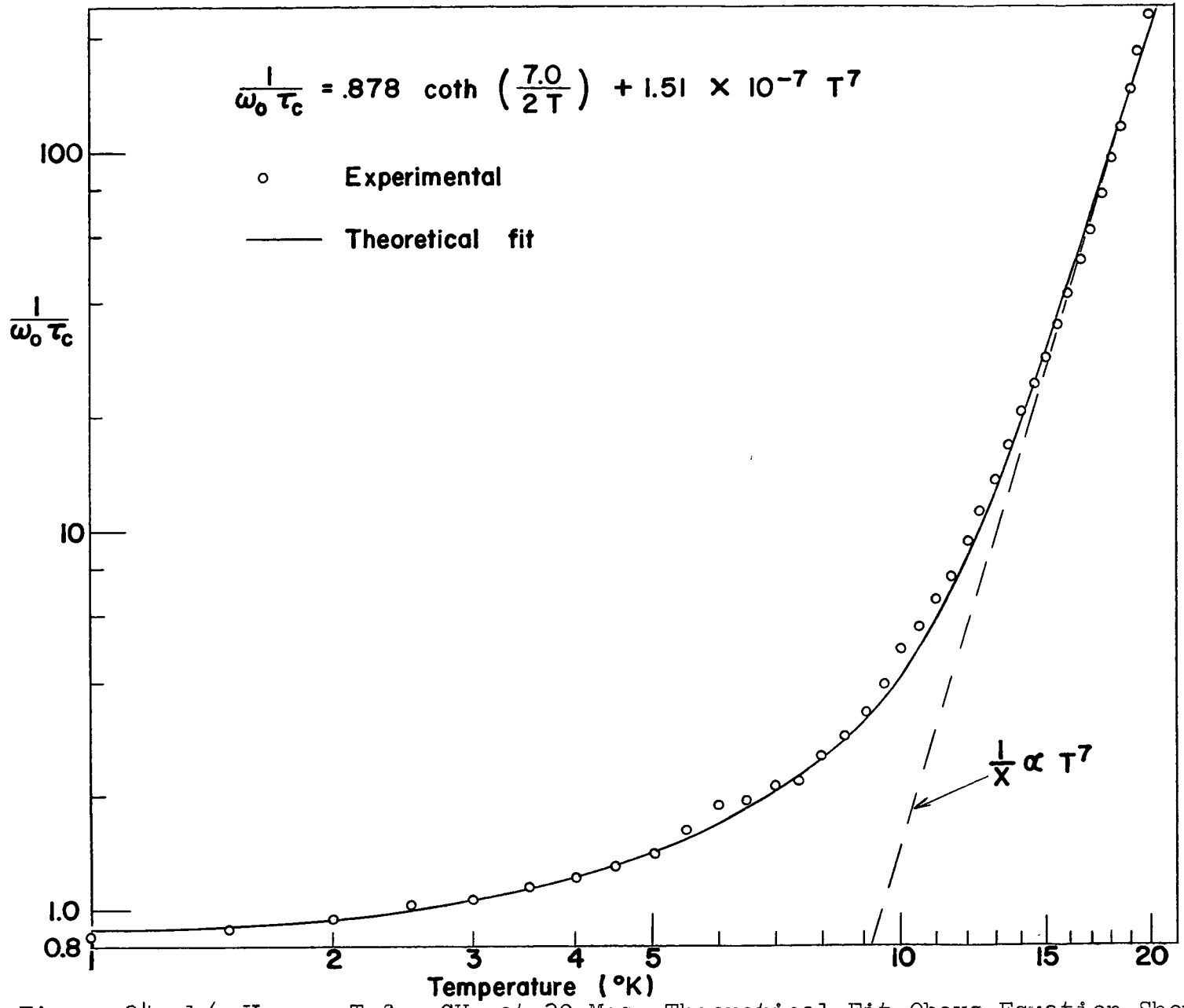

Figure 24. 1/x Versus T for CH_4 at 30 Mcs. Theoretical Fit Obeys Equation Shown

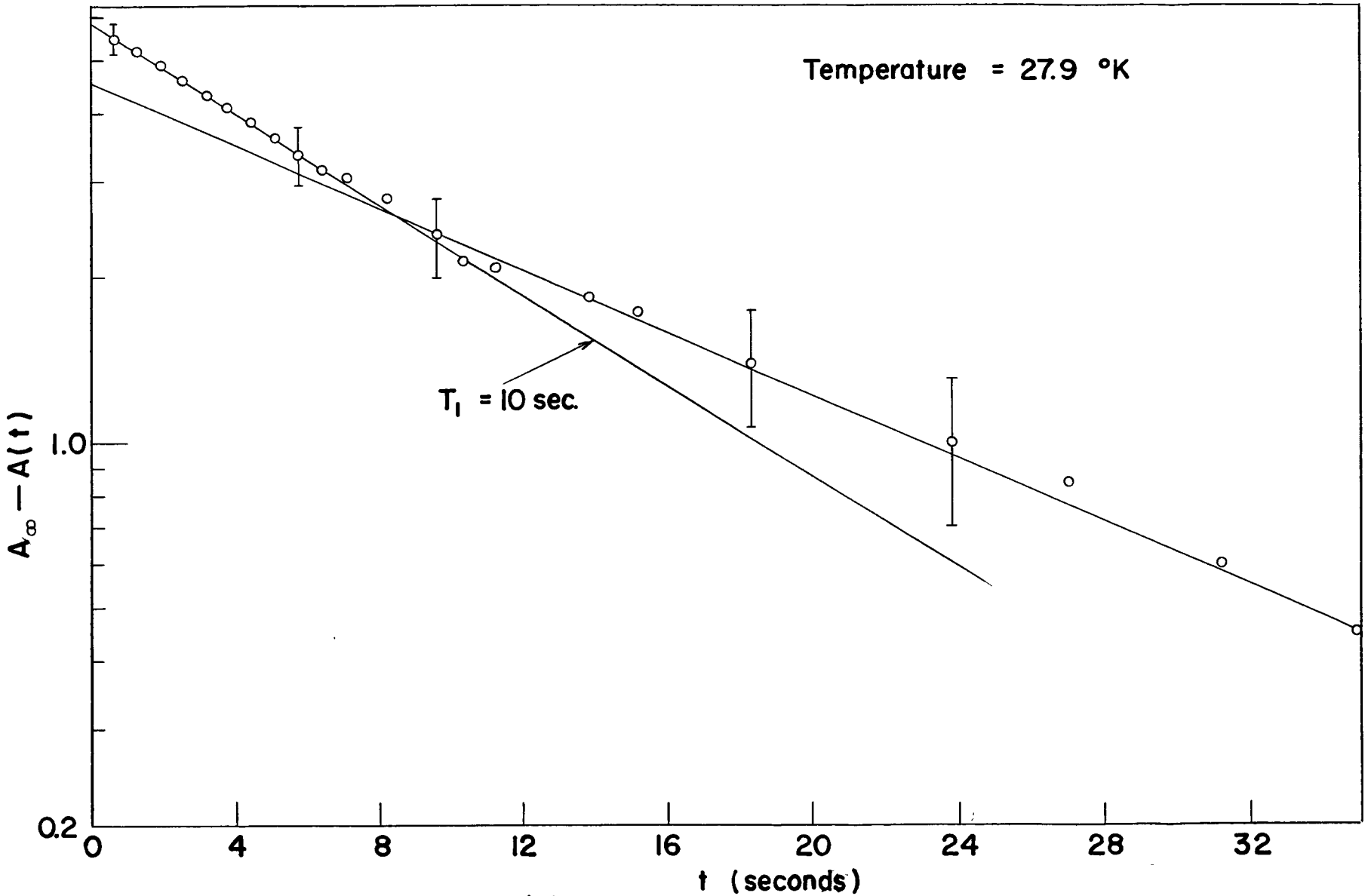

Figure 25. A Typical Plot of $A_\infty - A(t)$ Versus t Showing the Non-exponential Relaxation Observed at the Upper $(T_1)_{min}$ in CH_4

correlation time of 2.2×10^{-8} sec. at 23.2°K implied by the second T_1 minimum discussed above. It appears very likely that there is a connection between these two observations, but at the present time neither the mechanism responsible for the anomalous ultrasonic attenuation, nor that associated with the upper T_1 minimum is known.

CH_4 - Kr Mixtures: 5:7

The CH_4-Kr mixtures again exhibit an upper minimum in T_1 very similar to that observed in pure CH_4. The data are shown in Figures (26) and (27) for the 10% and 50% Kr mixtures. However, no evidence for non-exponential relaxation was observed. The explanation for this difference may be contained in the fact that the measurements were terminated when $A(t) \approx 0.15\ A(\infty)$, although in the case of CH_4, the non-exponential behaviour was noticeable when the measurement was terminated at that point. Surprisingly, the values of the lower $(T_1)_{min}$ are very strongly dependent on the Kr concentration, being 160, 300, and 5000 millisec. for 100%, 90%, and 50% CH_4, respectively. This behaviour of $(T_1)_{min}$ is surprising in view of the assumption, which is supported by other evidence, that all spin-lattice relaxation interactions are intramolecular. A possible explanation will be provided in the next chapter. Moreover, the temperature dependence below the $(T_1)_{min}$ is drastically changed by the addition of Kr. The high temperature values above and

below the upper $(T_1)_{min}$ are the same for 10% and 50% Kr providing additional evidence that at least down to 20°K the relaxation mechanisms are intramolecular. Another peculiar feature is the large shift to higher temperatures of the upper T_1 minimum as the Kr concentration is increased.

CD_4-CH_4 Mixtures: 5:8

The proton and deuteron spin-lattice relaxation times were measured for a 67% CD_4 - 33% CH_4 mixture, shown in Figures (28) and (29). Only the proton spin-lattice relaxation time was measured for a 10% CD_4 - 90% CH_4 mixture shown in Figure (30).

If the relaxation due to intermolecular interactions was appreciable this should be reflected in longer values of $(T_1)_{min}$ with increasing concentration of CD_4. In fact no such effect was observed; $(T_1)_{min}$ is 155, 195, and 175 millisec for 100% CH_4, 90% CH_4 and 33% CH_4, respectively. Within the experimental error, the variation in T_1 minimum is negligible.

The addition of CD_4 to CH_4 seems to have a marked effect on the temperature dependence of T_1 below the minimum. The upper minimum in the T_1 data for the proton resonance is also evident in the mixtures as it was in pure CH_4. As in the case of CH_4, the relaxation behaviour for the proton resonance in the region of the upper minimum is also non-exponential. The temperature at which the upper minimum

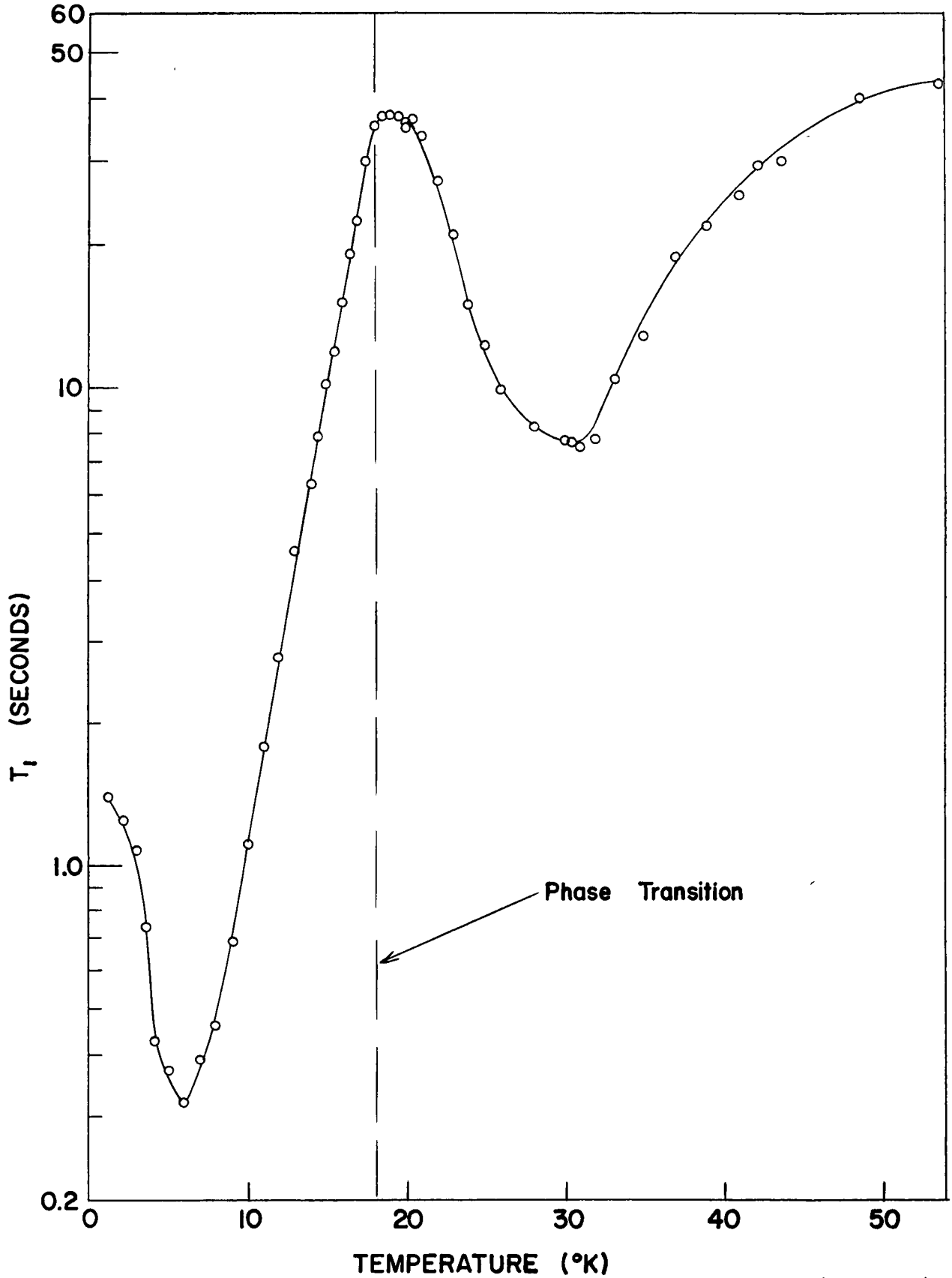

Figure 26. Experimental Values of T_1 Versus T for 10% Kr-90% CH_4 mixture

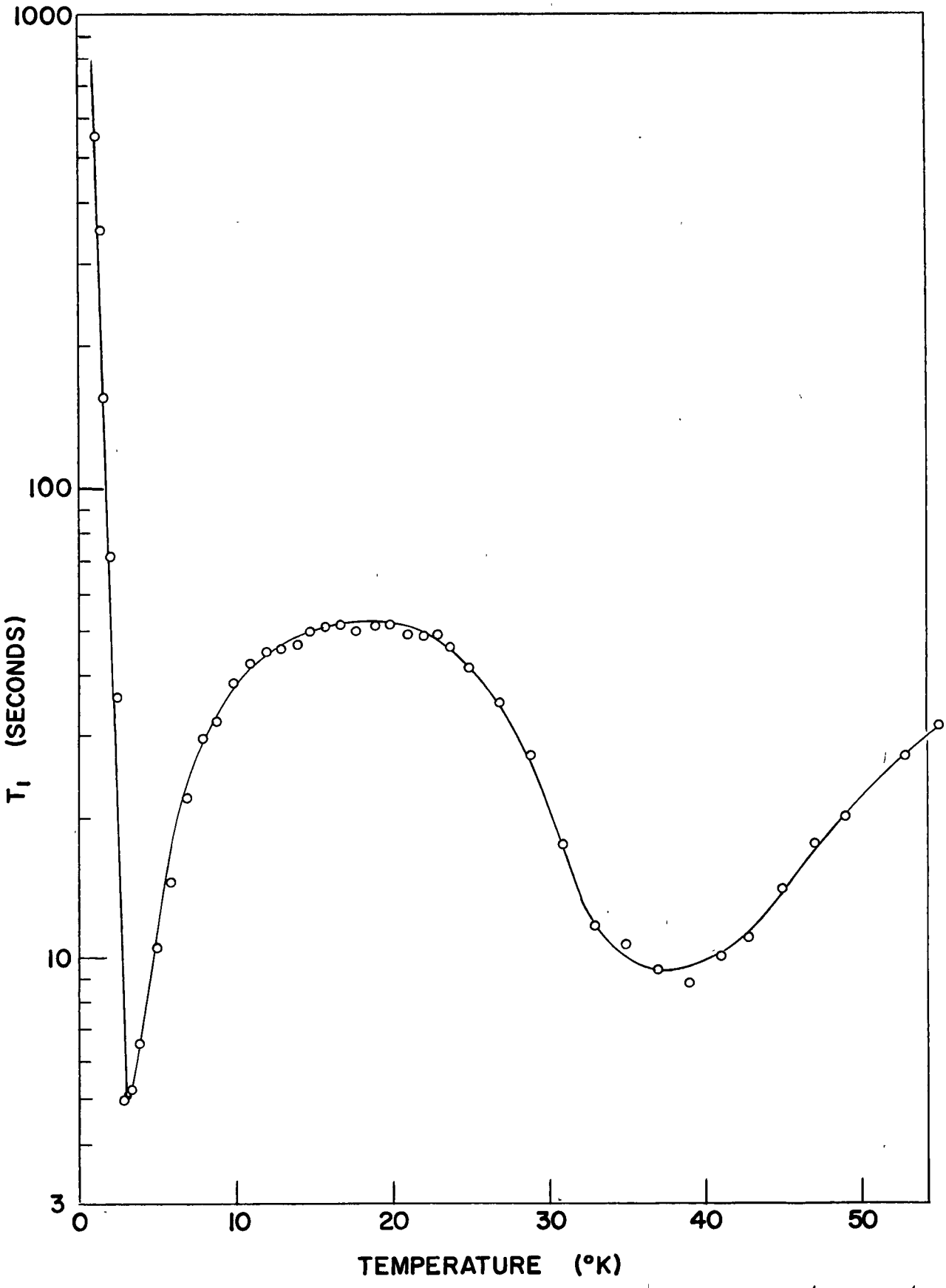

Figure 27. Experimental Values of T_1 Versus T for 50% Kr-50% CH_4 Mixture

occurs is apparently independent of the CD_4 concentration, whereas it is very concentration dependent for the CH_4-Kr mixtures.

A Distribution of Correlation Times: 5:9

It has been observed in solid high-concentration ortho H_2, that the relaxation of M_z towards its equilibrium value is non-exponential. This non-exponential behaviour has been attributed to a distribution of correlation times existing in the solid because it is inhomogeneous, i.e., the crystalline fields vary greatly from site to site, the crystalline fields being highly dependent on the local configuration of the ortho and para H_2 molecules. Consequently, a "spin temperature" (to be discussed in the next chapter) does not exist, because the energy levels of the neighbouring nuclear spins are not even approximately equidistant. A detailed examination of the relaxation function for M_z shows (Sugawara et al. 1956) that a distribution of correlation times has the net effect of introducing a distribution of T_1's. This could have the effect of increasing the mean value of T_1 at the minimum, and of broadening the T_1 minimum. Non-exponential relaxation behaviour was not observed in any of our experiments in the lowest temperature phases in methane. However, this does not prove conclusively that a distribution of correlation times does not exist, since, unlike H_2, it may still be possible to describe the spin system

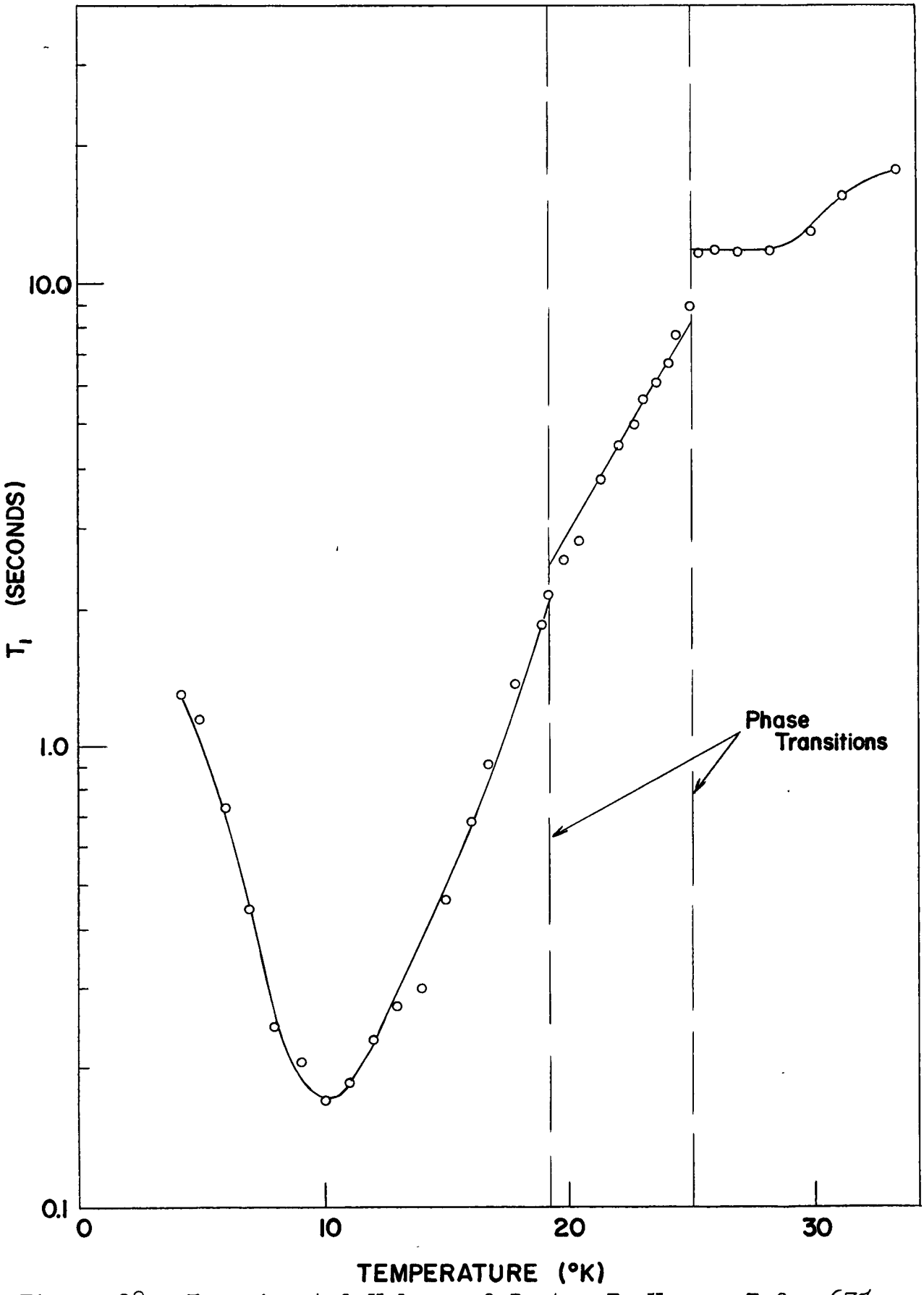

Figure 28. Experimental Values of Proton T_1 Versus T for 67% CD_4-33% CH_4 Mixture

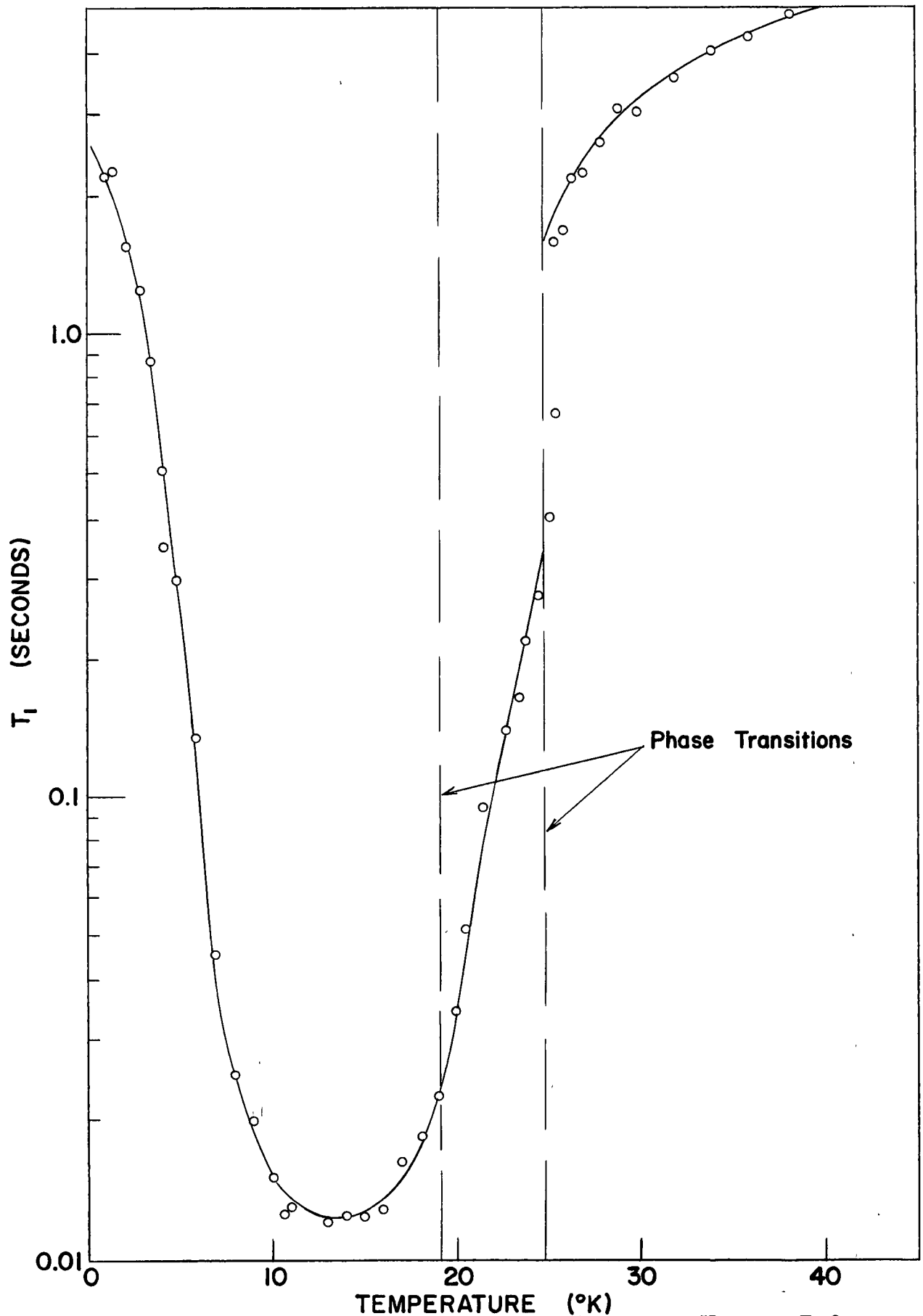

Figure 29. Experimental Values of Deuteron T_1 Versus T for 67% CD_4-33% CH_4 Mixture

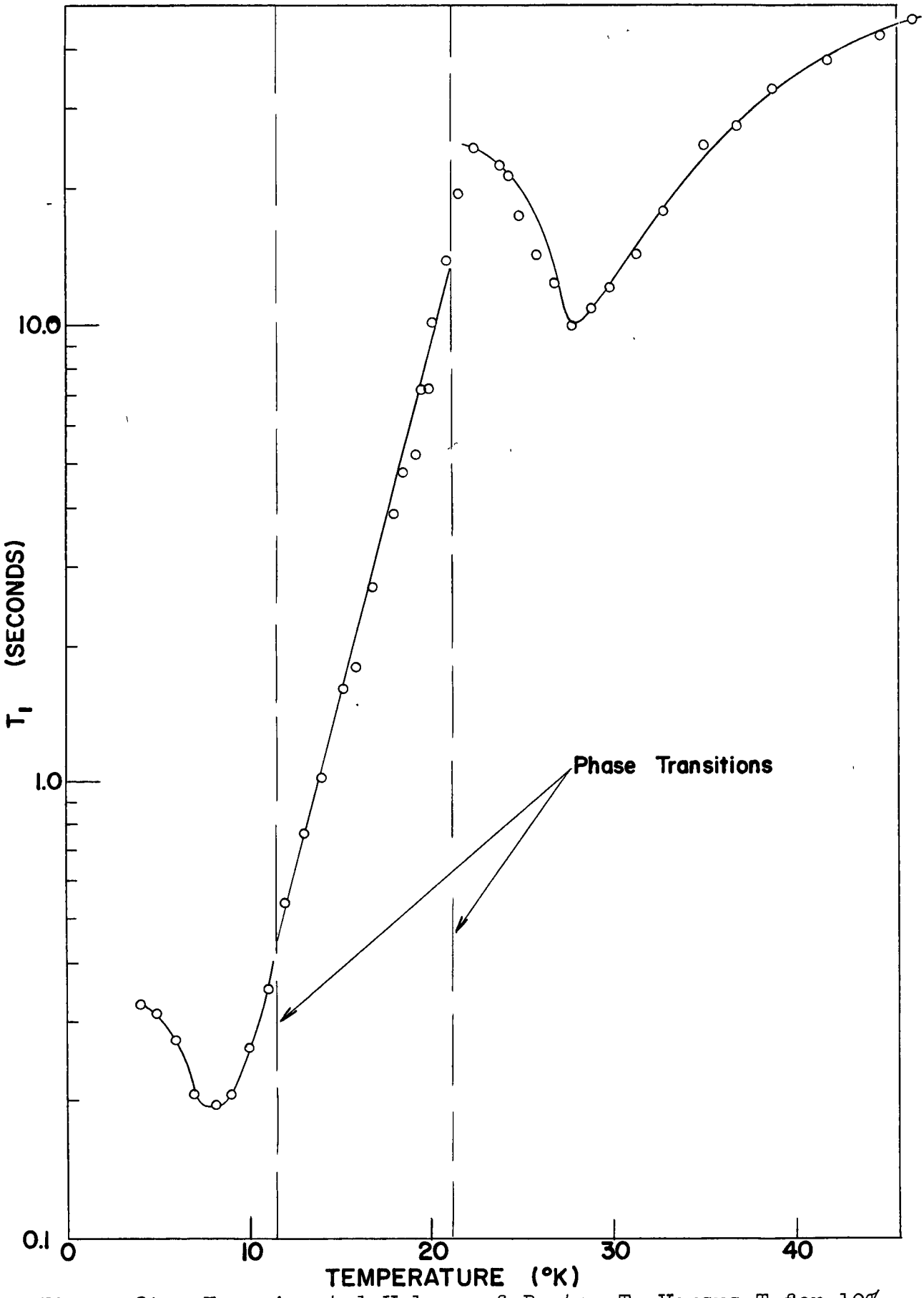

Figure 30. Experimental Values of Proton T_1 Versus T for 10% CD_4-90% CH_4 Mixture

by a "spin temperature". As far as our experiments are concerned the lengthening of T_1 could help to explain the long $(T_1)_{min}$ for CH_4. On the other hand, why should a distribution of correlation times only show up for CH_4 and not for CD_4? Non-exponential relaxation has only been observed for CH_4 and CH_4 - CD_4 mixtures, although only in a small temperature range near the upper minimum.

The Line Shape: 5:10

For all the systems studied, oscilloscope photographs were taken of the induction tail at a number of temperatures. As the shape of the induction tail varied only very slightly throughout the temperature range for all of the systems, the results will not be presented. The results agree in principle with those reported for the proton spin system by Wolf (1964). The line shape in particular T_2 of the deuteron resonance also shows very little change with temperature. A cursory examination of the data does show that the higher moments of the line are slightly temperature dependent. It has also been checked in a couple of instances, and shows that the Lowe beats can be fitted using the equation (4-14).

Summary: 5:11

As has been shown in this chapter, the relaxation properties of the methane system at low temperatures have many interesting features. These results can be used, in principle, to arrive at a better understanding of the nature of the various phase transitions and of the properties of the three phases. The main qualitative features of the results are:

1. Rapid changes of T_1 occur in the immediate vicinity of many of the phase transitions. In cases where rapid changes of T_1 were not observed, it was possible to give experimental reasons for their non-appearance. One can tentatively conclude that all of the phase transitions have associated with them large changes in the orientational states and/or in the rates of molecular reorientation. This is in qualitative agreement with entropy measurements.

2. Above the upper phase transition (phase I), T_1 is slowly temperature dependent in all cases, except that a pronounced minimum occurs in all measurements of T_1 in CH_4 (including experiments done on mixtures). The mechanism for these high temperature minima is not understood at all. The slow overall temperature dependence also remains to be explained.

3. T_1 decreases very rapidly with decreasing temperature below the upper phase transition (phases II and III) in all cases and goes through a minimum value in phase III.

In this chapter, the T_1 measurements were discussed in terms of the conventional theory of relaxation by intra-molecular interactions due to molecular reorientation. In the conventional theory the effective strength of the intra-molecular interactions is usually taken to be independent of temperature so that the variation of T_1 versus T gives the temperature dependence of the correlation time τ_c for molecular reorientation. In the discussion here, it was assumed that the relevant correlation functions decay exponentially in time. Some of the difficulties involved in using this type of interpretation to obtain quantitative information about the systems studied are as follows:

1. The minimum values of T_1 are known from the conventional theory if the intra-molecular interactions are known. For the protons, the observed $(T_1)_{min}$ are all too long, and in many cases by factors of 20 or even more. Furthermore, the values of $(T_1)_{min}$ in the CH_4-Kr mixtures at low temperatures depend strongly on the Kr concentration although the temperature independent values of T_1 at high temperatures are independent of Kr concentration.

2. The dependences of τ_c versus T extracted from the T_1 data are not governed by a single activation energy as is common for many classical systems.

3. There is no existing theory of molecular reorientation which is capable of describing the nature of the phase transitions in methane.

4. The present inadequate knowledge of the crystal structure of solid methane above and below the phase transition (see section 2:4) does not exclude the possibility of a small change in the crystal structure on passing through the phase transition. Such a change could account for the discontinuities in T_1 versus T through its effect on the molecular energy levels. Recent investigations have revealed such a structure change in solid H_2 at its phase transition occurring at $1.5^{\circ}K$ (Clouter et al. 1965, and Mills et al. 1965).

The conventional theory does give approximately the correct values of $(T_1)_{min}$ for the deuterons, but the uncertainty in the quadrupole coupling constant is great. In addition, the temperature dependence of T_1 in CH_4 at 4.4 mcs can be predicted approximately from the results at 28.5 mcs.

In the next chapter, the consequences of the detailed model of the molecular energy levels in phase III proposed by Morrison et al. will be examined. When this is combined with a simple picture of the phonon-molecular rotation interactions, there are indications that the results can be quantitatively interpreted in terms of molecular parameters. Also, some of the possible consequences of the quantum mechanical nature of the systems being considered will be discussed.

CHAPTER 6.

FURTHER DISCUSSION OF THE EXPERIMENTAL RESULTS

Review of the classical calculation of the correlation functions: 6:1

As has been discussed in Chapter 4, T_1 is related to Fourier transforms of correlation functions of functions of the molecular orientation insofar as contributions of intramolecular interactions to spin-lattice relaxation are concerned. The calculation of such correlation functions for a general class of systems is difficult. However, useful results have been obtained for simple models in which for example, the molecular orientations are taken to be random functions of time.

As an example, suppose that a given vector in a molecule is initially oriented in the solid angle between Ω_0 and $\Omega_0 + d\Omega_0$ with probability $p(\Omega_0)d\Omega_0$ and that reorientation proceeds by discrete random jumps with equal probability to any other element of solid angle between Ω and $\Omega + d\Omega$. Then the expression for the correlation function of a function of $\Omega(\tau)$, $y(\Omega(\tau))$, is given by

$$G(\tau) = \iint d\Omega\, d\Omega_0\, p(\Omega_0)\, P(\Omega, \Omega_0, \tau)\, y(\Omega_0)\, y^*(\Omega) \qquad (6\text{-}1)$$

where $P(\Omega, \Omega_0, \tau)d\Omega$ is the probability that the molecule is oriented between Ω and $\Omega + d\Omega$ at time τ if it is

initially oriented between Ω_o and $\Omega_o + d\Omega_o$. For the above model

$$P(\Omega_o, \Omega, \tau) = \delta(\Omega - \Omega_o)\, e^{-\tau/\tau_c} + \frac{1}{4\pi}\left(1 - e^{-\tau/\tau_c}\right) \tag{6-2}$$

where $\delta(\Omega - \Omega_o)$ is the Dirac δ-function and τ_c is the average time spent by a molecule in a given orientation.

Usually, it is appropriate to assume random a priori orientations, i.e.,

$$p(\Omega_o) = \frac{1}{4\pi} \tag{6-3}$$

in which case, substitution of equation (6-2) into equation (6-1) gives

$$G(\tau) = \langle |y|^2 \rangle\, e^{-\tau/\tau_c} \tag{6-4}$$

This type of model has been used recently for the interpretation of relaxation by quadrupolar interactions in solids (Alexander, 1965).

The opposite limiting case is the rotational diffusion model in which the individual jumps are assumed to be very small. As mentioned earlier, this case has been examined in great detail by Hubbard (1962) and others (Steele, 1963). This case would be most applicable to liquids composed of large (classical) molecules. The correlation function of $y(\tau)$ for the rotational diffusion model is of the same form as equation (6-4) and τ_c in this case is expressed in terms of the rotational diffusion constant. The passage from the small jump limit to the large jump limit has been discussed by Ivanov (1964).

In the preceding chapter, the experimental data have been analyzed under the assumption that the correlation functions are exponential as given in equation (6-4). However, the usual classical interpretation of the parameters appearing in equation (6-4) were found to be inconsistent with most of the data. The $y(\Omega)$ introduced above is identified with the spherical harmonic of order 2, namely $Y_{2m}(\Omega)$. The predicted minimum value of T_1 for a given resonance frequency is determined completely within the above models by $\langle |y|^2 \rangle$, which is $\frac{1}{4\pi}$ for $Y_{2m}(\Omega)$ if all orientations are equally probable. It has been found that the experimental values of $(T_1)_{min}$ are consistently larger than the theoretical predictions on this basis.

Secondly, the temperature dependences of τ_c as given by the experimental temperature dependence of T_1 assuming that $G(\tau)$ is given by equation (6-4) cannot be described in terms of an activation energy for most of the cases studied, i.e., the formula

$$\tau_c = \tau_o \, e^{T_o/T} \tag{6-5}$$

is not obeyed. For comparison with other systems where equation (6-5) is obeyed see Alexander (1965).

The Low Lying States of Methane: 6:2

The above mentioned discrepancies are not at all surprising in view of the fact that the methane molecules have

very small moments of inertia. For example, the rotational constant of CH_4 in equation (2-2) is B = (7.68°K)k. Therefore, it would not be surprising if it were necessary to take into account the quantum mechanical properties of the rotational energy levels in order to describe adequately the molecular reorientation in the temperature range in which these experiments were carried out.

There is in fact, some information available about the nature of the low lying molecular states on the basis of accurate heat capacity measurements by Morrison and his collaborators (Colwell, Gill and Morrison, 1965). Figure (31) is a schematic representation of the lowest rotational energy levels of CH_3D and CHD_3 according to their measurements. Roughly speaking, the 12 lowest rotational states are considered to consist of two groups of levels having degeneracies g_o and g_1 respectively, with $g_1/g_o = 3$. The average splittings between these groups are given as approximately 1.77°K for CH_3D and 1.26°K for CHD_3. For CH_4, the residual entropy indicates that the so-called T symmetry species' 3-fold spatial degeneracy is partially removed, the ground state corresponding to $g_o = 2$ and the excited state to $g_1 = 1$. The spatial degeneracies of the A and E species are completely removed. For CD_4, no removal of the 3-fold spatial degeneracy of the T modification is implied by the entropy measurements.

Calculation of the correlation functions for molecules having discrete energy levels: 6:3

Let the rotational states of a molecule be denoted by the index m = 1,2,- etc., and suppose that the expectation value of the intra-molecular interaction in question in the state m is y_m. The variable y is considered to be a random function of time because of the fact that transitions are induced between molecular states m,n, etc. by interactions which couple the molecular orientations to the lattice vibrations and so forth. If y is a "stationary", random function of time, the correlation function $G(\tau)$ of y may be written in the form (Abragam, 1961, p271)

$$G(\tau) = \sum_{m,n} p_m P_{mn}(\tau) y_m y_n \qquad (6\text{-}6)$$

where p_m is the a priori probability that a molecule is in the state m, $P_{mn}(\tau)$ is the probability that a molecule is in the state n at time τ if it is in the state m at time $\tau = 0$,

and it has been assumed that $P_{mn}(\tau) = P_{mn}(-\tau)$. For this case,

$$G(\tau) = G(-\tau) \qquad (6\text{-}7)$$

In Chapter 4, the consequences of an exponential form for the correlation function $G(\tau)$ have been examined. It should be noted that an exponential form does not hold in general for the $G(\tau)$ given by equation (6-6) even when $P_{mn}(\tau)$ are governed by rate equations, i.e.,

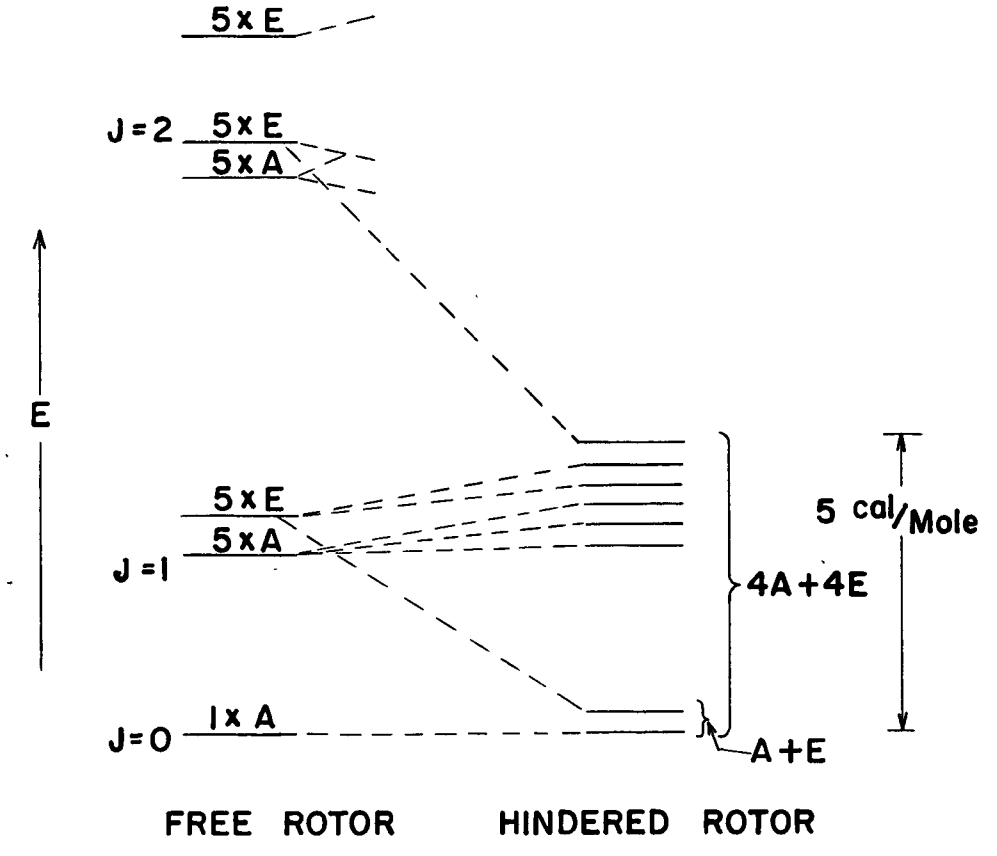

Figure 31. The Energy Level Diagram Proposed by Colwell, Gill and Morrison (1965) for CH_3D and CD_3H

$$\frac{dP_{mn}}{dt} = - P_{mm} \sum_{n' \neq n} W_{mn'} + \sum_{n' \neq n} W_{n'm} P_{mn'} \qquad (6\text{-}8)$$

where $W_{nn'}$ is the probability per unit time that a molecule undergoes a transition from the state n to the state n'. The initial conditions are

$$P_{mn}(0) = \delta_{mn} \qquad (6\text{-}9)$$

Two Energy Level Case: 6:4

In order to examine the model of Colwell, Gill, Morrison in more detail, assume a two energy level model in which the lower energy level is g_o fold degenerate and the upper level is g_1 fold degenerate. The energy separation of the levels is taken to be kT_o

$j = g_o+1, \ldots, g_o+g_1$ ——————— $E_1 = kT_o$

$i = 1,2,\ldots, g_o$ ——————— $E_o = o$

Let the index i denote the lower levels, $i = 1,2,\ldots,g_o$ and the index j denote the upper levels, $j=g_o+1, g_o+2,\ldots, g_o + g_1$.

Let $y = y_i$ in the i^{th} state of the lower level, and $y = y_j$ in the j^{th} state of the upper level.

Therefore,

$$\left.\begin{aligned} p_i &= p_o \quad \text{independent of } i \\ p_j &= p_1 \quad \text{independent of } j \end{aligned}\right\} \text{ equilibrium probabilities}$$

$$p_1/p_o = e^{-T_o/T} \tag{6-10}$$

$$g_o p_o + g_1 p_1 = 1 \qquad \text{Normalization} \tag{6-11}$$

To complete the model, the following simplifying assumptions are made,

W_0 = transition probabilities between any pair of states in 0,

W_1 = transition probabilities between any pair of states in 1,

W_+ = transition probabilities between any state in 0 and any state in 1,

W_- = transition probabilities between any state in 1 and any state in 0.

Then, $p_o W_+ = p_1 W_-$, by detailed balance. (6-12)

From equation (6-6) and the above definitions,

$$G(\tau) = p_o\left[\sum_{i,i'} P_{ii'}\, g_i g_{i'} + \sum_{i,j} P_{ij}\, g_i g_j\right] + p_1\left[\sum_{j,j'} P_{jj'}\, g_j g_{j'} + \sum_{i,j} P_{ij}\, g_i g_j\right] \tag{6-13}$$

Now, by substituting the transition probabilities defined above into the rate equations (6-8), the conditional probabilities P_{kl} in the expression for $G(\tau)$ may be found. The calculations are very lengthy, but straightforward and the results are:

$$\begin{aligned}
P_{ii'}(\tau) &= (\delta_{ii'} - 1/g_o)\, e^{-\tau/\tau_o} + g_1/g_o\, p_1\, e^{-\tau/\tau_{o1}} + p_o \\
P_{jj'}(\tau) &= (\delta_{jj'} - 1/g_1)\, e^{-\tau/\tau_1} + g_o/g_1\, p_o\, e^{-\tau/\tau_{o1}} + p_1 \\
P_{ij}(\tau) &= -p_1\, e^{-\tau/\tau_{o1}} + p_1 \\
P_{ji}(\tau) &= -p_o\, e^{-\tau/\tau_{o1}} + p_o
\end{aligned} \tag{6-14}$$

where use has been made of equations (6-11) and (6-12) and

$$\frac{1}{\tau_0} = g_0 W_0 + g_1 W_+$$

$$\frac{1}{\tau_1} = g_1 W_1 + g_0 W_- \qquad (6\text{-}15)$$

$$\frac{1}{\tau_{01}} = g_0 W_- + g_1 W_+$$

τ_0 and τ_1 are the average lifetimes of a molecule in an individual i and j level respectively, while τ_{01} is the time constant for the establishment of a Boltzman distribution between the two groups of levels.

Substituting equations (6-11), (6-12) and (6-14) into equation (6-13), the correlation function $G(\tau)$ may be written in the form,

$$\begin{aligned} G(\tau) = {} & g_0 p_0 \left[\langle y^2 \rangle_i - \langle y \rangle_i^2 \right] e^{-\tau/\tau_0} \\ & + g_1 p_1 \left[\langle y^2 \rangle_j - \langle y \rangle_j^2 \right] e^{-\tau/\tau_1} \\ & + g_0 g_1 p_0 p_1 \left[\langle y \rangle_i - \langle y \rangle_j \right]^2 e^{-\tau/\tau_{01}} \end{aligned} \qquad (6\text{-}16)$$

where $\langle y \rangle_i$ and $\langle y \rangle_j$ are the average values of y for a system of molecules restricted to the i and j states respectively, etc.

$$\langle y \rangle_i = \frac{1}{g_0} \sum_i y_i \quad , \text{ etc.}$$

$$\langle y^2 \rangle_i = \frac{1}{g_0} \sum_i y_i^2 \quad , \text{ etc.} \qquad (6\text{-}17)$$

Using equations (6-10) and (6-11))

$$p_0 = \left(g_0 + g_1 e^{-T_0/T} \right)^{-1}$$

$$p_1 = \left(g_0 + g_1 e^{-T_0/T} \right)^{-1} e^{-T_0/T} \qquad (6\text{-}18)$$

If all three terms in equation (6-16) are non-zero, the analysis of the experimental data in Chapter 5 is invalid, since it was assumed there that the correlation function could be expressed in terms of a single correlation time. The expressions for the relaxation rate would be expressed in terms of the Fourier transform of $G(\tau)$ as in equations (4-6) and (4-7), but the Fourier transform would then consist of the sum of 3 terms of the form of equations (4-11).

As will be discussed later, there are systems of interest in which the first two terms in equation (6-16) are zero or small. In this case, one obtains,

$$\frac{1}{T_1} = C_{c1}\, 4\pi\, g_0 g_1 P_0 P_1 \left[\langle y\rangle_i - \langle y\rangle_j\right]^2 J(x_{01}) \qquad (6\text{-}19)$$

where $C_{c1} = \frac{6}{5}\frac{\gamma^4\hbar^2 I(I+1)}{b^6\omega_0}$ (CH_4, dipolar interactions) see equation (4-11) (6-20)

$$= \frac{3}{80}\frac{1}{\omega_0}\left[\frac{eQ}{\hbar}\frac{\partial^2 V}{\partial z^2}\right]^2 \quad (CD_4, \text{ quadrupolar interactions}) \text{ see equation (4-12)} \qquad (6\text{-}21)$$

is the classical coefficient,

$$x_{01} = \omega_0 \tau_{01} \qquad (6\text{-}22)$$

The quantity y is identified with the spherical harmonic Y_{2m}. Whereas, in the classical case $\langle |Y_{2m}|^2\rangle = 1/4\pi$ (equation 4-9)), this is replaced by

$$\langle |Y_{2m}|^2\rangle_{eff} = \langle |Y_{2m}|^2\rangle - \langle Y_{2m}\rangle^2 \qquad (6\text{-}23)$$

$$= g_0 g_1 P_0 P_1 \left[\langle y\rangle_i - \langle y\rangle_j\right]^2$$

for this special case. Therefore, the effective strength of the interaction is temperature dependent in general.

The Temperature Dependence of the Transition Probabilities: 6:5

In the previous section the correlation times were expressed in terms of the transition probabilities W_+, W_-, W_o and W_1. If one believes that the molecular reorientations are caused by the coupling between the molecules and the phonons, then the temperature dependences of the transition probabilities can be predicted using a formalism very similar to that used in the theory for electron spin-lattice relaxation (Jeffries, 1963). In electron spin-lattice relaxation the only important relaxation processes for a two-level system are the "direct" and the "Raman processes." Higher-order relaxation processes are also possible, but the transition probabilities due to these processes are negligible.

In the direct process one imagines that the molecules are coupled to the phonons by the crystal field interaction with the molecule. This interaction acts as a time-dependent relaxation perturbation inducing a transition between the states of the molecule simultaneously with the creation or annihilation of a phonon of energy $\delta = kT_o$, thus conserving energy. Using the properties of the matrix elements for the creation and annihilation of phonons, one

can derive the following:

$$W_- = A\left(\bar{m}_\delta + 1\right)$$

$$W_+ = A\,\bar{m}_\delta$$

where $\bar{m}_\delta = \left(e^{T_0/T} - 1\right)^{-1}$

The constant A is dependent on the nature of the relaxation perturbation. Substituting these in equation (6-15)

$$\frac{1}{\tau_{01}} = A\,\frac{g_0 + g_1 e^{T_0/T}}{e^{T_0/T} - 1} \qquad (6\text{-}24)$$

The usual case considered in Electron Spin Resonance is $g_0 = g_1 = 1$,

$$\frac{1}{\tau_{01}} = A \coth\left(T_0/2T\right)$$

Unlike the direct process, the Raman process involves the simultaneous absorption of a phonon of energy δ_1 and the emission of another of energy $\delta_2 = \delta_1 + \delta$ along with a transition of the molecule from state $|j\rangle$ to state $|i\rangle$ and vice versa. In contrast to the direct process where the phonon energy must equal the energy level splitting, the only requirement now is that difference of the two phonon energies be δ for energy conservation. Since $\delta << k\,\Theta_D$ (the Debeye temperature), the entire phonon spectrum is available.

$$W_- \propto \int_\delta^{k\Theta_D} \frac{e^{\delta_1/kT}}{\left(e^{\delta_1/kT} - 1\right)\left(e^{\delta_2/kT} - 1\right)}\,\delta_1^3\,\delta_2^3\,d\delta_1$$

$$W_+ \propto \int_\delta^{k\Theta_D} \frac{e^{\delta_2/kT}}{\left(e^{\delta_1/kT} - 1\right)\left(e^{\delta_2/kT} - 1\right)}\,\delta_1^3\,\delta_2^3\,d\delta_2$$

Now if $\delta \ll kT$ in the temperature range where Raman process is dominant then $W_- \approx W_+$. Moreover, if $\delta \ll kT \ll k\Theta_D$ then (Abragam, 1961, p. 408)

$$W_+ \approx W_- \propto T^7 \tag{6-25}$$

For the special case of nuclear quadrupolar relaxation in a cubic crystal, it has been shown (van Kranendonk, 1954) that the T^7 law only holds for $T \leq 0.02\ \Theta_D$. Until the form of the phonon-molecule interaction is known for solid methane, it will not be known over what range of temperatures the T^7 law is valid for the systems being considered.

Transitions between any pairs of levels within the degenerate sets of levels, which are described by the transition probabilities W_1 and W_o can occur as a resonant process through the intermolecular coupling which exists between neighbouring molecules in these states. Since no energy is exchanged with the phonons in such a process, it is likely that W_o and W'_1 would be temperature independent.

Temperature dependence of T_1 for some special cases: 6:6

A. Two-level system:

The simplest case is that in which the degeneracy of the molecular levels is completely removed and in which only the lowest two levels are appreciably populated. In this case, it is obvious that

$$\langle y^2\rangle_i = y_o^2 = \langle y\rangle_i^2$$
$$\langle y^2\rangle_j = y_1^2 = \langle y\rangle_j^2$$

$$g_o = g_1 = 1 \tag{6-26}$$

$$P_o = \frac{1}{1 + e^{-T_o/T}}$$

$$P_1 = \frac{e^{-T_o/T}}{1 + e^{-T_o/T}}$$

At high temperatures, $T_o/T \ll 1$ and hence $P_o \approx P_1 \approx \frac{1}{2}$, so that equations (6-16) and (6-26) give

$$G(\tau) \simeq y^2 e^{-\tau/\tau_{o1}} \tag{6-27}$$

where we have defined y by

$$2y = y_o - y_1 \tag{6-28}.$$

Therefore, we conclude that at high temperatures, for a two-level system, the correlation time τ_c obtained from the analysis of Chapter 5 is to be identified with τ_{o1}. Therefore, using equations (6-15), (6-24) and (6-25)

$$\frac{1}{\tau_c} = \frac{1}{\tau_{o1}} \approx W_+ + W_- \tag{6-29}$$
$$\approx A \coth(T_o/2T) + B T^7$$

It has been shown in Figures (16) and (24) that equation (6-29) does fit the plot of τ_c versus T derived from the experimental data. The curves shown in Figures (16) and (24) correspond to the values of the parameters

$$
\begin{aligned}
A &= 0.88 \ \text{sec}^{-1} && CH_4 \\
&\quad 0.36 \ \text{sec}^{-1} && CH_3D \\
B &= 1.5 \times 10^{-7} \ \text{sec}^{-1}(^{\circ}K)^{-7} && CH_4 \\
&\quad 5.9 \times 10^{-8} \ \text{sec}^{-1}(^{\circ}K)^{-7} && CH_3D \\
T_o &= 7.0 \ ^{\circ}K && CH_4 \\
&\quad 8.8 \ ^{\circ}K && CH_3D.
\end{aligned}
\tag{6-30}
$$

This analysis is now seen to be inconsistent with the assumption that $T_o << T$ in the experimental region. If one includes the temperature dependences of p_o and p_1, equation (6-16) is replaced by

$$G(\tau) = 4g^2 \frac{e^{-T_o/T}}{(1+e^{-T_o/T})^2} \quad e^{-\tau/\tau_{o1}} \tag{6-31}$$

Therefore, $\langle |Y_{2m}|^2 \rangle_{eff}$ is now strongly temperature dependent as indicated by equations (6-23) and (6-31). It is therefore concluded that in spite of the excellent agreement given by equation (6-29) and (6-27), the two-level model is inconsistent with the experimental data for CH_4 and CH_3D.

B. The two energy-level system with degeneracies

There are many two energy-level systems in which the conditions under which equation (6-19) is valid are satisfied. These conditions are $\langle y^2 \rangle_i = \langle y \rangle_i^2 = y_o^2$, etc. For example, a molecule in the J = 1 state subjected to an axially symmetrical crystalline field has its degeneracy partially removed such that $g_o/g_1 = \frac{1}{2}$ of 2. Similarly, a molecule in the J = 2 state subjected to a field having cubic symmetry

has two energy levels with degeneracies which satisfy the equation $g_o/g_1 = 3/2$ or $2/3$. For these and other similar cases, the expectation values of Y_{2m} are identical for all degenerate states. Therefore, the assumption that the first two terms of equation (6-16) vanish is valid for such systems. This is not necessarily true of the spin-rotation interaction as will be discussed in section 6:8.

As stated earlier, the model of Colwell, Gill and Morrison, 1965 for CH_3D and CHD_3 corresponds to a two energy-level system with $\omega = 3$, where ω is defined as

$$\omega = g_1/g_o \tag{6-32}$$

The other parameters are

$$\begin{aligned} T_o &= 1.77^oK \qquad \text{for } CH_3D \\ T_o &= 1.26^oK \qquad \text{for } CHD_3. \end{aligned} \tag{6-33}$$

For these systems, the expression for T_1 given by equation (6-19) becomes

$$\frac{1}{T_1} = D\, f(T_o/T)\, y[x_{o1}(T_o/T)] \tag{6-34}$$

where

$$D = 16\pi\omega y^2 C_{C1} \tag{6-35}$$

$$f(T_o/T) = \frac{e^{-T_o/T}}{(1 + \omega e^{-T_o/T})^2} \tag{6-36}$$

and $y(x_{o1})$ has been given by equations (5-5) and (6-22). It is seen from equations (6-34) and (6-36) that T_1 is dependent on temperature because the effective strength of the spin-lattice interaction is temperature dependent as given by

$f(T_o/T)$ and x_{o1} is temperature dependent because of the temperature dependence of the correlation time τ_{o1}. The dependence of y on x has been plotted in Figure (15). The dependence of f on T_o/T is shown in Figure (32). The limiting value of f at the high and low temperature ends corresponds to

$$\lim_{\frac{T_o}{T}\to 0} f(T_o/T) = \frac{1}{1+\omega^2}$$

$$\lim_{\frac{T_o}{T}\to \infty} f(T_o/T) = \exp(-T_o/T) \qquad (6\text{-}37)$$

Thus $f(T_o/T)$ decreases rapidly with decreasing temperature for $T \ll T_o$. At temperatures $T_o \ll T$ $f(T_o/T)$ closely approximates its asymptotic value which is sensitive to ω. For $\omega \leq 1$, f is a monotonically increasing function of T, but for $\omega > 1$ f goes through a maximum. As a consequence, the dependence of the effective strength of the spin-lattice interaction on temperature is a sensitive function of ω.

From the discussion in section 6:5, the effect of the interaction between the molecules and the phonons on τ_{o1} can be expressed in terms of the "direct" and "Raman" processes as follows

$$\frac{1}{\tau_{o1}} = A g_o \frac{1+\omega e^{-T_o/T}}{1-e^{-T_o/T}} + B T^7 \qquad (6\text{-}38)$$

where the approximations made in deriving the T^7 term (Raman term) are that $T_o \ll T \ll \theta_D$.

At low temperatures the direct process predominates and for $T \ll T_o$, it follows that τ_{o1}, and hence x_{o1}, is independent of temperature. Therefore, for $T \ll T_o$, T_1

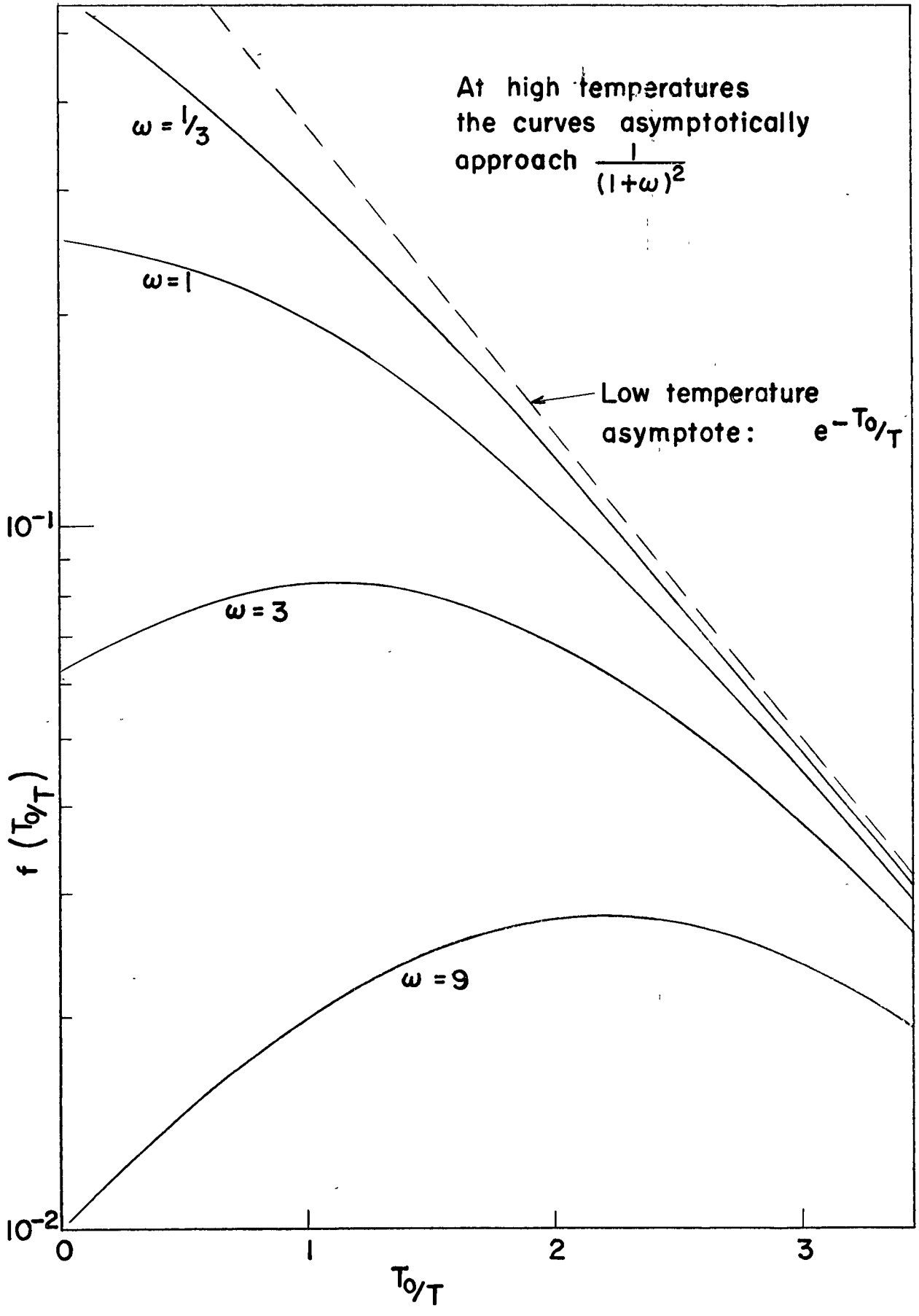

Figure 32. The Temperature Dependence of the Effective Interaction Strength for Several Values of ω

exp (+ T_o/T). For $T >> T_o$, on the other hand, f (T_o/T) is independent of temperature and $1/T_1 \propto y(x_{ol})$. The temperature T_{min} at which the minimum in T_1 versus T occurs depends on A, B, T_o, and the frequency ω_o, which can be varied experimentally. Figure (33) shows how T_1/T_{1min} depends on T/T_{min} for different values of T_o/T_{min}. These plots are valid for a special case characterized by $\omega = 3$, B = 0. This assumes that the temperature is sufficiently low that the Raman term is negligible.

For comparison, the experimental data for CH_4, CH_3D and CD_4 are plotted on the same graph. It is seen that the experimental values of T_1 for CD_4 and CH_3D vary much more rapidly with temperature just below T_{min} than any of the theoretical curves. The most plausible reason for this is that the Raman term has been neglected since B has been chosen to be zero. That the Raman term is probably important for these cases is indicated by Figures (19) and (16) in Chapter 5, where the term giving the high temperature behaviour $\tau_c^{-1} \propto T^7$ is still important at T_{min}. The reader is reminded, however, that $f(T_o/T)$ has been taken to be constant in the analyses of Figures (19) and (16). For CH_4, Figure (24) indicates that the T^7 term is small near T_{min}. Indeed, the experimental values of T_1 for CH_4 are in reasonable agreement with the theoretical curves of Figure (33) for T_o/T_{min} between 0.05 and 0.175 for T/T_{min} between 0.5 and 1.5. Because there are several parameters in the theoretical expression whose values have been

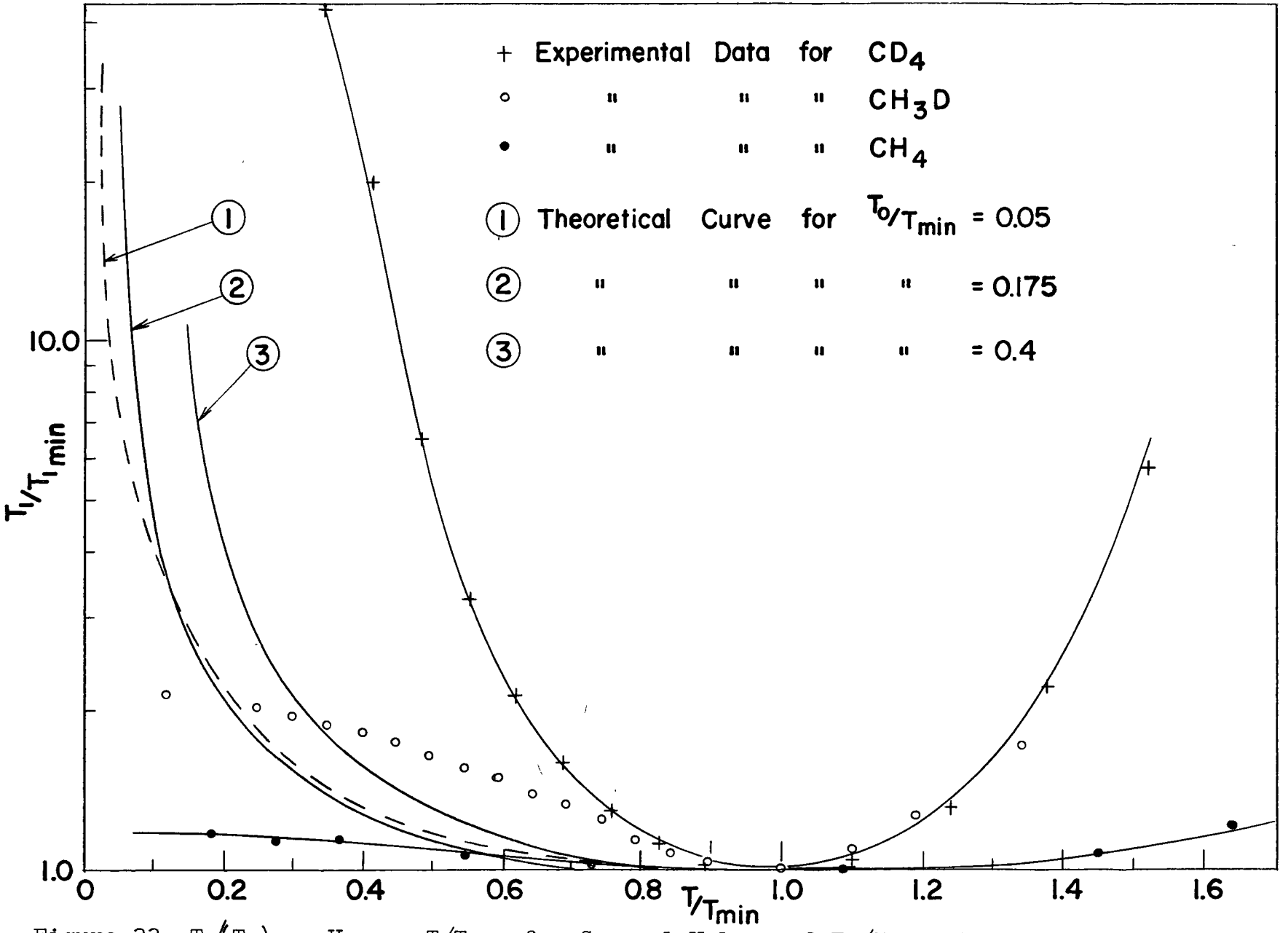

Figure 33. $T_1/(T_1)_{min}$ Versus T/T_{min} for Several Values of T_o/T_{min}, Taking into Account Only the Direct Process

chosen arbitrarily, this agreement has only qualitative significance.

Colwell, Gill and Morrison (1965) give the parameters $\omega = 3$ and $T_o = 1.77^oK$ for CH_3D. For this value of T_o, $f(T_o/T)$ varies by only about 10% for $T > T_{min}$. If this is so and if the contribution to $1/\tau_{01}$ due to the Raman term really does vary as T^7, then using the extrapolation of the T^7 curve in Figure (16), the fractional contribution of the BT^7 term to τ_{01}^{-1} in equation (6-38) may be estimated at $T_{min} = 10.1^oK$. This is sufficient information to determine Ag_o and B in equation (6-38) since it is known that $\omega_o \tau_{01} = 0.62$ at T_{min}. Then using the value of $T_o = 1.77^oK$, we have calculated τ_{01}^{-1} versus T for different values of ω as given by equation (6-38). Using the calculated values of $f(T_o/T)$ shown in Figure (32) and equation (6-34), calculated values of T_1 versus T have been plotted in Figure (34) for $\omega = 1/3$, 1, 3, and 9. The experimental values of T_1 versus T for CH_3D are shown on the same plot. A comparison between Figures (33) and (34) shows that this crude correction for the Raman term results in better agreement between the model and experiment, but it is impossible to distinguish between different values of ω on the basis of the available data. Better agreement with experiment could be obtained between 5^oK and 10^oK for $\omega = 3$, if B were chosen to be a little larger, but the very slow dependence of T_1 on T below 5^oK could not be reproduced for $\omega = 3$ and $T_o = 1.77^o$ K. It would appear that very similar remarks apply to CD_3H.

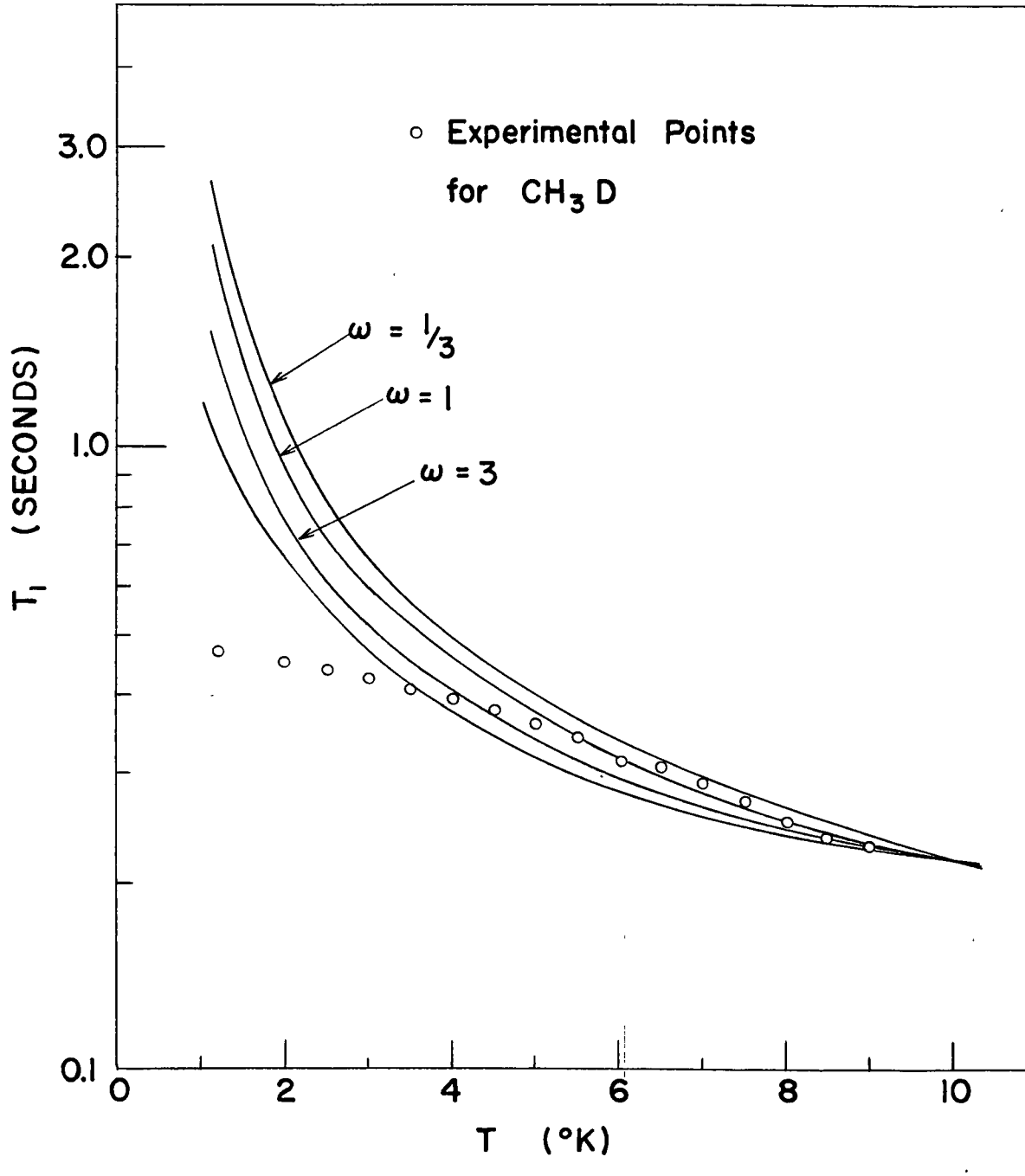

Figure 34. Theoretical Curves of T_1 Versus T Taking into Account the Raman Term for CH_3D as Described in the Text

It would be very desirable to have an independent check using NMR of the parameters T_o and ω which appear in the model of Colwell, Gill and Morrison. To do this T_1 must be studied in the region $T \ll T_o$ where $T_1 \propto \exp(T_o/T)$. This means going down to temperatures of the order of 0.3^oK using a liquid He^3 cryostat. In this region, the relationship $\omega_o \tau_{o1} \gg 1$ should be satisfied so that T_1 is given by

$$\frac{1}{T_1} = \frac{2D}{\omega_o} \frac{f(T_o/T)}{\tau_{o1}} \qquad T \ll T_{min} \qquad (6\text{-}39)$$

Figure (35) shows a plot of $\log(1/T_1)$ versus T_o/T for different values of ω in the region $T \ll T_{min}$ if only "direct" processes are important.

The study of T_1 down to 0.3^oK is a very important experiment insofar as the evaluation of the parameters in this model is concerned. If a rapidly increasing T_1 is not observed at these temperatures, then the assumption that $\langle \mathcal{J}^2 \rangle_i = \langle \mathcal{J} \rangle_i^2$ made earlier would have to be re-considered (see section 6:8).

Spin Temperature: 6:7

In the discussion of the experimental results in this thesis it has been assumed that the approach to equilibrium of the nuclear magnetization can be described in terms of a single time constant T_1. Experimentally, this has indeed been found to be true, except for some cases in the vicinity

of the unexplained high temperature "T_1 minimum" in CH_4. Yet, there are at least two reasons for expecting a possible deviation from exponential behaviour.

Case (1) The splittings of the molecular energy levels may vary from molecule to molecule because the crystalline electric fields may vary. Thus, there may not be a unique correlation time for this system. This seems to be the case in solid H_2 below $2^{\circ}K$, where a non-exponential relaxation is observed (Sugawara et al., 1956 and Hardy, 1965).

Case (2) There may exist different spin species each having non-zero nuclear spins. If so, and if these species have different orientational states, they may relax at different rates. Indeed, one implication of Tomita's (1953) analysis of the low temperature properties of CH_4 is that the A species (I = 2) cannot relax. According to his results, only the T species (I = 1) can relax.

The two effects described above need not manifest themselves in a non-exponential relaxation behaviour. The reason for this is indicated in the following diagram (Figure 36) in which we imagine two spin species a and b which have spin-lattice relaxation times T_1^a and T_1^b respectively. The two spin systems can also exchange energy with each other and, if not coupled to the lattice, their spin temperatures approach a common spin temperature with a time constant T_2^{ab}.

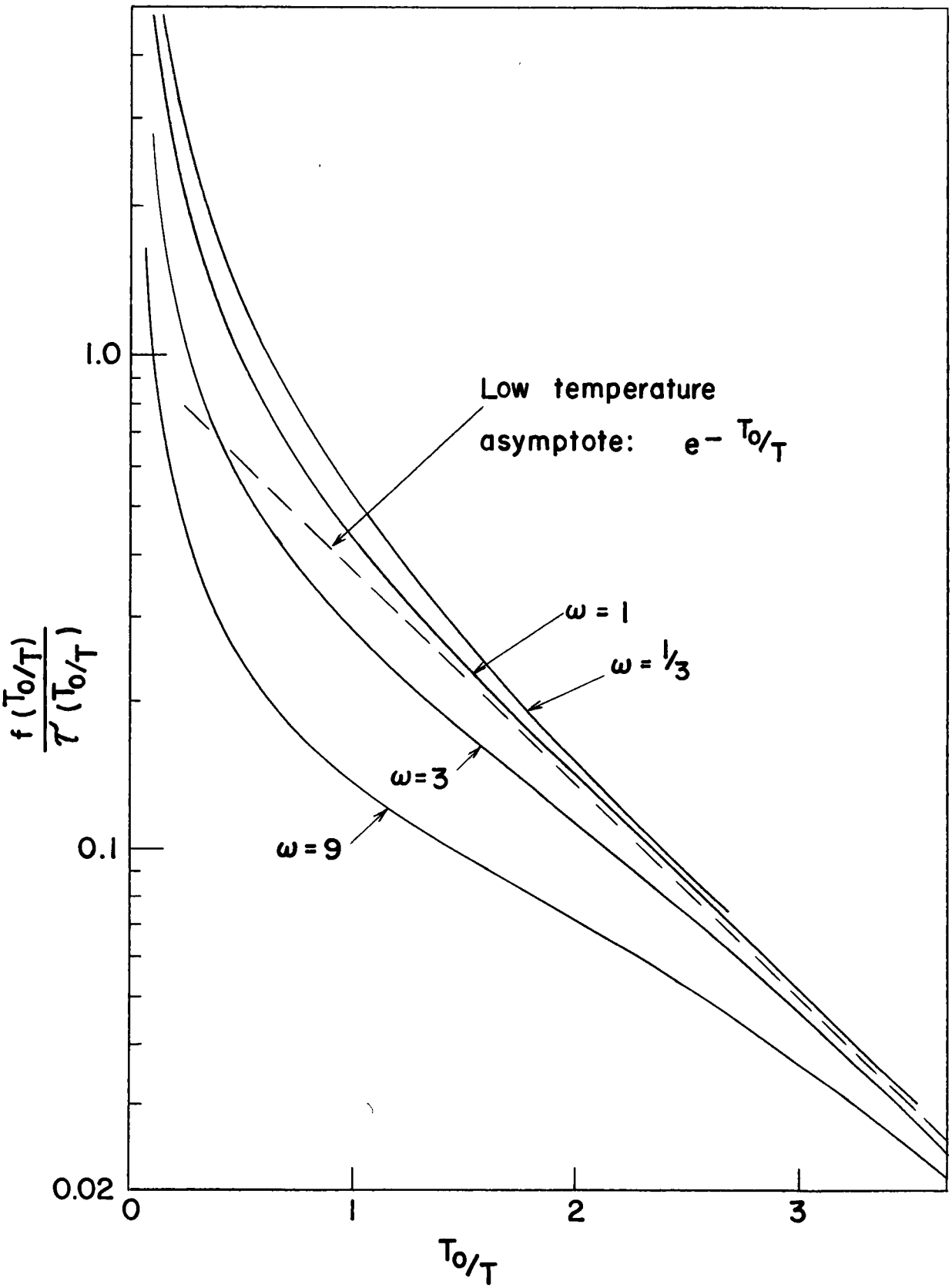

Figure 35. Theoretical Plots of $1/T_1$ Versus T_0T^{-1} in the Low Temperature Limit, $\omega_0 \tau_c >> 1$, Including Direct Process Only

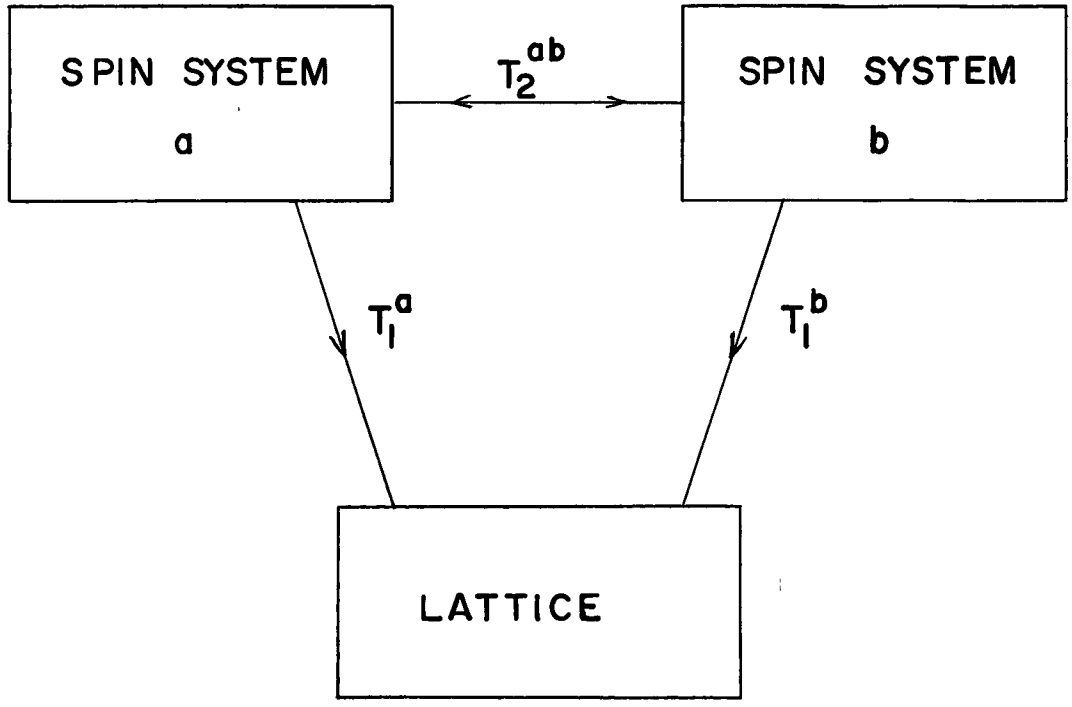

Figure 36. Illustrates the Coupling of Two Spin Systems 'a' and 'b' to the Lattice and to Each Other

If $T_2^{ab} << T_1^a, T_1^b$, the spin temperatures of the a and b systems are almost equal at all times and it may be shown that the magnetization of the composite system approaches equilibrium with the lattice exponentially with a time constant

$$\frac{1}{T_1^{eff}} = \frac{C_a}{C_a + C_b} \frac{1}{T_1^a} + \frac{C_b}{C_a + C_b} \frac{1}{T_1^b} \qquad (6\text{-}40)$$

where C_a and C_b are the heat capacities of the a and b systems respectively.

The time constant T_2^{ab} should be closely related to the "transverse relaxation time" T_2 which may be measured for the composite systems as the time constant for the decay of the x-y components of magnetization. For CH_4 at low temperatures T_2 = 12 μsecs, while for CD_4, T_2 = 500 μsecs so that the conditions required for equation (6-40) to be valid would seem to be well satisfied. The experimental results give a postiori justification of this.

If the a and b systems are associated with different local environments (Case (I)), the effect of a distribution of correlation times would result in an increase in the value of $T_{1_{min}}$ over that predicted for a single correlation time.

For the special example of case (2) for CH_4 given above, if a is associated with A symmetry molecules and b with T symmetry molecules, so that $1/T_1^A = 0$, then

$$\frac{1}{T_1^{eff}} = \frac{C_T}{C_A + C_T} \frac{1}{T_1^T}$$

with

$$\frac{C_T}{C_A} = \frac{N_T\, I_T\, (I_T + 1)}{N_A\, I_A\, (I_A + 1)}$$

where N_A, N_T are the number of molecules having A and T symmetry respectively and I_A, I_T are the total nuclear angular momenta for molecules having A and T symmetry respectively. For CH_4, it is known that $I_A = 2$, $I_T = 1$, while the high temperature ratio of N_A/N_T is 5/9. If this ratio is unchanged at low temperatures (no conversion between different spin species)

$$\frac{1}{T_{1\,\mathrm{eff}}} = \frac{3}{8}\,\frac{1}{T_1{}^T}$$

This would also give rise to an increase in the predicted value of $T_{1_{min}}$.

Some Comments about Matrix Elements of the Intramolecular Interactions: 6:8

To conclude this discussion of some of the manifestations of the quantum nature of the methane system, one more aspect of this problem will be discussed, namely, the effect that restricting the molecules to a small set of states has on the correlation function. In the classical treatment of rotational Brownian motion, the molecules are assumed to have a definite orientation $\Omega_0(t)$, i.e., the wave function,

$$\delta(\Omega - \Omega_0(t)) = \sum_{J m_J} Y_{J m_J}(\Omega)\; Y^*_{J m_J}(\Omega_0(t))$$

involves a superposition of all J, m_J states. The intramolecular interactions of the form $Y_{2m}(\Omega)$ are completely specified by $\Omega_o(t)$ at a particular time.

In the opposite extreme, for an ensemble of non-interacting symmetric top molecules where J, K, M are good quantum numbers, the orientation of each molecule is indeterminate. The eigenfunction of the system of N molecules is the product of the N free rotor wave functions $|JKM\rangle$. The correlation function of $Y_{2m}(\Omega)$ is then

$$G(\tau) = Tr\left\{ \rho\ Y_{2m}(\Omega(t))\ Y^*_{2m}(\Omega(t+\tau)) \right\}$$

where $Y_{2m}(\Omega(t))$ is a time-dependent operator in the Heisenberg representation and ρ is the density matrix describing the equilibrium populations of the various levels.

The correlation functions can be written as follows:

$$G(\tau) = \sum_{\substack{J=0 \\ J'=0}}^{\infty} \sum_{\substack{K=-J \\ K'=-J'}}^{+J} \sum_{\substack{M=-J \\ M'=-J}}^{J} P_{JKM} \left| \langle J'K'M' | Y_{2m}(\Omega) | JKM \rangle \right|^2 \cos(\omega_{JK} - \omega_{J'K'})\tau$$

where $E_{JK} = \hbar\omega_{JK} = \hbar\Omega_R J(J+1) + \hbar(\Omega_3 - \Omega_R)K^2$

and $$P_{JKM} = \frac{\exp -(E_{JK}/kT)}{\sum_J \sum_K (2J+1)\ \exp -(E_{JK}/kT)}$$

For spherical top molecules, the expression may be rewritten

$$G(\tau) = \frac{1}{4\pi}\left[\frac{1}{5} + \frac{1}{5}\sum_{J=0}^{\infty} P_J \left\{ \frac{2J+3}{2J+1} \cos\left[(2J+2)\Omega_R\tau\right] + \frac{2J-1}{2J+1} \cos\left[2J\Omega_R\tau\right] \right.\right.$$
$$\left.\left. + \frac{2J+5}{2J+1} \cos\left[(4J+6)\Omega_R\tau\right] + \frac{2J-3}{2J+1} \cos\left[(4J-2)\Omega_R\tau\right] \right\}\right]$$

Now the interactions between the molecules can be introduced in an arbitrary manner by multiplying $G(\tau)$ by an exponential

function $e^{-\tau/\tau_c}$ where τ_c is then a measure of the time interval during which the molecules behave essentially as free rotors. Now, if ω_o and $1/\tau_c$ are appreciably smaller than any frequencies occurring in the oscillatory terms, then these terms can be neglected and one sees that $G(\tau)$ has 1/5 of its classical value. At sufficiently low temperatures the correlation time will be long enough for this condition to be satisfied. This is another possible contributing factor to the lengthening of $(T_1)_{min}$.

The above considerations are intended only to illustrate how off-diagonal elements of the intra-molecular interactions can be suppressed insofar as their contribution to spin-lattice relaxation is concerned. They are not intended to imply that the wave functions of methane molecules in the solid are well approximated by free rotor wave functions. The model of Colwell, Gill and Morrison does implicitly assume that the wave functions of solid methane can be written as a product of N single molecule wave functions. No detailed description of these single molecule wave functions has yet been given.

Within the context of the above remarks this is an appropriate time to make some comments about the spin-rotation interactions. When the degeneracies of the molecular rotational levels are completely lifted by the crystalline electric field, the rotational angular momentum J is "quenched" (Abragam, 1961, p. 174). This means that the only non-zero matrix elements of J are between states of different energy. For

this reason, according to the preceding argument, the contribution of the spin-rotation interaction to nuclear spin relaxation is expected to be small in solids.

In fact, the spin-rotation interaction has been completely neglected in this thesis. For cases in which degeneracies do exist, it is not clear that this neglect is justified even in solids in which the molecule is subjected to large crystalline fields. In the discussion of the model proposed for solid methane, it has been assumed that for states i and j which have degeneracies g_o and g_1 respectively, $\langle y^2 \rangle_i = \langle y \rangle_i^2$ and $\langle y^2 \rangle_j = \langle y \rangle_j^2$ (see section 6:6B). It was pointed out that these equalities are satisfied in many cases of interest for $y = Y_{2m}$, for example. It is quite clear that for the examples given in section 6:6B, these equalities could not be satisfied for matrix elements of the operator J in the spin-rotation interaction. Then, the assumption that only the last of the three terms in equations (6-16) is non-zero, would not be valid and the correlation times τ_o and τ_1 would enter into the expression for T_1.

CHAPTER 7.

SUMMARY

In this thesis, the results of a study of the relaxation properties of the methane system at low temperatures have been presented. These were studied with the ultimate aim of gaining further insight into the nature of the phase transitions. To achieve this aim, N.M.R. pulse techniques were used with the hope that through the application of conventional N.M.R. theory, information about the nature of the relaxation mechanisms and the reorientational motions could be obtained. Instead, it was found that the conventional theory is inadequate. The experimental results and the analysis of the experimental results using the conventional theory have already been summarized at the end of Chapter 5. The results definitely indicate that the reorientational motion of the methane molecule is at least partially quenched at the phase transitions.

As a consequence, an attempt was made in Chapter 6, to modify the theory such as to take account of some of the effects due to the quantum nature of the system. The model for the low lying energy levels of solid methane proposed by Colwell, Gill, and Morrison (1965) was used as the starting point for our considerations in Chapter 6; the consequences of their model as far as the relaxation properties of methane are concerned were examined in some detail. The following consequences were established there:

(1) under conditions satisfied by many (but not all) systems of interest, it was found that a single exponential does indeed describe the correlation function.

(2) The effective strength of the interaction has been found to be temperature dependent for a two level system, thus invalidating the analysis of the experimental results carried out in Chapter 5.

(3) It is postulated that phonon-molecular interactions involving direct (one phonon) and Raman (two phonon) processes cause transitions between the energy levels. The observed temperature dependence of the correlation time is consistent with this picture, at least qualitatively.

(4) Some considerations leading to a reduction in the strength of the relaxation perturbation and consequently in a lengthening of T_1 were discussed in Chapter 6.

The following conclusions can be drawn from this study of the relaxation properties of the methane system. The molecular reorientations are definitely partially quenched at the phase transitions, but not completely. It seems likely that the direct and Raman processes in part account for the observed temperature dependence of the observed correlation time at low temperature; this to our knowledge is the first time that these types of processes have been observed to play a role in the magnetic relaxation in diamagnetic

substances. The conventional theory appears incapable of explaining the details of the relaxation phenomena in solid methane.

In conclusion, some further experiments will be proposed. In Chapter 6, it was proposed that carrying the relaxation measurements down to 0.3°K allows a determination of T_o. A word of warning is appropriate here; if the spin-rotation interaction is an effective relaxation perturbation, then the considerations which led us to propose that experiment are not correct. It would be intriguing to measure the relaxation properties of a CH_4-Kr mixture containing a very small amount of CH_4 in view of the drastic changes exhibited by the 50%Kr-50%CH_4 data. A more detailed examination of the upper minimum in T_1 for CH_4, and CH_4 mixtures with CD_4 of Kr, if performed carefully, may allow a separation of the two time constants observed. A study of CH_2D_2 could be interesting, as the energy level scheme proposed by Colwell, Gill and Morrison (1965) for CH_2D_2 consists of <u>three</u> sets of low-lying energy levels.

On the theoretical side, there seems to exist no theory of the interaction between molecular rotation and lattice vibration which is applicable to a quantum system like solid methane.

BIBLIOGRAPHY

1. Abragam, A. 1961. The Principles of Nuclear Magnetism (Oxford University Press, London)

2. Alexander, S. and Tzalmona, A. 1965. Phys. Rev. 138, A845.

3. Anderson, C. H. 1961. Ph.D. Thesis, Harvard University.

4. Andrew, E. R. and Eades, R. G. 1953. Proc. Roy. Soc. A, 218, 537.

5. Bartholome, E., Drikos, G., and Eucken, A. 1938. Z. Physik. Chem. B 39, 371.

6. Berman, R. 1952. Rev. Sci. Instr. 25, 94.

7. Bloch, F. 1946. Phys. Rev. 70, 460.

8. Bloch, F. 1956. Phys. Rev. 102, 104.

9. Bloembergen, N., Purcell, E. M., and Pound, R. V. 1948. Phys. Rev. 73, 679.

10. Bloom, M. and Sandhu, H. S. 1962. Can. J. Phys. 40, 289.

11. Clark, W. 1964. Rev. Sci. Instr. 35, 316.

12. Clement, J. R. and Quinnell, E. H. 1952. Rev. Sci. Inst. 23, 213.

13. Clouter, M. and Gush, H. P. 1965. Phys. Rev. Lett. 15, 200.

14. Clusius, K. 1929. Z. Phys. Chem. B 3, 41.

15. Clusius, K., Popp, L., and Frank, A. 1937. Physica 4, 1105.

16. Colwell, J. H., Gill, E. K., Morrison, J. A. 1962. J. Chem. Phys. 36, 2223.

17. Colwell, J. H., Gill, E. K., Morrison, J. A. 1963. J. Chem. Phys. 39, 635.

18. Colwell, J. H., Gill, E. K., Morrison, J. A. 1963. J. Chem. Phys. 42, 3144.

19. Dasanraoharya, B. A. to be published.

20. de Wit, G. A. and Bloom, M. 1965. Can. J. Phys. 43, 986.

21. Eucken, A. and Veith, H. 1936. Z. Physik. Chem. B34, 275.

22. Ewing, G. 1964. J. Chem. Phys. 40, 179.

23. Gordon, R. G. 1965. J. Chem. Phys. 43, 1307.

24. Hahn, E. L. 1950. Phys. Rev. 80, 580.

25. Hardy, W. N. 1965. Private Communication.

26. Hubbard, P. S. 1961. Rev. Mod. Phys. 33, 249.

27. Hubbard, P. S. 1962. Phys. Rev. 128, 650.

28. Hubbard, P. S. 1963. Phys. Rev. 131, 275.

29. Ivanov, E. N. 1964. Soviet Physics. JETP 18, 1041.

30. James, H. M. and Keenan, T. A. 1959. J. Chem. Phys. 31, 12.

31. Jeffries, C. D. 1963. Dynamic Nuclear Polarization (Interscience, New York)

32. Maue, A. 1937. Ann. Physik. 30, 555.

33. McLannen, J. and Plummer, W. 1929. Phil. Mag. 7, 761.

34. Mills, R. L. and Schuch, A. F. 1965. Phys. Rev. Lett. 15, 722.

35. Mooy, H. 1931. Nature 127, 707.

36. Nagamiya, T. 1951. Prog. Theor. Phys. 6, 702.

37. Pauling, L. 1930. Phys. Rev. 36, 430.

38. Redfield, A. G. 1957. I.B.M. J. Res. Develop. 1, 19.

39. Rosenberg, H. M. 1963. Low Temperature Solid State Physics (Oxford University Press).

40. Rosenshein, J. S. and Whitney, W. M. 1965. Low Temperature Physics LT9 (Plenum Press, New York).

41. Sandhu, H. S., Lees, J., and Bloom, M. 1960. Can. J. Chem. 38, 493.

42. Savitzky, G. B., and Hornig, D. F. 1962. J. Chem. Phys. 36, 2634.

43. Schallamach, A. 1939. Proc. Roy. Soc. A 171, 569.

44. Speriandio, A. 1961. Thesis, University of Zürich.

45. Stackelberg, M., Quatram, F., and Antweiler, H. 1936. Z. Electrochemie 42, 552.

46. Steele, W. A. 1963. J. Chem. Phys. 38, 2404.

47. Stevenson, R. 1957. J. Chem. Phys. 27, 646.

48. Stewart, J. W. 1959. J. Phys. Chem. S olids 12, 122.

49. Stiller, H. and Hautecler, S. 1963. Inelastic Scattering of Neutrons in Solids and Liquids (International Atomic Energy Agency, Vienna, 1963).

50. Sugawara, T., Masuda, Y., Kanda, T. and Kanda, E. 1956. Rep. Res. Insts. Tohoku Univ. A7, 67.

51. Thiele, A., Whitney, W. and Chase, C. 1965. Low Temperature. Physics LT 9 (Plenum Press, New York).

52. Thomas, J., Alpert, N. and Torrey, H. 1950. J. Chem. Phys. 18, 154.

53. Tomita, K. 1953. Phys. Rev., 89, 429.

54. Van Kranendonk. 1954. Physica 20, 781.

55. Welsh, H. L., Crawford, M. F., and Harrold, J. H. 1952. Can. J. Phys. 30, 81.

56. Wolf, R. P. 1963. Ph. D. Thesis, M. I. T.